

DOE/ET-53088-210

IFSR #210

**The Linear Instability and  
Nonlinear Motion of Rotating Plasma**

*Jixing Liu*

Institute for Fusion Studies  
The University of Texas at Austin  
Austin, Texas 78712

October 1985

THE LINEAR INSTABILITY AND NONLINEAR MOTION  
OF ROTATING PLASMA

Publication No. \_\_\_\_\_

Jixing Liu, Ph.D.

The University of Texas at Austin, 1985

Supervising Professor: C. Wendell Horton, Jr.

Two coupled nonlinear equations describing the flute dynamics of the magnetically confined low- $\beta$  collisionless rotating plasma are derived. The linear instability and nonlinear dynamics of the rotating column are analyzed theoretically.

In the linear stability analysis, a new sufficient condition of stability is obtained. From the exact solution of eigenvalue equation for Gaussian density profile and uniform rotation of the plasma, we find that the stability of the system strongly depends on the direction of plasma rotation, FLR effect and the location of the conducting wall. An analytic expression showing the finite wall effect on different normal modes is obtained and it explains the different behavior of (1,0) normal mode from other modes. The sheared rotation driven instability is investigated by using three model equilibrium profiles and the analytic expressions of eigenvalues

which includes the wall effect are obtained. The analogy between shear rotation driven instability and the instability driven by sheared plane parallel flow in the inviscid fluid is analyzed.

Applying the linear analysis to the central cell of tandem mirror system, the trapped particle instability with only passing electrons is analyzed. For uniform rotation and Gaussian density profile, an analytic expression which determines the stability boundary is found. For a typical sheared rotation profile numerical calculations are carried out and the results are presented.

The nonlinear analysis shows that the nonlinear equations have a solitary vortex solution which is very similar to the vortex solution of nonlinear Rossby wave equation. In the rest frame the vortex has dipole structure, keeps finite amplitude inside a small region and exponentially decays to zero at large distances. This solitary vortex propagates with constant speed in the azimuthal direction and keeps its shape when it moves. Also the propagating speeds of vortices are complementary to the phase velocities of corresponding linear modes. Two exact vortex solutions are obtained for the flute case and the case when the flute dynamics was modified by small amounts of passing electrons, respectively. These theoretical results may suggest a new picture of the dynamics of rotating low- $\beta$  plasma: complete description of fluctuations should include the coherent vortex component as well as the conventional modes.

**TO**  
**MY PARENTS**  
**MY WIFE AND MY SONS**

THE LINEAR INSTABILITY  
AND NONLINEAR MOTION OF ROTATING PLASMA

APPROVED BY SUPERVISORY COMMITTEE

Wendell Horton, Jr.  
J. B. Swift  
Henry L. Berkman  
Edward J. Power Jr.  
James S. Mass

**THE LINEAR INSTABILITY  
AND NONLINEAR MOTION OF ROTATING PLASMA**

by

**LIU, JIXING**

**DISSERTATION**

Presented to the Faculty of the Graduate School of

The University of Texas at Austin

in Partial Fulfillment

of the Requirements

for the Degree of

**DOCTOR OF PHILOSOPHY**

**THE UNIVERSITY OF TEXAS AT AUSTIN**

(August, 1985)

## Acknowledgements

I wish to thank my supervising professor, Dr. C. Wendell Horton, for introducing me to this topic and for his continuing guidance for my work.

The members of my Supervisory Committee, Dr. Jim Meiss, Dr. Edward Powers, Dr. Jack Swift and Dr. Harry Swinney, provided me with helpful suggestions to improve my work, for which I am grateful.

The more-than-generous assistance I received from my friend and co-worker, Dr. Joseph Sedlak, was invaluable in enabling me to complete my doctorate.

I am also grateful to a number of people during the course of my study. Dr. Herbert Berk, by providing me with his unpublished work, deepened my understanding of the concepts contained in Ch.IV. Dr. Swadesh Mahajan gave me much support and encouragement. Mrs. Winnie Schild helped to edit my manuscript.

Finally I would like to thank both The Institute of Theoretical Physics, Academia Sinica, for giving me the opportunity to come to The University of Texas and The Institute for Fusion Studies for providing me with an outstanding scientific atmosphere in which to pursue my studies.

## TABLE OF CONTENTS

Chapter	page
I INTRODUCTION.....	1
II FLUTE DYNAMICAL EQUATIONS	
FOR ROTATING PLASMA.....	11
Introduction	11
II.1. Derivation of nonlinear equations .....	14
II.2. The conservation laws .....	30
III THE LINEAR STABILITY ANALYSIS .....	36
Introduction.....	36
III.1. The linearized stability equations .....	38
III.2. The general stability properties .....	47
III.3. An analytic solution of the eigenvalue problem	
for the uniform rotating plasma .....	53
III.4. The instability due to the shear of	
the rotation frequency.....	76
IV THE TRAPPED PARTICLE MODES WITH	
PASSING ELECTRONS AND ROTATION SHEAR	
IN THE CENTRAL CELL OF TANDEM MIRROR.....	89
Introduction .....	89
IV.1. The derivation of the trapped particle mode equation	



from the hydrodynamic equations .....	93
IV.2. Analytic solution for solid body rotation	
with passing particles.....	102
IV.3. Differential rotation and passing particles .....	116
IV.4. Summary and conclusion .....	131
V    NONLINEAR MOTION-	
-THE SOLITARY VORTEX SOLUTION.....	133
Introduction.....	133
V.1. A brief historical summary .....	135
V.2. Reduction of the nonlinear equations	
of rotating plasma.....	145
V.3. Solitary flute-vortex in the rotating plasma .....	148
V.4. Solitary flute-vortex modified by the passing electrons	
in the rotating plasma.....	151
V.5. Properties of the vortices.....	153
V.6. Summary and conclusions .....	166
VI    CONCLUSIONS.....	168
Appendix A .....	173
Appendix B .....	178
Appendix C.....	182
Appendix D .....	186
References .....	191

## LIST OF FIGURES

Figure	page
2.1 The configuration of the rotating plasma column.....	13
3.1 Eigenvalue spectrum for (1,0) and (2,0) modes.....	46
3.2 The equilibrium density and electrostatic potential profile corresponding to section <b>III.3</b> .....	55
3.3 Radial perturbation function $\delta\phi_m(r)$ .....	58
3.4 Eigenvalue $\nu_{m,n}(b/a)$ versus $b/a$ .....	60
3.5 The growth rate of (1,0) mode.....	63
3.6 The growth rate of (2,0) mode.....	64
3.7 The growth rate of (5,0) mode.....	65
3.8 The real frequency and growth rate versus mode number $m$ .....	66
3.9 The stability boundary ( $\hat{g}$ versus $\hat{\Omega}$ ) .....	70
3.10 The stability boundary ( $T_i/T_e$ versus $\Omega$ ) .....	71
3.11 The wall effect on the real frequency and growth rate of low $m$ modes .....	74
3.12 The equilibrium profiles corresponding to <b>III.4A, 4B, 4C</b> .....	77
3.13 The real frequency and growth rate for rotation shear driven instability .....	82
3.14 The perturbed $\mathbf{E} \times \mathbf{B}$ flow seen in the frame rotating with $\Omega = (\Omega_1 + \Omega_2)/2$ .....	88

4.1	The schematic picture of three cell tandem mirror system .....	92
4.2	The stability boundary ( $A_p$ versus $\Omega$ ) with $\hat{g} = 0, b/a = 3$ , and $m = 1, 2$ .....	109-10
4.3	The same as Fig.4.2 with $\hat{g} = 1$ .....	111
4.4	The same as Fig.4.2 with $\hat{g} = -1$ .....	112
4.5	The wall effect to low $m$ modes .....	113
4.6	The same as Fig.4.3, with $b/a=1$ .....	114
4.7	The same as Fig.4.4, with $b/a=1$ .....	115
4.8	The equilibrium density and shear rotation profile .....	117
4.9	Low $m$ spectra for uniform rotation .....	122
4.10	The perturbation function for different density profiles .....	123-4
4.11(a)	The real and imaginary frequencies for $m=1$ mode in shear rotation with Gaussian density profile .....	125
4.11(b)	The same as Fig.4.11(a) for $m=2$ mode .....	126
4.12(a)	The same as Fig.4.11(a) with parabolic density profile .....	127
4.12(b)	The same as Fig.4.11(b) with parabolic density profile .....	128
4.13	The contours of constant potential for uniform rotation .....	129
4.14	The same as Fig.4.13 for shear rotation .....	130
5.1	Schematic diagram of the parameter representation for vortices .....	159
5.2	The constant $\phi(r, \theta)$ contour of the vortex .....	160
5.3	Propagation regions of vortices and linear wave modes .....	161

5.4	The vortex propagation speed versus $k$ ( $\Omega < 0$ ) .....	162
5.5	The same as Fig.5.4, ( $\Omega > 0$ ) .....	161
5.6	The radial structure of electron diamagnetic vortices .....	163
5.7	The radial structure of ion diamagnetic vortices .....	165

# CHAPTER I

## INTRODUCTION

This thesis is devoted to the study of linear instability and nonlinear motion of magnetically confined rotating plasma.

For a long time there has been considerable interest in rotating plasmas in various research areas from controlled fusion experiments to theoretical astrophysics. In astrophysics, the plasma confined in the strong magnetic field of rapidly rotating neutron stars plays an important role in the radiation of the pulsars [ Zheleznyakov, 1977 ]; the possibility of using the instability of the laboratory rotating plasma to simulate the spiral arm formation process of galaxies also was suggested [Fridman and Polyachenko, 1984]. In the controlled fusion study the centrifugal confinement concept was proposed to reduce the end loss from magnetic mirror devices [Bishop, 1958; Artshimovich 1964], where the plasma has to be put into fast rotation. Beside this, the plasma rotation has been observed in several magnetic confinement devices such as  $\theta$  -pinch, field reversed pinch, tandem mirror and tokomaks. It made the investigation of instability due to rotation in these devices important from the point of confinement. In addition, theoretical and experimental research on rotating plasma are also carried out in other fields. For example, nonneutral plasma needs to be rotating to maintain equilibrium [ Davidson, 1972], and plasma centrifuge device is expected to use

rotation to separate isotopes of various gases , especially Uranium-compound [McClura and Nathrath 1977]. More of the applications of the rotating plasma can be found in a review paper by Lehnert [Lehnert, 1971].

Since the early sixties many efforts have been put into the study of low-frequency instabilities of magnetically confined rotating plasma, since it is believed that the low-frequency, long wave length perturbation greatly influences the plasma confinement property.

As many theoretical investigations and experimental observations show, there are two basic mechanisms through which the rotation can drive low-frequency instability : first, since magnetically confined plasma generally is inhomogeneous and has negative density gradient from the center to the boundary, the centrifugal force experienced by the plasma plays a role similar to destabilizing gravity in Rayleigh-Taylor instability of a heavier fluid on top of a lighter fluid; second, when the density gradient of the plasma is very weak and negligible there is no driven mechanism for the Rayleigh-Taylor instability, but the shear associated with nonuniform rotation may drive instability similar to the Kelvin-Helmholz instability of parallel flow with velocity shear. In general these two mechanisms drive the instability simultaneously.

Before the late seventies, theoretical interest centered on  $\theta$ -pinch and Q-machine devices. For both devices the plasma confined by axial magnetic field and there is an equilibrium radial electric field which give an  $\mathbf{E} \times \mathbf{B}$  rotation and

drive both Rayleigh-Taylor and Kelvin-Helmholz type instabilities. These were observed experimentally. From the late seventies to now, the emphasis of research has gradually become the Tandem mirror device in the west and the SVIPP device in the Soviet Union. For the central cell of a Tandem mirror, considerable  $\mathbf{E} \times \mathbf{B}$  rotation due to the strong radial equilibrium electric field was observed in laboratory experiments [Hooper et al, 1983] and the related possible rotational instability is a topic of recent investigations [Freidberg and D'Ipoltto, 1984; Horton and Liu, 1984; Kesner and Lane, 1985]. For the SVIPP device, a very strong externally imposed radial electric field causes the rotation with a frequency several orders of magnitude higher than the ion diamagnetic drift frequency, which severely limits the MHD stability of this system [Breizman and Tsel'nik, 1984].

In the early studies of low frequency rotational instability the following theoretical models were developed and employed alternatively in calculations by different authors:

- (1) ideal magnetohydrodynamic model [Chandrasekhar, 1961; Taylor, 1962; Freidberg and Wesson, 1970 ; Spies, 1978];
- (2) Finite Larmor radius two-fluid model [Chen, 1965; Berge, 1966; Freidberg and Pearlstein, 1978 ];
- (3) the Vlasov equations [ Rosenbluth et al, 1962; Rosenbluth and Simon, 1965; Wright et al, 1976; Davidson, 1976];

(4) The Vlasov-Fluid model [Freidberg,1972; Seyle, 1979].

The publication on this topic is voluminous, but for the sake of finding a guide to our further work we would like to give a brief summary of the main results from the previous calculations.

- (1) In all the calculations based on the ideal magneto-hydrodynamic model for flute mode,  $m = 1, n = 0$  mode is marginal stable, other modes are unstable. If considering the axial variation of the perturbation, i.e. the modes are no longer flute,  $m = 1, n = 0$  mode can have growth rate for certain parallel wave number regime.
- (2) Calculations based on finite Larmor radius two-fluid model give a stable range of rotation frequency and conclude that for sufficient finite Larmor radius effect the modes with  $m \geq 2$  can be suppressed; this confirms the FLR stabilizing effect first proposed by Rosenbluth et al (1962). However, the  $m=1, n=0$  flute mode is also marginal stable in this model. Taking into account non-flute perturbations for a rigid-rotor equilibrium, Freidberg and Pearlstein (1978) obtained a positive growth rate for this mode.
- (3) The results from Vlasov equation are diverse, Using low- $\beta$  and flute approximations and solving Vlasov equation by direct integration along the unperturbed orbits [Rosenbluth et al, 1962] or by FLR expansion [Rosenbluth and Simon, 1965] the results are the same as the FRL two



fluid model. But for high- $\beta$  non-flute perturbation Bowers and Haines [1971] concluded that the  $m = 1, n = 1$  mode is more dangerous than would be expected from the two fluid model.

- (4) The Vlasov-fluid model results add new information to the rotating instability of  $\theta$ -pinch plasma. The numerical calculation by Seyler (1979) shows that due to the existence of small amounts of resonant ions interacting with the perturbation, beyond the region where FLR two fluid model and Vlasov equation calculations gave stable results, the system still can have residual instability. However the growth rate of this residual instability is very small.
- (5) Above calculations are carried out under the assumption that the rotation of the plasma column is uniform, so the conclusions drawn from them apply only to the Rayleigh-Taylor type instability. There are only few numerical calculations of instability with nonuniform rotation [Kent et al, 1969; Perkins et al, 1971; Rongline, 1973; Jassby 1972]. All these calculations are based on the FLR two-fluid model and take specific equilibrium density and rotation frequency profiles, so there is no general conclusion. All the calculations agree that the rotational shear instability differs qualitatively from the Rayleigh-Taylor type instability.

Due to lack of systematic and complete measurements of the relevant data, the comparison between theoretical results with experiment observations is

obscure and even controversial. There are several positive points can be made. (i) The fact that the  $\theta$ -pinch experiments always observed the unstable  $m = 1, n = 0$  mode but not  $m = 2$  and higher  $m$  modes is in direct conflict to the ideal MHD model, in a certain sense it may be a support to the concept of the FLR stabilizing although the theory including FLR effect predicted marginal stability of  $m = 1, n = 0$  flute mode. (ii) The nonflute FLR two-fluid model calculation by Freidberg and Pearstein (1978) has some success because the real frequency and growth rate of  $m = 1, n = 0$  mode given by them is quite close to the experiment value of the "wobble" mode and their calculation also showed that this mode has lowest threshold value for excitation. (iii) The calculations on instability due to nonuniform rotation have fair good agreement with experiment observations in edge oscillation of Q-machine plasma and instability in hollow cathode discharge plasma.

Since the Tandem mirror devices stepped to the stage of the open-ended confinement devices and the experiments in TMX showed the quite fast rotation of plasma in central cell of this device, theoretical works on rotational instability in Tandem mirror appeared recently. The theoretical models used here are the ones from the early studies with certain modifications. Freidberg and D'Ipollito (1984) discussed the low- $\beta$  rotational interchange marginal stability condition for a conventional tandem mirror on basis of the Vlasov-fluid model and concluded that low  $m$  modes are stable in the TMX experiment. Horton and Liu (1984), by using

two fluid model discussed rotation driven drift modes in central cell of tandem mirror and suggested the weak unstable modes observed in TMX experiment may be the rotation driven drift modes. Kesner and Lane (1985) discussed low  $\beta$  tandem mirror trapped particle instability for arbitrary azimuthal mode number including the effects of radial equilibrium electric fields by solving Vlasov equations and suggested a possible rotationally driven trapped particle mode.

The numerous articles and reports mentioned above show that the research of low frequency rotational instability in plasma is enriched a great deal during the past two decades, but unfortunately, all these works belong to the linear analysis. The only nonlinear work in this respect is reported by Janssen [Janssen, 1983]. In this work the equilibrium plasma parameters were adjusted to allow only one weakly unstable linear mode, then by using the multi-time method the author studied the saturation of the unstable mode and found that the amplitude of this mode is in recurrence, hence in average there is no radial transport. Janssen's model is an oversimplified case for the real rotating plasma but this work is a useful effort in the direction of nonlinear study of rotating plasma.

The purpose of this thesis is to achieve two goals: first, to derive a set of model nonlinear equations which is suitable to treat the nonlinear dynamics of inhomogeneous rotating plasma; second, to apply the model equations to investigate some practical problems, specifically, the mode structure of rotational trapped particle instability in the central cell of the Tandem mirror by linear analysis and

under some approximations give a nonlinear solution of the model equation. For this purpose, it is necessary to consider the balance between physical effects included in the theory and the mathematical tractability of the problem. From the physics side, the model equation should contain the physics effects which are important for description of the system under consideration; from the other side, the mathematical formalism used in the theory should not be too complicated to prevent solving the problem practically. After considering this balance, we choose a two-fluid description of the plasma, which unavoidable excludes kinetic effects from our consideration, but it was proved by the previous works on the linear analysis of rotational instability that for low frequency perturbation this description is quite fruitful. We also limit our study to low  $\beta$  isothermal plasma and flute-like perturbations, which reduce the number of perturbed quantities to two and make the problem two-dimensional; by this choice the mathematics become much less involved. Despite above mentioned limitations, we include following physical effects which were pointed out by the previous linear studies being essential to the rotational instability into our consideration: inhomogeneity of plasma; arbitrary radial equilibrium electric field ( in other words, arbitrary rotational frequency of plasma); magnetic field line curvature effect or pondermotive force effect of RF heating; FLR effects of ion component; and the finite boundary effect.

The arrangement of the materials of the thesis is as follows. In chapter II we derive the nonlinear equations from the two-fluid model of plasma and give

the conservative quantities kept by this set of equations. We prove that for a closed system the model equations keep the total mass, entropy, angular momentum and energy of the plasma conserved. In chapter III, we give three forms of the linearized stability equation from our nonlinear equations, among which the first one is convenient for treating uniform rotating case of plasma; the third one is a form convenient to the linear mode spectrum analysis for instability. The second linearized form of the model equations recovered the compact linear stability equation first derived by Rosenbluth and Simon (1965) from solving Vlasov equation. This means that, at least through the linear treatment, our model equations is as powerful as the Rosenbluth-Simon equation. Through a general discussion of this equation, besides recovering some previous reported conclusions we find a sufficient condition for stability of low- $\beta$  plasma rotating with arbitrary frequency which generalizes the condition given by others [Freidberg and Pearlstein, 1978]. By considering special equilibrium density and electric potential ( or rotation frequency) profiles, several analytic solutions for uniform and nonuniform rotation were given and the wall effect on  $m = 1, n = 0$  mode is analyzed.

In chapter IV, we modify the linearized stability equation derived in chapter III to include effect of small amounts of passing electrons and study the rotational trapped particle instability in central cell of simple Tandem mirror and give the stability boundary for the passing electron ratio versus plasma rotation frequency. In this chapter we also numerically treat the shear rotation effects for

a specific rotation profile and two continuously varying density profiles.

In chapter V we treat the nonlinear problem of uniform rotating plasma. By introducing certain approximations, we find a solitary dipole solution of our nonlinear equations. The vortex moves with constant velocity in the azimuthal direction in the rotating frame of plasma. This solitary vortex solution is similar to the solitary vortex discovered in nonlinear Rossby wave equation for planetary atmosphere study by Larichev and Reznik ( 1976) and adds two new members to the recently rapid growing family of solitary vortex solutions in magnetically confined plasma study. The propagation and spatial properties and the possible implication of these vortices on plasma transport are discussed.

In chapter VI, the conclusions of this thesis is given.

Chapter II  
FLUTE DYNAMICAL EQUATIONS  
FOR ROTATING PLASMA

**Introduction**

In this chapter we derive the nonlinear equations for flute dynamics of low  $\beta$  rotating plasma and give the constants maintained by these equations.

We assume the plasma under consideration is a dense, collisionless plasma column confined in a constant, uniform axial magnetic field  $\mathbf{B} = B_0 \hat{z}$ . Most importantly, we suppose the plasma has a radial equilibrium electric field  $\mathbf{E}_0 = E_0(r) \hat{r}$  which causes the plasma column to rotate transverse to the crossed electric and magnetic field: in cylindrical coordinates, the plasma rotates in the azimuthal direction  $\hat{\theta}$  with frequency  $\Omega = \frac{cE}{rB}$ . This configuration is shown in Fig. 2.1. Since our purpose is to study the low frequency (characteristic frequency  $\omega \ll \omega_{ci} = \frac{eB}{m_i c}$ , ion cyclotron frequency) instability of rotating plasma, we require the basic equations to include the following essential effects: equilibrium electric potential, inhomogeneity of plasma density, finite Larmor radius (FLR), magnetic field line curvature.

Instead of using the most accurate description of plasma-electromagnetic fields system by Vlasov equations for electron and ion components and Maxwell equations for the fields we describe our system by using two component hydrody-

dynamic equations and Maxwell equations which neglect the kinetic effects included in the first description but retain the fluid like properties of plasma. Due to the fact we are dealing with low frequency electrostatic perturbations for low  $\beta$  ( $\beta = 4\pi \sum_{j=i,e} n_j T_j / B^2$ ), dense plasma, the Maxwell equations are legitimately replaced by a quasineutrality condition. This choice of description greatly reduces the mathematical complexity of the problem. The flute approximation also is assumed in the derivation of equations which limits our consideration to the plane perpendicular to equilibrium magnetic direction.

This chapter consists of two sections. In section II.1 we derive the equations appropriate to stability analysis of rotating plasma, and in section II.2 we derive the conservation law of these equations.



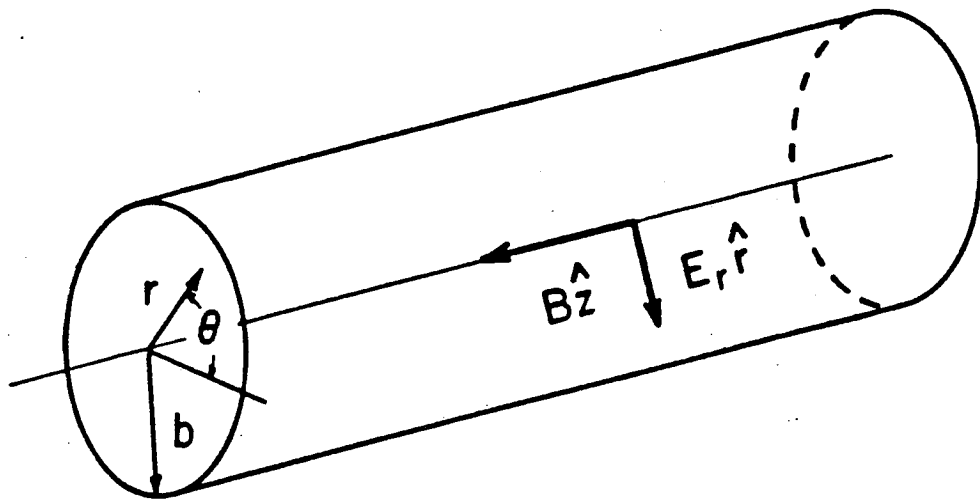


**Fig.2.1** The configuration of the system. a plasma column confined in a constant axial magnetic field  $B_0 \hat{z}$ , the equilibrium electric field  $\mathbf{E} = E(r) \hat{r}$ , the  $\mathbf{E} \times \mathbf{B}$  drift causes the plasma rotating in  $\hat{\theta}$  direction, where  $b$  is the location of a conducting boundary.

## II.1 Derivation of Nonlinear Equations

We take two component hydrodynamic equations to describe the dynamics of the ion and electron fluids and the Maxwell equations to describe the electromagnetic fields which interact with the plasma.

The full hydrodynamic equations consist of the continuity equations, the momentum balance equations, and the thermal energy equations for both components.

The continuity equations:

$$\frac{\partial n_j}{\partial t} + \nabla \cdot (n_j \mathbf{V}_j) = 0, \quad (II.1)$$

The Momentum equations:

$$m_j n_j \frac{d\mathbf{V}_j}{dt} = n_j q_j \left( \mathbf{E} + \frac{\mathbf{V}_j \times \mathbf{B}}{c} \right) - \nabla p_j - \nabla \cdot \mathbf{\Pi}^{(j)} + \mathbf{F}_j \quad (II.2)$$

The thermal energy equations

$$\frac{3}{2} n_j \frac{dT_j}{dt} + p_j \nabla \cdot \mathbf{V}_j + \nabla \cdot \mathbf{Q}_j + \mathbf{\Pi}^{(j)} : \nabla \mathbf{V}_j = 0 \quad (II.3)$$

Equations (II.1)-(II.3) can be obtained from the Vlasov equation by integrating the first three moments [Braginskii, 1963; Mikhailovskii, 1977]; they are not closed yet. To close the equations or to terminate the moment hierarchy we

need to introduce constitutive relations, i.e. the equations of state, the expression for viscosity tensor  $\Pi^{(j)}$  and the heat fluxes  $\mathbf{Q}_j$ .

The equations of state for a hot plasma ( $nT \gg e^2 n^{\frac{1}{3}}$ ) are the same as that for an ideal gas:

$$p_j = n_j T_j. \quad (II.4)$$

In Cartesian coordinates with the  $\hat{\mathbf{z}}$  in magnetic field direction, for collisionless plasma, the viscosity tensors for ion and electron components can be expressed as [Mikhailovskii, 1977]:

$$\begin{aligned} \Pi_{xx}^{(j)} = -\Pi_{yy}^{(j)} &= -\frac{p_j}{2\omega_{cj}} \left( \frac{\partial V_{jx}}{\partial y} + \frac{\partial V_{jy}}{\partial x} \right) - \frac{1}{5\omega_{cj}} \left( \frac{\partial Q_{jx}}{\partial y} + \frac{\partial Q_{jy}}{\partial x} \right) \\ \Pi_{xy}^{(j)} = \Pi_{yx}^{(j)} &= \frac{p_j}{2\omega_{cj}} \left( \frac{\partial V_{ix}}{\partial x} - \frac{\partial V_{jy}}{\partial y} \right) + \frac{1}{5\omega_{cj}} \left( \frac{\partial Q_{jx}}{\partial x} - \frac{\partial Q_{jy}}{\partial y} \right) \\ \Pi_{xz}^{(j)} = \Pi_{zx}^{(j)} &= -\frac{p_j}{\omega_{cj}} \left( \frac{\partial V_{jz}}{\partial y} \right); \\ \Pi_{yz}^{(j)} = \Pi_{zy}^{(j)} &= \frac{p_j}{\omega_{cj}} \left( \frac{\partial V_{jz}}{\partial x} \right) \\ \Pi_{zz}^{(j)} &= 0 \end{aligned} \quad (II.5)$$

and the heat fluxes are given by

$$\mathbf{Q}_j = \frac{5}{2} \frac{p_j}{m_j \omega_{cj}} \hat{\mathbf{z}} \times \nabla T_j \quad (II.6)$$

The Maxwell equations should be introduced to describe the electromagnetic field:

$$\nabla \cdot \mathbf{E} = 4\pi \sum_j n_j q_j \quad (II.7)$$

$$\nabla \times \mathbf{E} = -\frac{1}{c} \frac{\partial \mathbf{B}}{\partial t} \quad (II.8)$$

$$\nabla \cdot \mathbf{B} = 0 \quad (II.9)$$

$$\nabla \times \mathbf{B} = \frac{1}{c} \frac{\partial \mathbf{E}}{\partial t} + \frac{4\pi}{c} \sum_j n_j q_j \mathbf{V}_j \quad (II.10)$$

The set of equations (II.1)–(II.10) is a closed complete set of equations describing the dynamics of collisionless plasma in electromagnetic fields. Here we list the definition of the notations appeared in Eqns.(II.1)–(II.10):

$j = i, e \equiv$  The species of charged particles of plasma.

$m_i, m_e \equiv$  The mass of ion and electron.

$q_i, q_e \equiv$  The electric charge of ion and electron.

$n_i, n_e \equiv$  The number density of ion and electron fluid.

$p_i(\mathbf{x}, t), p_e(\mathbf{x}, t) \equiv$  The pressure of ion and electron fluid.

$\mathbf{V}_i(\mathbf{x}, t), \mathbf{V}_e(\mathbf{x}, t) \equiv$  The velocity vector of ion and electron fluid.

$\Pi^{(i)}, \Pi^{(e)} \equiv$  The viscosity tensor of ion and electron fluid.

$T_i(\mathbf{x}, t)$ ,  $T_e(\mathbf{x}, t) \equiv$  *The temperature of ion and electron fluid.*

$\mathbf{Q}_i(\mathbf{x}, t)$ ,  $\mathbf{Q}_e(\mathbf{x}, t) \equiv$  *The heat flux vector of ion and electron fluid.*

$\mathbf{F}_i(\mathbf{x}, t)$ ,  $\mathbf{F}_e(\mathbf{x}, t) \equiv$  *The nonelectromagnetic forces exerted  
on ion and electron fluids.*

$\omega_{ci} = \frac{q_i B}{m_i c} \equiv$  *The cyclotron frequency of ions.*

$\omega_{ce} = \frac{q_e B}{m_e c} \equiv$  *The cyclotron frequency of electrons.*

$c \equiv$  *The velocity of light.*

$\mathbf{E}(\mathbf{x}, t) \equiv$  *The electric field vector.*

$\mathbf{B}(\mathbf{x}, t) \equiv$  *The magnetic field vector.*

$$\left(\frac{d}{dt}\right)_i = \frac{\partial}{\partial t} + \mathbf{V}_i \cdot \nabla$$

$$\left(\frac{d}{dt}\right)_e = \frac{\partial}{\partial t} + \mathbf{V}_e \cdot \nabla$$

To further reduce the equations, we introduce the following assumptions:

1. the flute approximation, all the quantities of the plasma under consideration have no variations along the axial direction and  $V_{iz} = V_{ez} = 0$
2. the plasma is isothermal, i.e.  $\nabla T_i = \nabla T_e = 0$ ;
3. low  $\beta$  plasma, i.e. the thermal pressure of plasma is much less than the magnetic pressure. ( $\beta = \frac{4\pi(n_i T_i + n_e T_e)}{B^2} \ll 1$ );

4. the plasma is dense, i.e.  $\left(\frac{\omega_{pi}}{\omega_{ci}}\right)^2 \gg 1$ ; where  $\omega_{pi} = \left(\frac{4\pi n_i q_i^2}{m_i}\right)^{\frac{1}{2}}$  is ion plasma frequency;
5. the plasma is hydrogen,  $q_i = -q_e = e$ , where  $e$  is the electron charge. and due to  $m_e/m_i \ll 1$ , we neglect the inertia of the electron component.

Due to the assumptions we made above, the set of equations (II.1)-(II.10) can be greatly simplified. By assumption 1, the flute approximation, the problem becomes two-dimensional, all the fields only depend on the two coordinates  $x, y$  in an Cartesian coordinate system or  $r, \theta$  in a cylindrical coordinate system at the plane perpendicular to  $\mathbf{B}$ . By the assumption 2 (the isothermal approximation), equations (II.3) is eliminated as well as the free energy for driving an instability from the temperature gradient. By the low- $\beta$  approximation (the assumption 3), the thermal energy of the plasma is too low to disturb the magnetic field; from the Maxwell equations we can eliminate the temporal and spatial variation of the magnetic field. Then only the electrostatic perturbation needs to be considered and two equations for  $\nabla \cdot \mathbf{E}(r, \theta, t)$  and  $\nabla \times \mathbf{E}(r, \theta, t)$  remain and they can be reduced to a single Poisson equation:

$$\nabla^2 \phi = -4\pi \sum_j q_j n_j \quad (II.11),$$

by taking

$$\mathbf{E} = -\nabla \phi. \quad (II.12)$$

One more step farther, by using the dense plasma assumption (assumption 4) we can use the quasineutrality condition

$$n_i = n_e \quad (II.13)$$

to replace the Poisson equation (II.11) as a good approximation [Rosenbluth and Simon,1965; Mikhailovskii,1977]. And finally, by assumption 5, we can neglect the term with electron viscosity tensor  $\Pi_{(e)}$  and the term  $\mathbf{F}_e(\mathbf{x}, t)$  from the momentum balance equation for electron component. Up to now we have not specified the non-electromagnetic force  $\mathbf{F}_i(\mathbf{x}, t)$ ; we identify this force as a fictitious force to model the magnetic field line curvature or the high frequency pondermotive force with the form

$$\mathbf{F}_i(\mathbf{x}, t) = m_i \mathbf{g}(\mathbf{x}, t) = -m_i \nabla U(\mathbf{x}, t),$$

where in modeling curvature of magnetic field line,  $g \sim (T_i + T_e)/m_i R$ ,  $R = R(\mathbf{x}, t)$  is the curvature of magnetic field line. Then the momentum balance equations (II.2) can be written as

$$en_e \left( \mathbf{E} + \frac{\mathbf{V}_e \times \mathbf{B}}{c} \right) + \nabla p_e = 0 \quad (II.14)$$

$$m_i n_i \frac{d\mathbf{V}_i}{dt} = n_i e \left( \mathbf{E} + \frac{\mathbf{V}_i \times \mathbf{B}}{c} \right) - \nabla p_i - \nabla \cdot \Pi + m_i \mathbf{g} \quad (II.15)$$

where the ion gyroviscosity tensor  $\Pi$  is a  $2 \times 2$  matrix which can be written in the polar coordinates as

$$\Pi = \begin{pmatrix} \Pi_{rr} & \Pi_{r\theta} \\ \Pi_{\theta r} & \Pi_{\theta\theta} \end{pmatrix} \quad (II.16)$$

where

$$\Pi_{rr} = -\Pi_{\theta\theta} = \frac{n_i T_i}{2\omega_{ci}} \left( \frac{\partial V_\theta}{\partial r} - \frac{1}{r} \frac{\partial V_r}{\partial \theta} - \frac{V_\theta}{r} \right) \quad (II.17)$$

$$\Pi_{r\theta} = \Pi_{\theta r} = \frac{n_i T_i}{2\omega_{ci}} \left( \frac{\partial V_r}{\partial r} - \frac{1}{r} \frac{\partial V_\theta}{\partial \theta} - \frac{V_r}{r} \right) \quad (II.18)$$

After the simplifications, the problem becomes two dimensional and the number of independent equations describing the plasma is greatly reduced. There are two continuity equations, two momentum equations (4 scalar equations), two state equations, two constitutive relations (8 scalar relations), an equation defines electric field (2 scalar relations), and a quasineutrality condition. In total 19 scalar equations remain independent, which correspond to 19 unknown functions  $n_i(r, \theta, t)$ ,  $n_e(r, \theta, t)$ ,  $\mathbf{V}_i(r, \theta, t)$ ,  $\mathbf{V}_e(r, \theta, t)$ ,  $p_i(r, \theta, t)$ ,  $p_e(r, \theta, t)$ ,  $\Pi_i(r, \theta, t)$ ,  $\Pi_e(r, \theta, t)$ ,  $\mathbf{E}(r, \theta, t)$   $\phi(r, \theta, t)$ .

To set up the model equations suitable to the stability study, it is necessary to further reduce the number of equations and corresponding unknown functions. For this purpose we introduce the FLR (finite Larmor radius) ordering into the analysis. The FLR theory [Rosenbluth and Simon, 1965] assumes the



following ordering of frequency of the waves:

$$\omega = O(\epsilon^2 \omega_{ci}) \quad (II.19)$$

where  $\epsilon = \frac{\rho_i}{L} \ll 1$ ,  $\rho_i = \frac{v_{th,i}}{\omega_{ci}}$  is the ion cyclotron radius,  $v_i = \left(\frac{T_i}{m_i}\right)^{\frac{1}{2}}$  is ion thermal velocity and  $L$  is a typical gradient length of plasma.

Also the  $\mathbf{E} \times \mathbf{B}$  drift frequency  $\Omega = \frac{-cE}{rB}$  is assumed of the same order as the characteristic frequency  $\omega$ ,

$$\Omega = O(\epsilon^2 \omega_{ci}) \quad (II.20)$$

and then the  $\mathbf{E} \times \mathbf{B}$  drift velocity  $\mathbf{V} = c\mathbf{E} \times \mathbf{B}/B^2$  is of the order

$$V = O(\epsilon v_{th,i}) \quad (II.21)$$

According to equation (II.21) the electric force is of the same order as the pressure gradient  $enE \sim \nabla p$ .

Taking this ordering into account, we find that the ion momentum balance equation can be solved iteratively. Substituting Eqns. (II.3), (II.12) into Eqn.(II.15), taking  $\mathbf{z} \times$  (II.15) gives

$$\mathbf{V}_i = \frac{c}{B} \hat{\mathbf{z}} \times \nabla \phi + \frac{cT_i}{Ben_i} \mathbf{z} \times \nabla p_i + \frac{c}{Ben_i} \hat{\mathbf{z}} \times \nabla \cdot \Pi - \frac{1}{\omega_{ci}} \hat{\mathbf{z}} \times \mathbf{g} + \frac{1}{\omega_{ci}} \hat{\mathbf{z}} \times \frac{d\mathbf{V}_i}{dt} \quad (II.22)$$

for the ion fluid velocity field.

According to the FLR ordering we find that the first two terms of Eqn. (II.22) are of order  $\epsilon$  while other terms are two orders higher, of order  $\epsilon^3$ , so to the lowest order

$$\mathbf{V}_i^{(1)} = \frac{c}{B} \hat{\mathbf{z}} \times \nabla \phi + \frac{cT_i}{Ben_i} \hat{\mathbf{z}} \times \nabla n_i = \frac{cT_i}{Be} \hat{\mathbf{z}} \times \nabla \psi \quad (II.23)$$

where we define

$$\psi = \frac{e\phi}{T_i} + \ln n_i$$

For constant B it follows that  $\nabla \cdot \mathbf{V}_i^{(1)} = 0$ .

By iteration, the third order correction of the velocity is given by

$$\mathbf{V}_i^{(3)} = \frac{1}{\omega_{ci}} \hat{\mathbf{z}} \times \frac{d\mathbf{V}_i^{(1)}}{dt} + \frac{c}{Ben_i} \hat{\mathbf{z}} \times \nabla \cdot \mathbf{\Pi}^{(1)} - \frac{1}{\omega_{ci}} \hat{\mathbf{z}} \times \mathbf{g} \quad (II.24)$$

Repeating the same operation on electron fluid momentum equation (II.14) gives

$$\mathbf{V}_e^{(1)} = \frac{c}{B} \hat{\mathbf{z}} \times \nabla \phi - \frac{cT_e}{Ben_e} \hat{\mathbf{z}} \times \nabla n_e \quad (II.25)$$

since we neglect the inertia of the electron component, there is no need to look for higher order corrections to the electron fluid velocity.

Substitute Eqns. (II.23)-(II.25) into the continuity equations (II.1),(II.2), respectively, considering the quasineutrality condition (II.13), to the first order of  $\epsilon$ , for both electron and ion components we have

$$\frac{\partial n}{\partial t} + \mathbf{V}_{\mathbf{E} \times \mathbf{B}} \cdot \nabla n = 0 \quad (II.26)$$

where

$$n_i = n_e \equiv n(r, \theta, t)$$

and

$$\mathbf{V}_{\mathbf{E} \times \mathbf{B}} \equiv \frac{c}{B} \hat{\mathbf{z}} \times \nabla \phi \quad (II.27)$$

is the  $\mathbf{E} \times \mathbf{B}$  drift velocity of ion and electron. Subtracting the ion and electron continuity equations, the  $\mathbf{E} \times \mathbf{B}$  drift cancels for both components. Since the diamagnetic drift due to pressure gradient of isothermal fluids not participate in the continuity equation, the lowest order equation becomes

$$\nabla \cdot (n \mathbf{V}_i^{(3)}) = 0 \quad (II.28)$$

We take the equations (II.26) and (II.28) as our basic nonlinear equations, because after substituting (II.27) into (II.26), (II.23) into (II.24) explicitly, Eqns. (II.26) and (II.27) become two independent equations in respect to two unknown functions  $n(r, \theta, t)$  and  $\phi(r, \theta, t)$ .

Here for convenience we introduce the Poisson bracket  $[ , ]$  to represent the following linear differential operation on arbitrary function  $f(\mathbf{x}, t)$ ,  $g(\mathbf{x}, t)$

$$\begin{aligned} [f, g] &= (\hat{\mathbf{z}} \times \nabla f) \cdot \nabla g \\ &= \frac{\partial f}{\partial x} \frac{\partial g}{\partial y} - \frac{\partial f}{\partial y} \frac{\partial g}{\partial x} \\ &= \frac{1}{r} \left( \frac{\partial f}{\partial r} \frac{\partial g}{\partial \theta} - \frac{\partial f}{\partial \theta} \frac{\partial g}{\partial r} \right) \end{aligned}$$

By using the Poisson bracket notation we can write the equation (II.27) as

$$\frac{\partial n}{\partial t} + \frac{cT_i}{Be} [\tilde{\phi}, n] = 0 \quad (II.29)$$

where

$$\tilde{\phi} \equiv \frac{e\phi}{T_i}$$

To express (II.28) in terms of  $n$  and  $\phi$  we need to calculate the terms  $n\mathbf{z} \times \frac{d\mathbf{V}_i^{(1)}}{dt}$  and  $\mathbf{z} \times \nabla \cdot \mathbf{\Pi}^{(1)}$ .

### A. Calculation of $n\hat{\mathbf{z}} \times \frac{d\mathbf{V}_i^{(1)}}{dt}$

Substituting (II.23) into

$$n\hat{\mathbf{z}} \times \frac{d\mathbf{V}_i^{(1)}}{dt} = n\hat{\mathbf{z}} \times \left( \frac{\partial}{\partial t} + \mathbf{V}_i^{(1)} \cdot \nabla \right) \mathbf{V}_i^{(1)}$$

we have

$$\begin{aligned} n\hat{\mathbf{z}} \times \frac{d\mathbf{V}_i^{(1)}}{dt} &= -\frac{cT_i}{Be} n \left( \frac{\partial}{\partial t} \nabla \psi + \left( \frac{cT_i}{Be} (\hat{\mathbf{z}} \times \nabla \psi) \cdot \nabla \nabla \psi \right) \right) \\ &= -\frac{cT_i}{Be} n \left( \frac{\partial}{\partial t} \nabla \tilde{\phi} + \frac{\partial}{\partial t} \nabla \ln n \right) - \left( \frac{cT_i}{Be} \right)^2 n [\psi, \nabla \psi] \end{aligned} \quad (II.30)$$

Notice that

$$n \frac{\partial}{\partial t} \nabla \ln n = \frac{\partial}{\partial t} \nabla n - \frac{\nabla n}{n} \frac{\partial n}{\partial t}$$

and equation (II.29) gives

$$\frac{\partial n}{\partial t} = \frac{cT_i}{Be} [n, \tilde{\phi}]$$

then

$$n \frac{\partial}{\partial t} \nabla \ln n = \frac{cT_i}{Be} \left( [\nabla n, \tilde{\phi}] + [n, \tilde{\phi}] - \frac{\nabla n}{n} [n, \phi] \right) \quad (II.31)$$

Using the property of Poisson bracket

$$n [\tilde{\phi}, \nabla \ln n] = [\tilde{\phi}, \nabla n] - \frac{\nabla n}{n} [\tilde{\phi}, n] \quad (II.32)$$

Substitute (II.31), (II.32) into (II.30), after some cancelations finally we obtain

$$n \hat{\mathbf{z}} \times \frac{d\mathbf{V}_i^{(1)}}{dt} = -\frac{cT_i}{Be} n \frac{\partial}{\partial t} \nabla \phi - \left( \frac{cT_i}{Be} \right)^2 n \left( [\psi, \nabla \tilde{\phi}] + \frac{1}{n} [n, \nabla \psi] \right). \quad (II.33)$$

### B. Calculation of $\hat{\mathbf{z}} \times \nabla \cdot \mathbf{\Pi}^{(1)}$

Substitute (II.23) into the expression of gyroviscosity tensor (II.16), then the tensor can be expressed in terms of  $\psi$ .

$$\mathbf{\Pi}^{(1)} = -\frac{1}{2} m_i \left( \frac{cT_i}{Be} \right)^2 n \begin{pmatrix} \left( \frac{\partial^2}{\partial x^2} - \frac{\partial^2}{\partial y^2} \right) \psi & 2 \frac{\partial^2}{\partial x \partial y} \psi \\ 2 \frac{\partial^2}{\partial x \partial y} \psi & -\left( \frac{\partial^2}{\partial x^2} - \frac{\partial^2}{\partial y^2} \right) \psi \end{pmatrix} \quad (II.34)$$

Operating with  $\nabla \cdot$  on (II.34), after some algebra one finds

$$\nabla \cdot \mathbf{\Pi}^{(1)} = -m_i \left( \frac{cT_i}{Be} \right)^2 \left\{ \hat{\mathbf{z}} \times [n, \nabla \psi] + \frac{1}{2} \nabla (n \nabla^2 \psi) \right\} \quad (II.35)$$

Acting  $\hat{\mathbf{z}} \times$  on (II.35) gives

$$\hat{\mathbf{z}} \times \nabla \cdot \Pi^{(1)} = m_i \left( \frac{cT_i}{Be} \right)^2 \left\{ [n, \nabla\psi] - \frac{1}{2} \hat{\mathbf{z}} \times \nabla (n \nabla^2 \psi) \right\} \quad (II.36)$$

The third term in equation (II.28) comes from the fictitious gravity drift, after introducing an effective potential  $U(r, \theta, t)$  such that

$$\mathbf{g} = \nabla U$$

the divergence of this term can be written as

$$\nabla \cdot \left( \frac{1}{\omega_{ci}} n \hat{\mathbf{z}} \times \mathbf{g} \right) = - \frac{1}{\omega_{ci}} [U, n] \quad (II.37)$$

Substitute (II.33), (II.36), (II.37) into (II.28) and notice that

$$\nabla \cdot \{ \hat{\mathbf{z}} \times \nabla (n \nabla^2 \psi) \} = 0$$

and

$$[\ln n, \tilde{\phi}] = \frac{1}{n} [n, \tilde{\phi}]$$

then equation (II.28) is expressed in terms of  $n, \tilde{\phi}$  as

$$\frac{cT_i}{Be} \nabla \cdot \left( n \frac{\partial}{\partial t} \nabla \tilde{\phi} \right) + \frac{cT_i^2}{Be} \nabla \cdot \left\{ n [\tilde{\phi}, \nabla \tilde{\phi}] + [n, \nabla \tilde{\phi}] \right\} + [n, U] = 0 \quad (II.38)$$

From this derivation we have obtained the nonlinear model equations (II.29) and (II.38) which describe the flute dynamics of rotating plasma. Physically

they are the lowest order continuity equation for the ion and electron components of the plasma and the lowest order quasineutrality condition in the FLR ordering. The equation (II.29) shows that the change rate of the density of each component of the plasma fluid is caused by the  $\mathbf{E} \times \mathbf{B}$  convection while the equation (II.38) shows that the total current caused by all the drifts produced by the inertial force must be divergenceless to keep the plasma quasineutral. The meaning of each term in equation (II.38) is clear: the first term and the first Poisson bracket in the second term represent the charge separation caused by the ion polarization drift, the second Poisson bracket is the charge separation comes from FLR of the ions, and the third term is the charge separation due to the drift caused by magnetic field line curvature or RF pondermotive force. Previously Horton and Liu (1984) derived a similar set of nonlinear equations under an MHD ordering where they assume that the  $\mathbf{E} \times \mathbf{B}$  drift is dominant over the ion diamagnetic drift. In this ordering the ion FLR term, the second Poisson bracket of equation (II.38), is dropped.

The equations (II.29), (II.38) are written in the laboratory frame. When the plasma is rotating uniformly, we can write them in the rotating frame under the coordinate transformation

$$r_{lab.frame} \longrightarrow r_{rot.frame}$$

$$\theta_{lab.frame} \longrightarrow \theta_{rot.frame} + \Omega t_{rot.frame}$$

$$t_{lab.frame} \longrightarrow t_{rot.frame}$$

where

$$\Omega = \frac{c}{B} \hat{\mathbf{z}} \times \nabla \phi_o(r) = \text{constant}$$

$\phi_o(r)$  is the equilibrium electric potential in lab. frame.

After completing the transformation we obtain the following set of non-linear equations in the rotating frame:

$$\frac{\partial n}{\partial t} + [\tilde{\phi}, n] = 0 \quad (II.39)$$

$$\begin{aligned} \frac{cT_i}{Be} \nabla \cdot \left( n \frac{\partial}{\partial t} \nabla \tilde{\phi} \right) + \left( \frac{cT_i}{Be} \right)^2 \left\{ n [\tilde{\phi}, \nabla \tilde{\phi}] + [n, \nabla \tilde{\phi}] \right\} - 2\Omega \frac{cT_i}{Be} [n, \tilde{\phi}] \\ + \left[ n, U - \frac{r^2 \Omega^2}{2} \right] = 0 \end{aligned} \quad (II.40)$$

From equations (II.39),(II.40) we can see the characteristic terms in a rotating frame, the Coriolis drift term  $2\Omega \frac{cT_i}{Be} [n, \nabla \tilde{\phi}]$  and the centrifugal drift term which joins the gravity term as a centrifugal potential  $\frac{1}{2} r^2 \Omega^2$ . We have shown that the above explanation in fact can be justified by a more elementary derivation from the single particle picture of plasma [**Horton and Liu, (1984)**]. The equations (II.39) and (II.40) are more convenient to be linearized than the equations (II.29) and (II.38) when we treat the linear problem of uniformly rotating plasma because in the rotating frame equilibrium electrical field is eliminated by the transformation and the term proportional to  $\nabla \cdot \{n[\tilde{\phi}, \nabla \tilde{\phi}]\}$  is at least second



order in the perturbation; in equation (II.38) the corresponding term contains several terms linear in the perturbation and needs to be treated carefully.

In the following chapters of this thesis we will use the equations (II.29) and (II.38), or (II.39) and (II.40) as the basic nonlinear equations to treat the low frequency electrostatic instability of rotating plasma. To conclude this section we would like to point out that although the approximations introduced for derivation of the equations limit the validity of the equations only to the flute perturbations of low  $\beta$  collisionless dense plasma, these two mathematically relatively simple nonlinear equations still retain quite a few essential physical factors for the motion of the inhomogeneous, rotating plasma including the magnetic field line curvature or RF pondermotive force effects and the finite Larmor radius effect. Within the limit of the flute perturbation the equations can be used to treat the  $\mathbf{E} \times \mathbf{B}$  rotation driven electrostatic instabilities of inhomogeneous plasma with or without FLR effects. In addition to these, since we have not specified the equilibrium electric potential, our equations can be used to treat either uniformly or nonuniformly rotating plasma.

## II.2 The Conservation Laws

In the previous section we derived a pair of nonlinear equations under certain approximations; in this section we will derive the basic conservation laws of these equations. Here we suppose our system is a closed, that means the system we considered will not exchange mass with outside sources. We also suppose the plasma column is surrounded by a conducting wall on which the electric potential of plasma is zero.

### A. The conservation of the total mass and the total entropy

Since equation (II.29) is in fact a particular version of the continuity equation of ion and electron fluids under convection by  $\mathbf{E} \times \mathbf{B}$  and ion and electron diamagnetic drift motion respectively, obviously the basic physics law, the conservation of total mass expressed by this equation must obtain, i.e.

$$\frac{d}{dt} \int n(\mathbf{x}, t) d\mathbf{x} = 0 \quad (II.41)$$

Mathematically, (II.41) can be verified simply integrating the equation (II.29) over the whole volume (the whole cross sectional area in the two dimensional problem) filled by the plasma and using the integral property of the Poisson bracket

$$\int n[\phi, n] d\mathbf{x} = \int \phi[n, n] d\mathbf{x} = 0$$

Furthermore, since the fluids only experience the  $\mathbf{E} \times \mathbf{B}$  and the  $\nabla p$  drift (the diamagnetic drift) motions in a constant axial B field,  $\nabla \cdot \mathbf{V}_{i,e}^{(1)} = 0$ , the fluids

are incompressible. This means they are only mixed but not compressed in the motion. This fact implies that equation (II.29) will give a family of constants of motion, i.e. any physical quantity which only depends on  $n$  is conserved by the motion:

$$\frac{d}{dt} \int f(n(\mathbf{x}, t)) \mathbf{d}\mathbf{x} = 0 \quad (II.42)$$

Specifically, in the isothermal case the entropy  $S(n) = \sum_{j=i,e} n_j \ln(n_j^{-1} T_j^{\frac{3}{2}})$  [Braginskii, 1963] belongs to this family, so it is a constant of motion

$$\frac{d}{dt} \int S(n) \mathbf{d}\mathbf{x} = 0 \quad (II.43)$$

(II.42) and (II.43) can be easily proved by multiplying  $f(n)$  or  $S(n)$  by the equation (II.29) and integrating over the whole volume, remembering the property of Poisson bracket

$$\int f(n)[\phi, n] \mathbf{d}\mathbf{x} = \int \phi[n, f(n)] \mathbf{d}\mathbf{x} = 0.$$

### B. The conservation of total energy

We define the total energy of our system as the sum of two parts, the kinetic energy

$$\frac{1}{2} \sum_{j=i,e} m_j n_j(\mathbf{x}, t) V_{\mathbf{E} \times \mathbf{B}}^2$$

and the potential energy density

$$m_i n_i(\mathbf{x}, t) U(\mathbf{x}, t)$$

. Due to the smallness of  $\frac{m_e}{m_i}$  the electron's contribution to the kinetic energy can be neglected. Then the conservation law of the system can be expressed as

$$\frac{d}{dt} \int m_i n_i (V_{\mathbf{E} \times \mathbf{B}}^2 / 2 + U) \mathbf{d}\mathbf{x} = 0 \quad (II.44).$$

To prove that the equations (II.29) and (II.38) conserve energy, some algebra manipulations are necessary. Multiplying equation (II.38) by  $\tilde{\phi}$  and integrating over the whole region occupied by the plasma yields

$$\int \tilde{\phi} \left\{ \frac{cT_i}{Be} \nabla \cdot \left( n \frac{\partial}{\partial t} \nabla \tilde{\phi} \right) + \left( \frac{cT_i}{Be} \right)^2 \nabla \cdot \left( n [\tilde{\phi}, \nabla \tilde{\phi}] + \nabla \cdot [n, \nabla \tilde{\phi}] \right) + [n, U] \right\} \mathbf{d}\mathbf{x} = 0 \quad (II.45)$$

By using the integral properties of Poisson bracket and integrating by parts, one finds the terms in equation (II.45) as

$$\text{Term 1} = -\frac{1}{2} \frac{cT_i}{Be} \int n \frac{d}{dt} (\nabla \tilde{\phi})^2 \mathbf{d}\mathbf{x}$$

$$\text{Term 2} = -\frac{1}{2} \left( \frac{cT_i}{Be} \right)^2 \int (\nabla \phi)^2 [n, \tilde{\phi}] \mathbf{d}\mathbf{x}$$

$$\text{Term 3} = 0$$

$$\text{Term 4} = - \int U [n, \tilde{\phi}] \mathbf{d}\mathbf{x}$$

Substitute the equation (II.29)  $\frac{\partial n}{\partial t} = \frac{cT_i}{Be} [n, \tilde{\phi}]$  into term 2 and term 4 and finish the integrations, one obtains

$$\frac{d}{dt} \int n \left\{ \frac{1}{2} \left( \frac{cT_i}{Be} \right)^2 (\nabla \tilde{\phi})^2 + U \right\} \mathbf{d}\mathbf{x} = \int n \frac{\partial U}{\partial t} \mathbf{d}\mathbf{x}. \quad (II.46)$$

The meaning of (II.46) is the change of the total energy of the system comes from the time variation of the fictitious potential  $U$ .

Noticing that  $\frac{\partial U}{\partial t} = 0$  if we supposed the system considered can not exchange energy with outside. Then the right hand side of Eq.(II.46)=0, it means that

$$\text{The Total Energy} = \int m_i n_i \left( \frac{1}{2} V_{\mathbf{E} \times \mathbf{B}}^2 + U \right) d\mathbf{x} = \text{constant.} \quad (\text{II.47})$$

### C. Conservation of the total angular momentum

Multiplying equation (I.38) by  $\frac{1}{2} r^2$  and integrating over the entire volume of the plasma one can obtain the angular momentum conservation law of the system. The details of the proof follow.

$$\int \frac{1}{2} r^2 \left\{ \frac{cT_i}{Be} \nabla \cdot \left\{ n \frac{\partial}{\partial t} \nabla \tilde{\phi} + \left( \frac{cT_i}{Be} \right)^2 (n [\tilde{\phi}, \nabla \tilde{\phi}] + [n, \nabla \phi]) \right\} + \frac{1}{2} r^2 [n, U] \right\} d\mathbf{x} = 0 \quad (\text{II.48})$$

integrating by parts

$$\begin{aligned} \frac{cT_i}{Be} \int \frac{1}{2} r^2 \nabla \cdot \left( n \frac{\partial}{\partial t} \nabla \tilde{\phi} \right) d\mathbf{x} &= - \frac{cT_i}{Be} \int r n \frac{\partial}{\partial t} \frac{\partial \tilde{\phi}}{\partial r} d\mathbf{x} \\ &= - \int n \frac{\partial}{\partial t} r V_\theta d\mathbf{x} \end{aligned} \quad (\text{II.49})$$

where  $V_\theta = \frac{cT_i}{Be} \frac{\partial \tilde{\phi}}{\partial r}$  is the azimuthal component of  $\mathbf{V}_{\mathbf{E} \times \mathbf{B}}$ .

$$\begin{aligned} \int \frac{1}{2} r^2 \nabla \cdot (n[\tilde{\phi}, \nabla \tilde{\phi}]) \mathbf{d}\mathbf{x} &= - \int nr [\tilde{\phi}, \nabla \tilde{\phi}]_r \mathbf{d}\mathbf{x} \\ &= - \int nr \left( \frac{\partial \tilde{\phi}}{\partial r} \frac{\partial^2 \tilde{\phi}}{\partial \theta \partial r} - \frac{\partial \tilde{\phi}}{\partial \theta} \frac{\partial^2 \tilde{\phi}}{\partial r^2} - \frac{1}{r} \frac{\partial \tilde{\phi}}{\partial r} \frac{\partial \tilde{\phi}}{\partial \theta} \right) d\theta dr \end{aligned} \quad (II.50)$$

where  $[\tilde{\phi}, \nabla \tilde{\phi}]_r$  denotes the r component of  $[\tilde{\phi}, \nabla \tilde{\phi}]$ . Integrate the first two terms of (II.50) by parts

$$\begin{aligned} - \int nr \frac{\partial \tilde{\phi}}{\partial r} \frac{\partial^2 \tilde{\phi}}{\partial \theta \partial r} dr d\theta &= \frac{1}{2} \int \frac{\partial n}{\partial \theta} \left( \frac{\partial \tilde{\phi}}{\partial r} \right)^2 \mathbf{d}\mathbf{x} \\ \int nr \frac{\partial \tilde{\phi}}{\partial \theta} \frac{\partial^2 \tilde{\phi}}{\partial r^2} dr d\theta &= \frac{1}{2} \int \frac{\partial n}{\partial \theta} \left( \frac{\partial \tilde{\phi}}{\partial r} \right)^2 \mathbf{d}\mathbf{x} - \int \frac{n}{r} \frac{\partial \tilde{\phi}}{\partial \theta} \frac{\partial \tilde{\phi}}{\partial r} \mathbf{d}\mathbf{x} - \int \frac{\partial n}{\partial r} \frac{\partial \tilde{\phi}}{\partial \theta} \frac{\partial \tilde{\phi}}{\partial r} \mathbf{d}\mathbf{x} \end{aligned}$$

substituting these two terms back into (II.50) and use equation (II.29), one gets

$$\begin{aligned} \left( \frac{cT_i}{Be} \right)^2 (II.50) &= \left( \frac{cT_i}{Be} \right)^2 \int \left( \frac{\partial n}{\partial \theta} \frac{\partial \tilde{\phi}}{\partial r} - \frac{\partial n}{\partial r} \frac{\partial \tilde{\phi}}{\partial \theta} \right) \frac{\partial \tilde{\phi}}{\partial r} \mathbf{d}\mathbf{x} \\ &= - \left( \frac{cT_i}{Be} \right)^2 \int r [n, \tilde{\phi}] \frac{\partial \tilde{\phi}}{r} \mathbf{d}\mathbf{x} \\ &= - \int \frac{\partial n}{\partial t} r V_\theta \mathbf{d}\mathbf{x} \end{aligned} \quad (II.51)$$

other terms in equation (II.48) are integrated and give

$$\int \frac{1}{2} r^2 \nabla \cdot [n, \nabla \tilde{\phi}] = 0 \quad (II.52)$$

and

$$\int \frac{1}{2} [n, U] \mathbf{d}\mathbf{x} = \int nr F_\theta \mathbf{d}\mathbf{x} \quad (II.53)$$

where  $F_\theta = -\frac{\partial U}{\partial \theta}$ .

Finally, substituting the relations (II.49), (II.51)-(II.53) into equation (II.48) one obtains

$$\frac{dL_z}{dt} = \frac{d}{dt} \int nrV_\theta dx = \int nrF_\theta dx \quad (II.54)$$

Equation (II.54) states that the total angular momentum of the system is driven by the external torque. The change rate of the angular momentum of the system equals the total torque of the external force. For the axisymmetric system like the central cell of the Tandem mirror devices,  $F_\theta = 0$ , there is no torque acting on the system the total angular momentum is conserved

$$\begin{aligned} \text{The Total Angular Momentum } L_z &= \int nrV_\theta dx \\ &= \int nr^2\Omega(x, t) dx = \text{constant} \end{aligned} \quad (II.55)$$

## Chapter III

### LINEAR STABILITY ANALYSIS

#### Introduction

Based on the nonlinear equations derived in chapter II, we study the linear instability of rotating plasma in this chapter. In section III.1 we derive the radial eigenequation of the normal mode by linearizing equations (II.29) and (II.38). The radial eigenvalue problem is presented in three different forms. The first form is written in terms of perturbed radial potential  $\delta\phi_m(r)$ , the second one in terms of radial Lagrangian displacement  $\xi_m(r)$  and the third one is written in a matrix form. Each of these three forms has own advantages. The first form has the virtue of transparency of physical meaning for each term in it and is convenient for treatment of the uniformly rotation case. The second form which is often referred to in publications has the advantage of compactness of the form and is conveniently used to discuss the general property of stability of rotating plasma. The last one is an appropriate form to be used to solve the problem numerically; it can give the radial structure of density and potential perturbations of all radial normal modes for given  $m$  together with complex frequency of the mode by one run.

In section III.2 we discuss the flute instability of rotating plasma by the



method of energy integration and give some general conclusions about the rotation driven instability. A new sufficient condition for stability is derived.

In sections III.3 and section III.4 we treat two typical cases of rotational instability of plasma by solving the eigenvalue problems analytically in order to reveal the basic features of the Rayleigh-Taylor type and Kelvin-Helmholtz type instability of rotating plasma. In section III.3, we choose a diffusive equilibrium density profile (Gaussian density profile) and a quadratic equilibrium electrical potential profile which gives a uniform  $\mathbf{E} \times \mathbf{B}$  rotation of plasma to model the stationary equilibrium state of plasma. The instability driven by plasma rotation in this case is of the Rayleigh-Taylor type. In section III.4 we choose the model equilibrium profiles of density and electrical potential which are favored to drive the Kelvin-Helmholtz type instability, three analytically solvable model profiles are discussed. In both uniform and nonuniform rotation cases the finite boundary effect is considered.

To avoid putting the lengthy derivations into the main text, the mathematical details of the equation derivations are put into three appendices at the end of this chapter.

### III.1 The Linearized Stability Equations

#### A. The equilibrium state and the linearized equations of perturbations

Denoting the equilibrium quantities of the plasma density  $n$  and the electrical potential  $\phi$  by subscript "o", since they are the quantities in equilibrium

$$\begin{aligned}\frac{\partial n_o}{\partial t} &= 0, \\ \frac{\partial \phi_o}{\partial t} &= 0.\end{aligned}$$

In equilibrium state, the equations (II.29) and (II.38) become

$$[\phi_o, n_o] = 0 \quad (III.1)$$

and

$$\nabla \cdot \left\{ \left( \frac{c}{B} \right)^2 n_o [\phi_o, \nabla \phi_o] + \frac{cT_i}{Bm_i \omega_{ci}} [n_o, \nabla \phi_o] \right\} + [n_o, U] = 0. \quad (III.2)$$

From the property of the Poisson bracket we can easily write down the solutions of (III.1) and (III.2) in the cylindrical coordinates as

$$\begin{aligned}\phi_o &= \phi_o(r) \\ n_o &= n_o(r)\end{aligned} \quad (III.3)$$

provided  $U = U(r)$ .

Suppose there are small time dependent perturbations of the density and the electrical potential  $\delta n(r, \theta, t)$ ,  $\delta \phi(r, \theta, t)$  around the equilibrium state:

$$\begin{aligned}\phi(r, \theta, t) &= \phi_o(r) + \delta \phi(r, \theta, t) \\ n(r, \theta, t) &= n_o(r) + \delta n(r, \theta, t)\end{aligned} \quad (III.4)$$

Substituting (III.4) into equations (II.29) and (II.38), after neglecting higher order terms one obtains the linearized equations of (II.29) and (II.38):

$$\frac{\partial \delta n}{\partial t} + \frac{c}{B} \{[\delta \phi, n_o] + [\phi_o, \delta n]\} = 0 \quad (III.5)$$

and

$$\begin{aligned} \nabla \cdot \left\{ \frac{c}{B} \left( n_o \frac{\partial}{\partial t} \nabla \delta \phi + \delta n \frac{\partial}{\partial t} \nabla \phi_o \right) + \left( \frac{c}{B} \right)^2 \left( \delta n [\phi_o, \nabla \phi_o] + n_o [\delta \phi, \nabla \phi_o] + n_o [\phi_o, \nabla \delta \phi] \right) \right. \\ \left. + \frac{c T_i}{B m_i \omega_{ci}} \left( [\delta n, \nabla \phi_o] + [n_o, \nabla \delta \phi] \right) \right\} + [\delta n, U(r)] = 0 \quad (III.6) \end{aligned}$$

## B. The linearized equations of normal mode

Considering the axial symmetry of equilibrium state (III.3), we can expand the perturbations  $\delta n$  and  $\delta \phi$  to the following Fourier series:

$$\delta n(r, \theta, t) = \sum_{m=0}^{\infty} \{ \delta n_m(r) e^{i(m\theta - \omega t)} + \text{complex conjugates} \} \quad (III.7)$$

$$\delta \phi(r, \theta, t) = \sum_{m=0}^{\infty} \{ \delta \phi_m(r) e^{i(m\theta - \omega t)} + \text{complex conjugates} \} \quad (III.8)$$

Substituting (III.7) and (III.8) into the linearized equations of the perturbations (III.5) and (III.6) and going through lengthy but straightforward algebra [ see appendices A-C], one obtains the following three forms of the equations for normal mode  $m$ .

Form 1:

$$\begin{aligned}
& \nabla_{\perp} \cdot [n_o(\tilde{\omega} - \omega_{*i})\nabla_{\perp}\delta\phi_m] + m\frac{d\Omega}{dr}\frac{d}{dr}[n_o(1 - \frac{\omega_{*i}}{\tilde{\omega}})\delta\phi] \\
& + \{[2m\Omega + \frac{m^2(\Omega^2 + g/r)}{\tilde{\omega}} - \frac{m^2cT_i}{\tilde{\omega}Ber}\frac{d}{dr}(r^2\frac{d\Omega}{dr})]\frac{1}{r}\frac{dn_o}{dr} \\
& + \frac{mn_o}{r}\frac{d}{dr}(\frac{1}{r}\frac{d}{dr}(r^2\Omega)) + \frac{1}{r}\frac{d}{dr}(n_o\omega_{*i})\}\delta\phi_m = 0 \tag{III.9}
\end{aligned}$$

where

$$\begin{aligned}
\tilde{\omega} &= \omega - m\Omega(r) \\
\Omega(r) &= \frac{c}{B}\frac{1}{r}\frac{d\phi_o}{dr} \\
g(r) &= -\frac{dU(r)}{dr} \\
\omega_{*i} &= \frac{mT_i}{m_i\omega_{ci}}\frac{1}{r}\frac{d\ln n_o}{dr}
\end{aligned}$$

Form 2:

$$\frac{d}{dr}(T\frac{d\xi_m}{dr}) + \left[\frac{1-m^2}{r^2}T + (m^2rg + r^2\omega^2)\frac{dn_o}{dr}\right]\xi_m = 0 \tag{III.10}$$

where

$$\begin{aligned}
\xi_m &= \frac{m}{r\tilde{\omega}}\delta\phi_m(r) \\
T &= \tilde{\omega}n_o(r)r^3(1 - \frac{\omega_{*i}}{\tilde{\omega}})
\end{aligned}$$

Form 3:

$$\mathbf{A} \begin{pmatrix} \delta \tilde{n}_m(x) \\ \delta \tilde{\phi}_m(x) \end{pmatrix} = \omega \mathbf{B} \begin{pmatrix} \delta \tilde{n}_m(x) \\ \delta \tilde{\phi}_m(x) \end{pmatrix} \quad (III.11)$$

where

$$x = \left(\frac{r}{a}\right)^2, \delta \tilde{n}_m = \frac{\delta n_m}{n_o}, \delta \tilde{\phi}_m = \frac{e \delta \phi_m}{T_e}$$

$\mathbf{A}$ ,  $\mathbf{B}$  are 2 by 2 matrices of differential operators

$$\mathbf{A} = \begin{pmatrix} A_{11} & A_{12} \\ A_{21} & A_{22} \end{pmatrix}$$

$$A_{11} = m \hat{\Omega}(x)$$

$$A_{12} = m \omega_{*e}(x)$$

$$A_{21} = m \left\{ -\frac{T_i}{T_e} x \frac{d\hat{\Omega}}{dx} \frac{d}{dx} + \frac{1}{4} (\hat{\Omega}^2 + x^{-\frac{1}{2}} g(x)) - \frac{T_i}{T_e} \left[ x^{-\frac{1}{2}} \frac{d}{dx} \left( x^{\frac{3}{2}} \frac{d\hat{\Omega}}{dx} \right) + x \frac{d\hat{\Omega}}{dx} \frac{d \ln n_o}{dx} \right] \right\}$$

$$A_{22} = m \left\{ x \left( \hat{\Omega} + 2 \frac{T_i}{T_e} \frac{d \ln n_o}{dx} \right) \frac{d^2}{dx^2} + \left[ \frac{\hat{\Omega}}{n_o} \frac{d}{dx} (x n_o) + \frac{2T_i}{T_e n_o} \frac{d}{dx} \left( x \frac{dn_o}{dx} \right) \right] \frac{d}{dx} - \frac{1}{x} \frac{d}{dx} \left( x^2 \frac{d\hat{\Omega}}{dx} \right) - \frac{d \ln n_o}{dx} \frac{d}{dx} (x \hat{\Omega}) - \frac{m^2 \hat{\Omega}}{4x} - \frac{T_i}{T_e n_o} \left( \frac{d^2 n_o}{dx^2} + \frac{m^2}{2x} \frac{dn_o}{dx} \right) \right\}$$

$$\mathbf{B} = \begin{pmatrix} B_{11} & B_{12} \\ B_{21} & B_{22} \end{pmatrix}$$

$$B_{11} = 1$$

$$B_{12} = 0$$

$$B_{21} = 0$$

$$B_{22} = x \frac{d^2}{dx^2} + \frac{1}{n_o} \frac{d}{dx} (x n_o) \frac{d}{dx} - \frac{m^2}{4x}$$

### C. The boundary conditions

To analyze the linear stability problem we must impose the appropriate boundary conditions on the second order differential equations derived in previous subsection to form the well-posed eigenvalue problems. Here we give the boundary conditions from the following physical considerations. On the axis of plasma column we naturally require the perturbation to be finite. At the outer edge of the plasma the boundary conditions may be imposed differently according to the different physical situations, for example, the plasma may be surrounded by neutral gases, vacuum magnetic field or a solid limiter. For simplicity of treatment we limit our discussion to the case of conducting wall boundary, which models the conducting limiter. Now we are in the position to write out the boundary conditions for each form of the differential equation of normal mode.

For the first form, the equation (III.9), the boundary conditions for the potential perturbation function  $\delta\phi_m(r)$  are

$$\begin{aligned} \delta\phi_m(r)|_{r=0} &= \text{Finite} \\ \delta\phi_m(r)|_{r=b} &= 0 \end{aligned} \tag{III.12}$$

where  $b$  is the position of the conducting wall.

For the second form, the equation (III.9), the boundary conditions for the radial displacement function  $\xi_m(r)$  are

$$\begin{aligned}\xi_m(r)|_{r=0} &= \textit{Finite} \\ \xi_m(r)|_{r=b} &= 0.\end{aligned}\tag{III.13}$$

For the third form, the equation (III.11), the boundary conditions for the normalized density and potential perturbations  $\delta\tilde{n}_m(r)$ ,  $\delta\tilde{\phi}_m(r)$  are

$$\begin{aligned}\delta\tilde{n}_m(x), \delta\tilde{\phi}_m(x)|_{x=0} &= \textit{Finite} \\ \delta\tilde{n}_m(x), \delta\tilde{\phi}_m(x)|_{x=\frac{b^2}{a^2}} &= 0\end{aligned}\tag{III.14}$$

After adding corresponding boundary conditions to the three forms of the differential equations we obtain three forms of the eigenvalue problem for the radial perturbation functions of the normal mode. By solving these problems we can analyze the linear instability of the rotating plasma.

Before going to the analysis of stability it is worthwhile to add a few remarks on these three forms of eigenvalue problems.

- (1) In the form 1 of the eigenvalue problem, equation (III.9) and the boundary condition (III.12), the unknown function is the radial perturbation function  $\delta\phi_m(r)$ . The equation looks lengthy, but the physical meaning of each term in it is quite clear. As we pointed out in the previous chapter, each term in the equation (III.9) represents the charge separation caused by corresponding drift motion: the term 1 is given by the usual

polarization drift convection modified by the FLR effect; the terms 3 and 4 are given by the Coriolis, the centrifugal ( proportional to  $\Omega^2$  ) and the gravity drifts; the terms 2,5 and 6 are caused by the shear of rotation; and the last term, the term 7 is purely due to the FLR effect. When the rotation is uniform, i.e.  $\Omega = constant$ , the equation (III.9) takes a simpler form because the three terms related to the shear of rotation are dropped. If we consider a cold ion system, it means that compared with the fast rotation of the plasma the finite ion temperature effect can be neglected, and suppose the rotation is uniform the equation (III.9) take its simplest form as

$$\frac{d}{dr} \left( r n_o \frac{d\delta\phi_m}{dr} \right) - \frac{m^2 n_o}{r} \delta\phi_m + \left[ \frac{2m\Omega}{\tilde{\omega}} + \frac{m^2(\Omega^2 + g/r)}{\tilde{\omega}^2} \right] \frac{dn_o}{dr} \delta\phi_m = 0 \quad (III.15)$$

which contains only the convection, the Coriolis, the centrifugal and the gravity drift terms. This equation describes the fast rotating confinement devices such as the SVIPP device, where the ion temperature can be neglected compared with the fast rotation speed. This equation was derived previously by a simpler way [Horton and Liu,1984].

- (2) The equation (III.10) has the virtue of compactness despite the fact that the physical meaning of each term in it is not as clear as the equation (III.9). This linearized equation was first derived by Rosenbluth and Si-



mon [1965] from solving the Vlasov equations by impose a FLR ordering and it has been cited in the plasma literature as the Rosenbluth-Simon equation. We have rederived it from the set of nonlinear equations based on two fluids model of plasma; this fact may partly justify our formalism. It is easy to see that the equation (III.10) is not a self-adjointed equation respect to the eigen frequency  $\omega$ . So there is not a very useful variational principle can be formulated for this equation. But this form of the equation is very convenient to analyze the general property of the stability of the system. We will give a general discussion of rotational instability by using the energy integral of this equation in the next section.

- (3) The equation (III.11) is of matrix form. This form is convenient for the study of the eigenvalue spectrum of the problem with arbitrary equilibrium density and potential profiles by numerical method using linear matrix algebra. As an testing example, we numerically solved the equation (III.11) with the uniform rotation and the Gaussian density profile without FLR effect and the gravity. In Fig.3.1 we give a picture of the eigenfrequency of the numerical calculation and find it is in good agreement with the analytic results of the same problem which we will give in section III.3. Since the main emphasis of this thesis is in the analytically solvable case we will not use this form in the further analysis. But as the problem needs to be analyzed numerically, this form of eigenvalue

problem should be very useful.

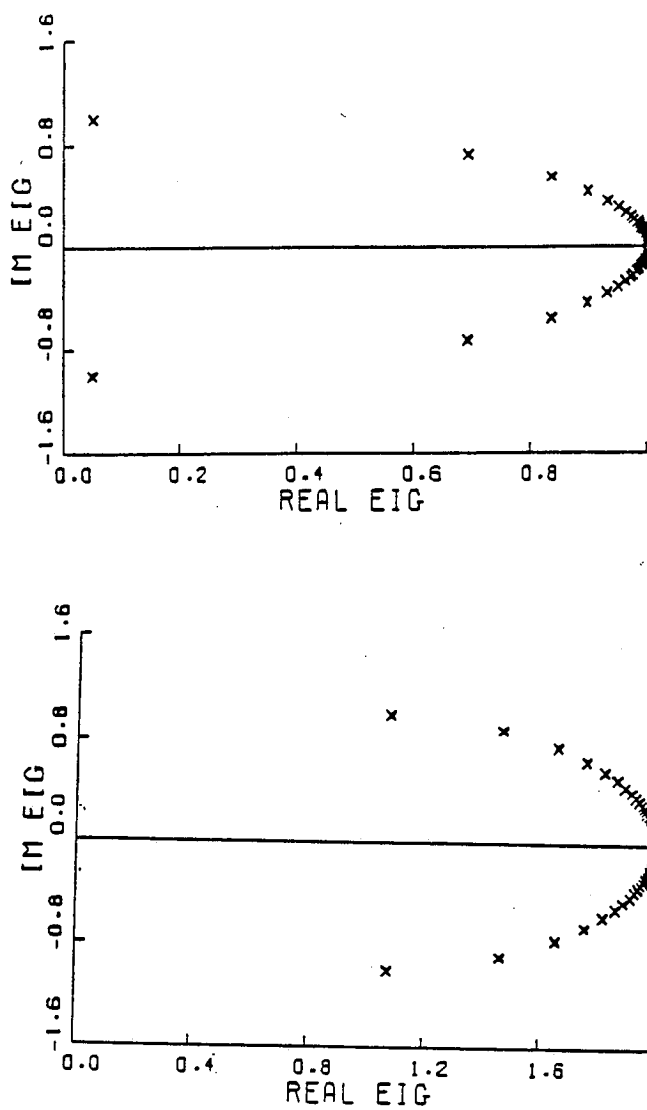


**Fig.3.1** The eigenfrequency calculated numerically from solving the eigenequation (III.11) for a uniform rotation and Gaussian density profile with a linear gravity  $g = g_0 r/a$ , and  $g_0/a = \Omega^2$ , the boundary set to infinity. The frequency is normalized to the rotation frequency  $\Omega$ . (a)  $m=1$ , (b)  $m=2$ . each cross corresponds to a mode  $(m,n)$ . Notice good agreement with formula (III.39) and (III.40).

### III.2 The General Stability Properties

In this section we analyze the general stability properties of the rotating plasma column by using the equation (III.9) and the boundary conditions (III.12). By the term "general" we mean that in the analysis we will not specify the equilibrium density profile and the rotation frequency  $\Omega$  particularly, so the conclusions drawn from this analysis should be generally applied to the different cases with specific equilibrium state. We notice that a analysis similar to the analysis for rotating plasma column also can be carried out for the plasma rotating inside an annular between two concentric conducting cylindrical walls with the radius  $r_1$ ,  $r_2$  respectively, a configuration very much like the Couette flow experiment in hydrodynamics, if the corresponding boundary conditions on inner and outer wall are imposed. The rotating plasma in SVIPP device corresponds to this configuration. Since we are interested in the rotating plasma in the central cell of Tandem Mirror devices here we only give the analysis of the plasma column.

Multiplying  $\xi_m^*(r)$ , the complex conjugate of function  $\xi_m(r)$ , to equation (III.10) and integrating over the region  $r = 0$  to  $r = b$ , taking the boundary conditions (III.13) into account, we obtain the quadratic form

$$A\omega^2 + B\omega + C = 0 \tag{III.16}$$

where

$$A = (m^2 - 1) \int_0^b r n_o |\xi_m|^2 dr + \int_0^b n_o r^3 \left| \frac{d\xi_m}{dr} \right|^2 dr - \int_0^b r^2 \frac{dn_o}{dr} |\xi_m|^2 dr \quad (III.17)$$

$$B = -2m \left\{ \int_0^b r^3 n_o \left( \Omega + \frac{\omega_{*i}}{2m} \right) \left| \frac{d\xi_m}{dr} \right|^2 dr + (m^2 - 1) \int_0^b r n_o \left( \Omega + \frac{\omega_{*i}}{2m} \right) |\xi_m|^2 dr \right\} \quad (III.18)$$

$$C = m^2 \left\{ \int_0^b n_o r^3 \Omega \left( \Omega + \frac{\omega_{*i}}{m} \right) \left| \frac{d\xi}{dr} \right|^2 dr + (m^2 - 1) \int_0^b n_o r \Omega \left( \Omega + \frac{\omega_{*i}}{m} \right) |\xi_m|^2 dr - \int_0^b r g \frac{dn_o}{dr} |\xi|^2 dr \right\} \quad (III.19)$$

The equation (III.16) is a constraint that every integrable solution of equation (III.10) which satisfies the boundary conditions (III.13) must satisfy. Solving the equation (III.16) respect to  $\omega$  we obtain

$$\omega = \frac{1}{2A} (-B \pm (B^2 - 4AC)^{\frac{1}{2}}) \quad (III.20)$$

From equation (III.20) we have the sufficient condition of stability for the system

$$\Delta = B^2 - 4AC \geq 0 \quad (III.21)$$

Since the coefficients of quadratic equation (III.16) A,B,C are integrals of a complicated combination of the equilibrium quantities  $n_o(r), \phi_o(r)$ , the unknown radial perturbation function  $\xi_m(r)$  and their derivatives, this sufficient condition is not

very convenient to use in the applications. But we still can draw several useful conclusions about the stability of the system by close observation of this condition. It is interesting to note that for the density profile with  $\frac{dn_o}{dr} \leq 0$ ,  $A > 0$  holds. This property of the integral will help us to analyze the condition (III.21).

- (1) The  $m=0$  mode is marginally stable because for  $m=0$  the two coefficients  $B$  and  $C = 0$ .
- (2) For the pure rotation driven magnetically confined plasma system, when the outer boundary is in the finite distance and the FLR effect can be neglected, the linear modes with  $m = 1$  are generally unstable.

The proof of this statement is as follows. since we neglect the curvature effect and FLR effect  $g = 0, \omega_{*i} = 0$ , under these conditions

$$\begin{aligned}
 A &= \int_0^b \left\{ n_o r^3 \left| \frac{d\xi_1}{dr} \right|^2 - r^2 \frac{dn_o}{dr} \left| \xi_1 \right|^2 \right\} dr \\
 B &= -2 \int_0^b r^3 n_o \Omega \left| \frac{d\xi_1}{dr} \right|^2 dr \\
 C &= \int_0^b r^3 n_o \Omega^2 \left| \frac{d\xi_1}{dr} \right|^2 dr
 \end{aligned} \tag{III.22}$$

From (III.22) we have

$$\begin{aligned}
 \Delta &= 4 \left\{ \left( \int_0^b r^3 n_o \Omega \left| \frac{d\xi_1}{dr} \right|^2 dr \right)^2 - \int_0^b r^3 n_o \Omega^2 \left| \frac{d\xi_1}{dr} \right|^2 dr \int_0^b (n_o r^3 \left| \frac{d\xi_1}{dr} \right|^2 dr \right. \right. \\
 &\quad \left. \left. + \int_0^b r^3 n_o \left| \frac{d\xi_1}{dr} \right|^2 dr \int_0^b r^2 \frac{dn_o}{dr} \left| \xi_1 \right|^2 dr \right\} \tag{III.23}
 \end{aligned}$$

By using the schwartz inequality

$$\left(\int_a^b f(x)g(x)dx\right)^2 - \int_a^b f^2(x)dx \int_a^b g^2(x)dx \leq 0 \quad (III.24)$$

and the fact that for magnetically confined plasma  $\frac{dn_o}{dr} \leq 0$  we can immediately see that

$$\Delta \leq 0$$

for both uniform and nonuniform rotation cases provided that  $\frac{d\xi_1}{dr}$  not disappear everywhere in the plasma region. In the uniform rotation case it is the last term of (III.23) destabilizes the system where as in the shear rotation case both destabilizing terms contribute.

It is noteworthy to mention that several authors [Freidberg and Pearlstein, 1978] claimed that  $m=1$  flute mode for rotating plasma is marginal stable based on the argument that this mode is so-called rigid mode, i.e.  $\left|\frac{d\xi_1}{dr}\right| = 0$  everywhere in the plasma region. We think this statement is dubious. Our argument is that although in the central region of the plasma column the  $m=1$  mode might be rigid, due to the boundary condition (III.13) at  $r=b$ , the perturbed displacement function  $\xi_1(r)$  must start to decrease from some place inside plasma in order to get its zero value at  $r=b$ . This means that the existence of a conducting wall requires the  $m=1$  mode being nonrigid. The closer the wall locates the farther the  $m=1$  mode deviates from the rigid mode. Intuitively, the relation between the "rigidness" of the  $m=1$  mode and the location of the conducting wall can be

explained as follows. If the conducting wall is located very far from the plasma center, due to the decreasing density profile for confined plasma, the region where  $\left| \frac{d\xi_1(r)}{dr} \right|$  is noticeable has negligible plasma density, the integral of (III.24) which contributes negative value of  $\Delta$  can be neglected and  $m=1$  become marginal stable. In this situation the rigid mode argument makes sense. But when the conducting wall locates quite close to the center of the plasma column, the region where the noticeable  $\left| \frac{d\xi_1(r)}{dr} \right|$  may penetrate into the main body of plasma where the plasma density still is high enough to contribute a considerable negative  $\Delta$ , in this case the rigid mode argument is unreasonable. We feel that this understanding about the rigid mode explains the discrepancy between the marginal stability of the  $m=1$  rigid mode expectation and the considerable growth rate of the same mode calculated numerically by some authors [Chen, 1967]. In the next section we will discuss this wall effect by solving the eigenvalue equation for a specific equilibrium profile, which quantitatively supports our argument.

- (3) **For the pure rotation driven magnetically confined plasma system with the FLR effect, if**

$$\left| \frac{\omega_{*i}(r)}{m} \right| \geq \Omega(r) \geq 0 \quad (III.25)$$

everywhere inside the plasma region, the system is stable.

The proof of this statement is straightforward. since for magnetically confined plasma  $\frac{dn_o}{dr} \leq 0$ , from equation (III.17)  $A > 0$ . Substituting condition

(III.25) into equation (III.19) gives  $C < 0$ . Thus we have  $\Delta > 0$ , the system is stable. Condition (III.25) was also derived previously by Freidberg and Pearlstein [ 1978 ] for uniform rotation case of the plasma with finite  $\beta$ . But in our low  $\beta$  plasma case the condition (III.25) is not limited to the uniform rotation; it also valid for rotation with shear. In certain sense this condition generalizes the one given by Freidberg and Pearlstein.

- (4) **For rotating plasma without the curvature effect, if the equilibrium density profile can be adjusted to  $\frac{dn_o}{dr} \geq 0$  everywhere in the plasma then the system is stable.**

The proof of this statement is straightforward, set  $g=0$  in (III.19) and substitute (III.17)-(III.19) into (III.20), many terms canceled and  $\Delta \geq 0$  is obtained which proves this statement.

As we mentioned at the beginning of this subsection the conclusions we obtained from the energy integral are quite general, they do not depend on specific equilibrium state of the rotating plasma. But on the other hand they are qualitative statements about the stability property of the system, they do not provide quantitative information such as the mode structure, the oscillation frequency and the linear growth rate of the unstable modes. To get this information we need to proceed to solve the eigenvalue problem given in section III.1. This is the task of the next two sections.



### III.3 An Analytic Solution of The Eigenvalue Problem For The Uniform Rotating Plasma

In this section we analyze the linear instability of an uniformly rotating, inhomogeneous plasma with a Gaussian density profile. To model the magnetic field line curvature effect we also suppose a gravity which is linear function of  $r$ . To study the wall effect on stability of the system, we assume there is a conducting wall located at finite distance from the center of the plasma. The nice point of this model case is that we can get the analytical solution of the eigenvalue problem (III.9) with the boundary condition (III.12). Through analyzing this model case of rotating plasma, we can get all the quantitative information about the stability of the rotating column and clearly reveal the role played by different physical effects on the stability of the system. Since we supposed the rotation of the plasma is uniform, the instability is of Rayleigh-Taylor type. Accordingly the solution of this model will show the basic feature of the instability of this type. Quite interestingly, since we take the effective gravity into account, the dispersion relation provides a possibility to discuss the difference between the pure gravity driven instability and the pure rotation driven instability of the plasma column in a unified formalism. We should mention that the similar model has been analyzed by various people previously. Rosenbluth et al [1962], Berge [1966] has discussed the pure rotation driven case with infinite boundary, Rognlien [1973] studied the finite wall effect

without taking account of the field line curvature term. Here we show that when we take the corresponding limit, all the previous results are recovered.

We take the following equilibrium profiles of the plasma column

$$\begin{aligned} n_o(r) &= N_o e^{-\frac{r^2}{a^2}} \\ \phi_o(r) &= \Phi_o + \frac{B\Omega_o}{2c} r^2 \\ g(r) &= \frac{g_o}{a} r \end{aligned} \quad (III.26)$$

as shown in Fig. 3.2, where  $n_o, a, \Omega_o, g_o$  are constants giving the plasma density at the center, the perpendicular dimension scale of the plasma, The equilibrium electric potential at the plasma center, plasma rotation frequency and the effective gravity constant, respectively.

Substituting (III.26) into equation (III.9) one obtains

$$\frac{d^2 \delta \phi_m}{dr^2} + \left( \frac{1}{r} - \frac{2r}{a^2} \right) \frac{d \delta \phi_m}{dr} + \frac{2}{a^2} \left( \nu - \frac{a^2 m^2}{2r^2} \right) \delta \phi_m = 0 \quad (III.27)$$

where

$$\nu = - \frac{\tilde{\omega}(2m\Omega + \omega_{*i}) + m^2(\omega^2 + g_o/a)}{\tilde{\omega}(\tilde{\omega} - \omega_{*i})} \quad (III.28)$$

With the substitution  $x = \sqrt{2} \frac{r}{a}$  equation (III.28) transforms to

$$\frac{d^2 \delta \phi_m}{dx^2} + \left( \frac{1}{x} - x \right) \frac{d \delta \phi_m}{dx} + \left( \nu - \frac{m^2}{x^2} \right) \delta \phi_m = 0 \quad (III.29)$$

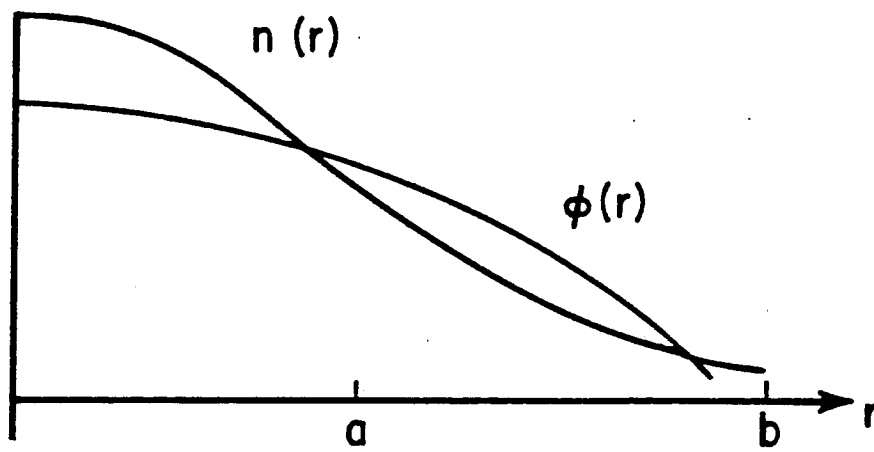


Fig.3.2 The equilibrium density and electrostatic potential in section III.3

Furthermore with the transform

$$\delta\phi_m(x) = e^{\frac{x^2}{4}} x^{-\frac{1}{2}} y(x)$$

one finds that  $y(x)$  satisfies the equation

$$\frac{d^2 y}{dx^2} + \left[ \nu + 1 - \frac{x^2}{4} - \frac{(m + 1/2)(m - 1/2)}{x^2} \right] y = 0 \quad (III.30)$$

We recognize the analogy between equation (III.30) and the standard form of radial equation of the quantum spherical harmonic oscillator [Flügge, 1974]

$$\frac{d^2 \chi_l}{dr^2} + \left[ k^2 - \lambda^2 r^2 - \frac{l(l+1)}{r^2} \right] \chi_l = 0 \quad (III.31)$$

where the potential  $V(r) = \lambda r^2$ . This analogy gives a qualitative picture of function  $y(x)$ . Like the particle is repulsed by the centrifugal force  $\frac{l(l+1)}{r^2}$  from the origin, the larger the equivalent angular quantum number  $l = m - 1/2$  in equation (III.30) is, the farther the peak of  $y(x)$  is located from the origin. However, we should notice that the analogy between our eigenvalue problem and the one of quantum oscillator is only a formal one. The difference of these two problem rests in two aspects. (i) The equivalent angular quantum number in (III.30) is half integers instead of the integers in the oscillator problem. (ii) The outer boundary conditions are different for both problems; for equation (III.30) it is

$$y(x) \Big|_{x=\frac{b^2}{a^2}} = 0$$

but for the oscillator problem the outer boundary condition is set as

$$\chi_i(r)|_{r=\infty} = 0$$

Due to these differences we cannot directly use the results already obtained in the well known oscillator problem. But this analogy suggests to us to solve our eigenvalue problem by the similar way of solving the oscillator problem. Completing all the steps necessary for solving the oscillator problem, we find that the solutions of equation (III.30) with boundary conditions (III.12) can be expressed by the Whittaker function  $W_{p,q}(\frac{r^2}{a^2})$  or the confluent hypergeometric function  ${}_1F_1(a, b; z)$  as

$$\delta\phi_m(r) = A_m r^m {}_1F_1\left(\frac{m-\nu}{2}, m+1; \frac{r^2}{a^2}\right) \quad (III.32)$$

with the eigenvalue  $\nu_{m,n}(b/a)$  determined by

$${}_1F_1\left(\frac{m-\nu}{2}, m+1; \left(\frac{b}{a}\right)^2\right) = 0 \quad (III.33)$$

where  $A_m$  is an arbitrary constant, the confluent hypergeometric function is defined by

$${}_1F_1(a, b; z) = \sum_{n=0}^{\infty} \frac{a_n z^n}{b_n n!}$$

$$a_n = a(a+1)\dots(a+n-1)$$

In Fig 3.3 we give the first three low  $m$  perturbation functions  $\delta\phi_{m,0}(r)$  for boundary distance  $b/a=3$ .

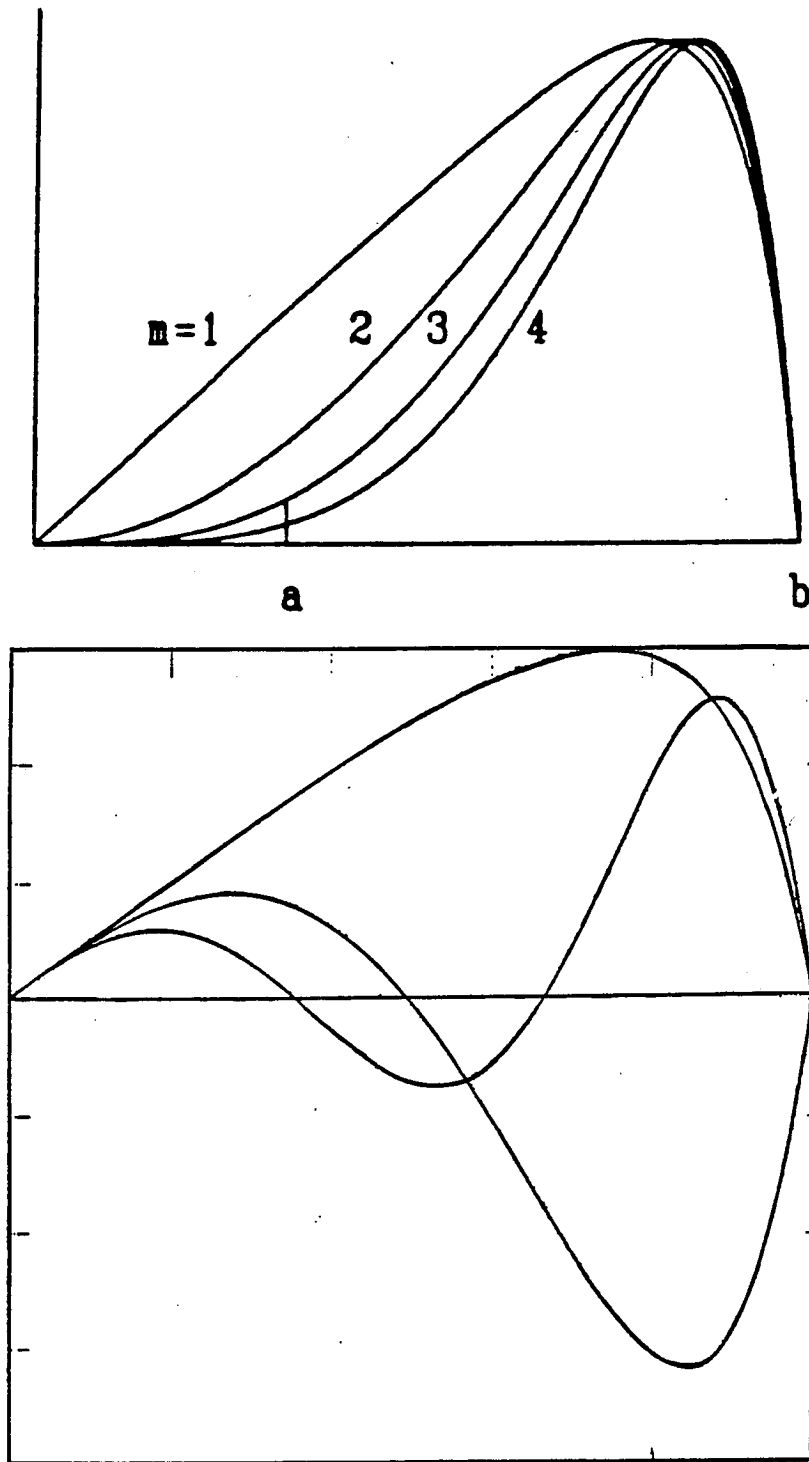


**Fig.3.3** The radial eigenfunction  $\delta\phi_m(r)$ . (a) For  $(1,0)$ ,  $(2,0)$ , and  $(3,0)$  modes with  $b/a=3$ . (b) For  $(1,0)$ ,  $(1,1)$ , and  $(1,2)$  modes with  $b/a=2.5$ .

From the pictures we see that the higher azimuthal mode number is the farther the peak of the function is removed from the origin, as we predicted by the analogy between our equation and the quantum spherical oscillator. From the theory on zeros of the confluent hypergeometric function [Buchholz, 1969] we can express  $\nu_{m,n}(b/a)$  as

$$\nu_{m,n}(b/a) = 2n + m + f_{m,n}(b/a) \quad (III.34)$$

where  $n$  is zero and positive integers which determine the node numbers of function  $\delta\phi_m(r)$  in the region between the origin and the boundary, and  $f_{m,n}(b/a)$  is a monotonous decreasing function of  $b/a$  which approaches zero as  $b/a$  tends infinity. Although the hypergeometric function is a well studied function the practically useful references about zeros of this function are hardly available. In Fig. 3.4 we give several graphs for function  $\nu_{m,n}$  numerically calculated from the equation (III.33) for our use.

Inserting the different values of  $\nu_{m,n}$  determined by (III.34) into equation (III.28) one obtains the dispersion relation corresponding to the perturbation function  $\delta\phi_{m,n}(r)$ , here we explicitly put the radial mode number  $n$  as a subscript to denote the fact that each azimuthal mode number  $m$  corresponds many eigenfunctions distinguished by the number of their radial nodes.

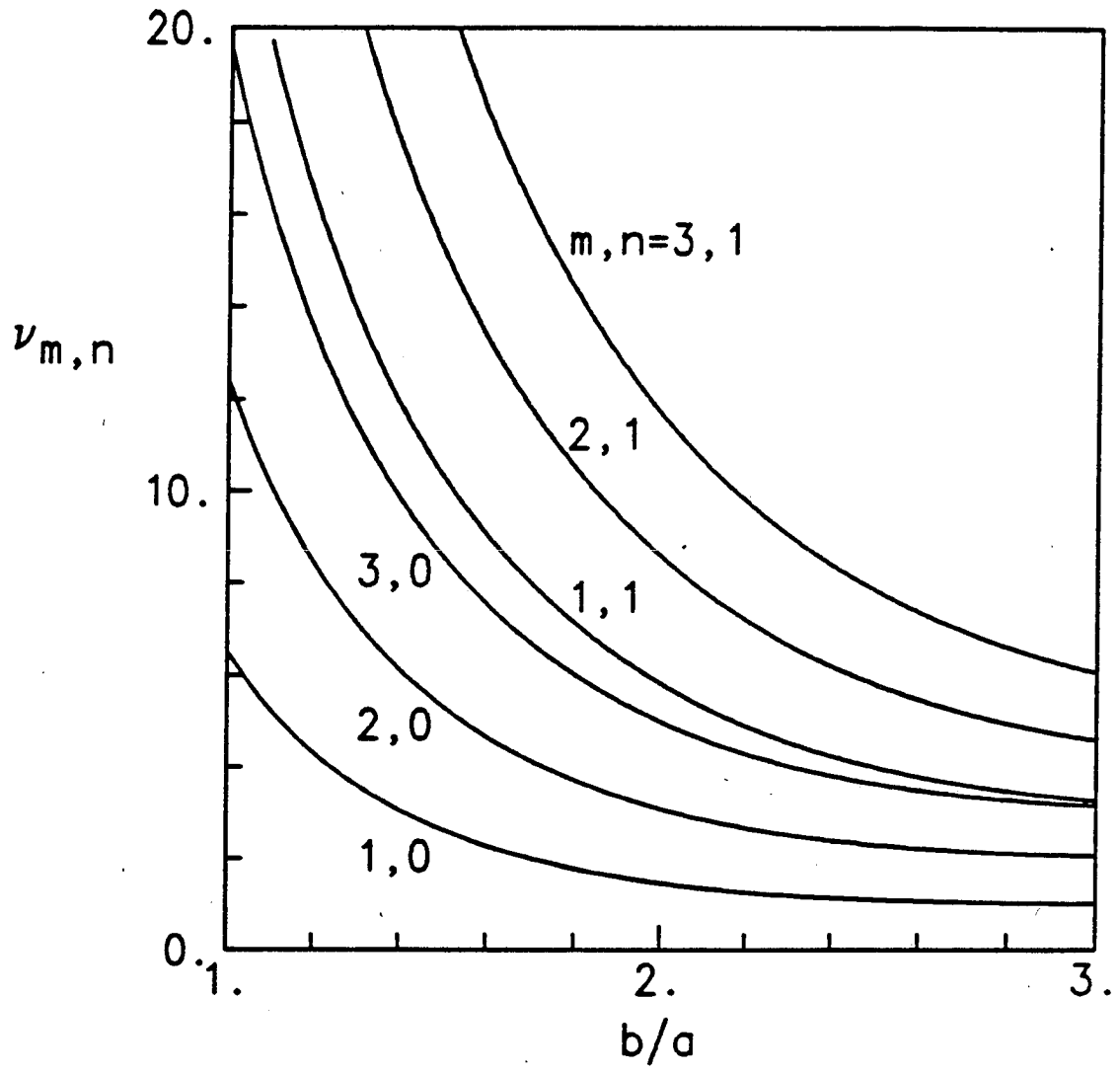


Fig.3.4 The eigenvalue  $\nu_{m,n}(b/a)$  calculated from Eq. (III.33) for low  $m$  modes.



$$A\tilde{\omega}^2 + B\tilde{\omega} + C = 0 \quad (III.35)$$

where

$$A = \nu_{m,n}$$

$$B = 2m\Omega + \omega_{*i}(1 - \nu_{m,n}) \quad (III.36)$$

$$C = m^2(\Omega^2 + g_o/a)$$

Solving (III.35) respect to  $\tilde{\omega}$  one obtains

$$\tilde{\omega} = -\frac{1}{2\nu_{m,n}} \left\{ [2m\Omega + \omega_{*i}(1 - \nu_{m,n}) \mp \{[(2m\Omega + \omega_{*i}(1 - \nu_{m,n}))^2 - 4\nu_{m,n}m^2(\Omega^2 + g_o/a)]\}^{\frac{1}{2}}] \right\} \quad (III.37)$$

which gives the Doppler shifted complex frequency for the normal mode (m,n) in the rotating frame. By using the relation

$$\tilde{\omega} = \omega - m\Omega$$

the complex frequency of the mode (m,n) in the laboratory is given by

$$\omega = m(\Omega + \omega_{*i}/2m)(1 - \frac{1}{\nu_{m,n}}) \left\{ 1 \pm i \left[ \frac{(\Omega + \frac{\omega_{*i}}{2m})^2 - \nu_{m,n}(\frac{\omega_{*i}^2}{4m^2} - \frac{g_o}{a(\nu_{m,n}-1)})}{(\nu_{m,n}-1)(\Omega + \frac{\omega_{*i}}{2m})^2} \right]^{\frac{1}{2}} \right\} \quad (III.38)$$

Writing the real part and the imaginary part of complex  $\omega$  separately we have the oscillation frequency and the growth rate for the mode (m,n)

$$\omega_r^{(m,n)} = m(\Omega + \frac{\omega_{*i}}{2m})(1 - \frac{1}{\nu_{m,n}}) \quad (III.39)$$

$$\gamma^{(m,n)} = \frac{m}{\nu_{m,n}} \left\{ (\nu_{m,n}-1) \left[ (\Omega + \frac{\omega_{*i}}{2m})^2 - \nu_{m,n}(\frac{\omega_{*i}^2}{4m^2}) \right] + \nu_{m,n} \frac{g_o}{a} \right\}^{\frac{1}{2}} \quad (III.40)$$

The graphs of the oscillation frequency and growth rate versus rotation frequency with fixed  $g$  and  $T_i/T_e$  for several low  $m$  modes and the growth rate versus mode number  $m$  for other parameters fixed are given in Figs. 3.5-3.8. This exact solution of the rotational plasma stability eigenvalue problem gives a good opportunity to study the mechanism of the instability caused by the plasma rotation in presence of the effects of the magnetic field line curvature and the the FLR, and to determine the stability boundary depending on various effects. Also the analytic expression of the dispersion relation which explicitly related to the boundary depending eigenvalue  $\nu_{m,n}$  enables us to investigate the wall effect analytically.

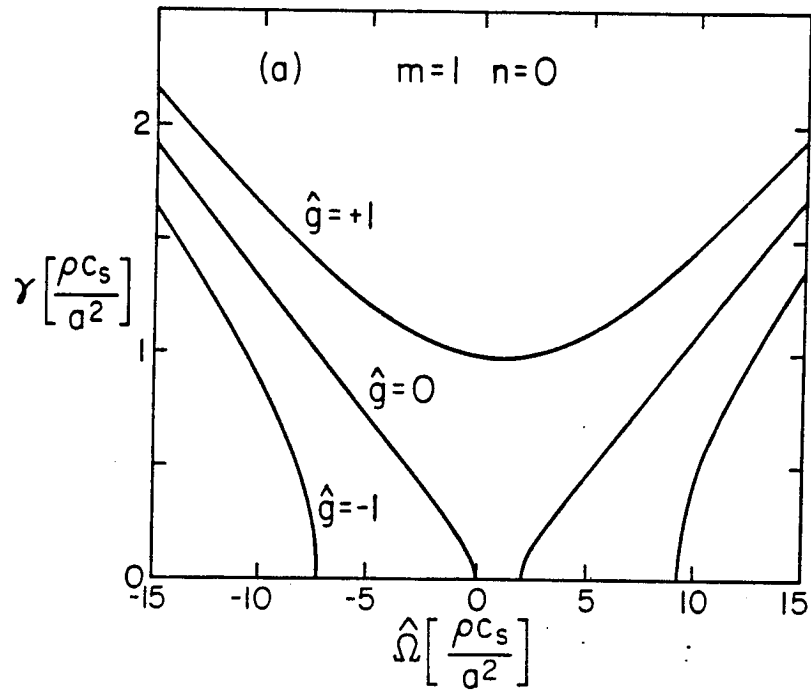


Fig.3.5 The growth rate for (1,0) mode, where  $\hat{\Omega}, \hat{g}$  are dimensionless value of  $\Omega$  and  $g_0/a$ , the frequency unit is  $\rho_s c_s / a^2$ . Other parameters are  $b/a=3, T_i/T_e = 1$ .

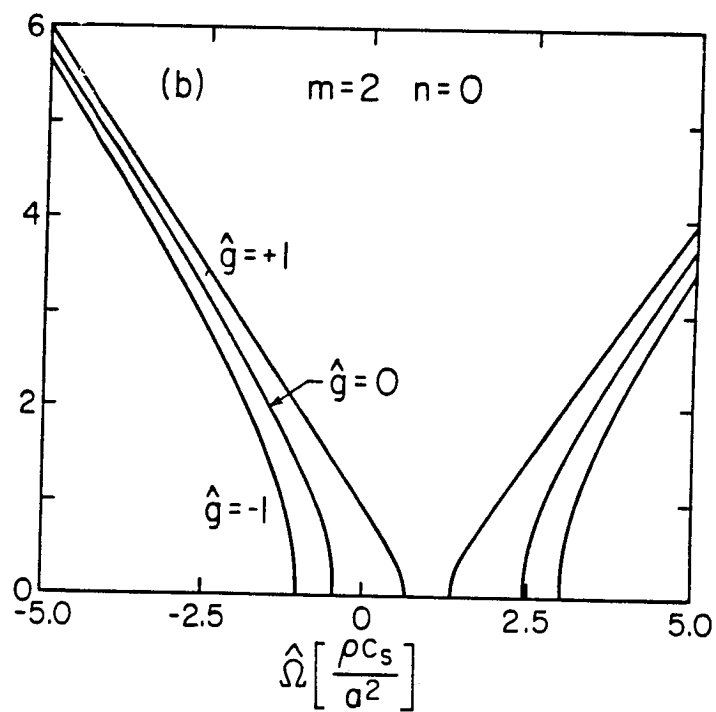


Fig.3.6 The growth rate for (2,0) mode, the parameter is the same as Fig.3.5.

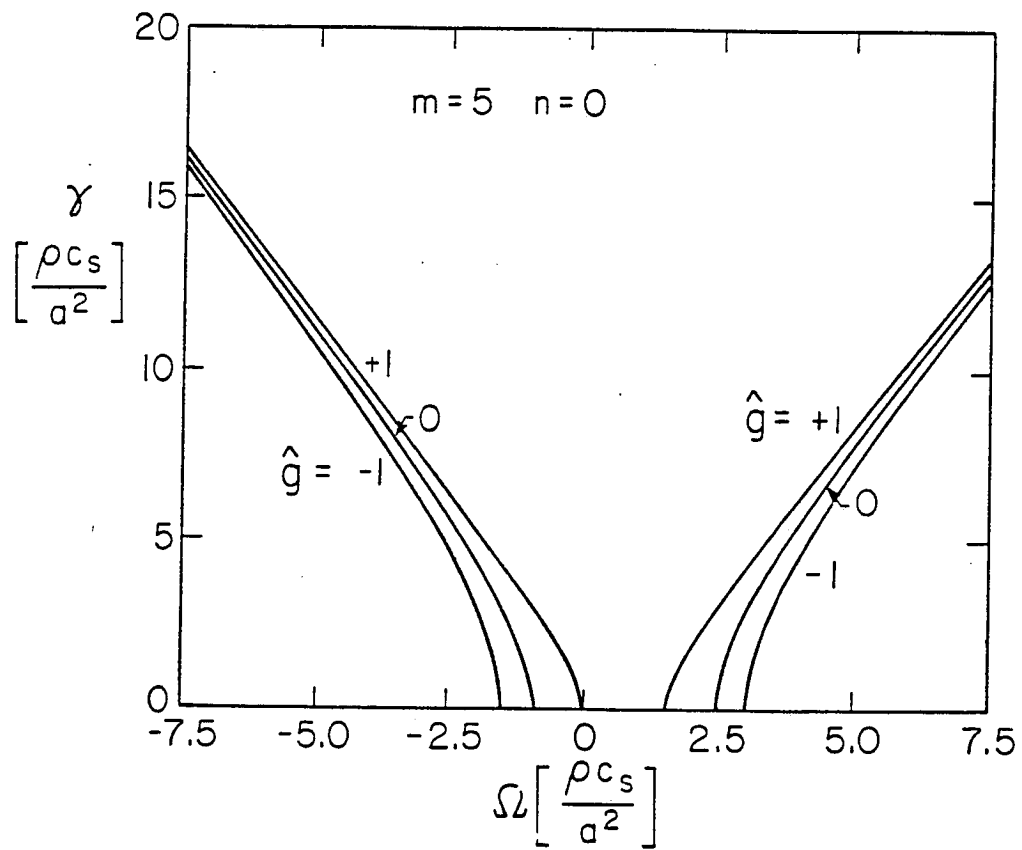


Fig.3.7 The growth rate for (5,0) mode, here  $T_i/T_e = .77, b/a = 3$ .

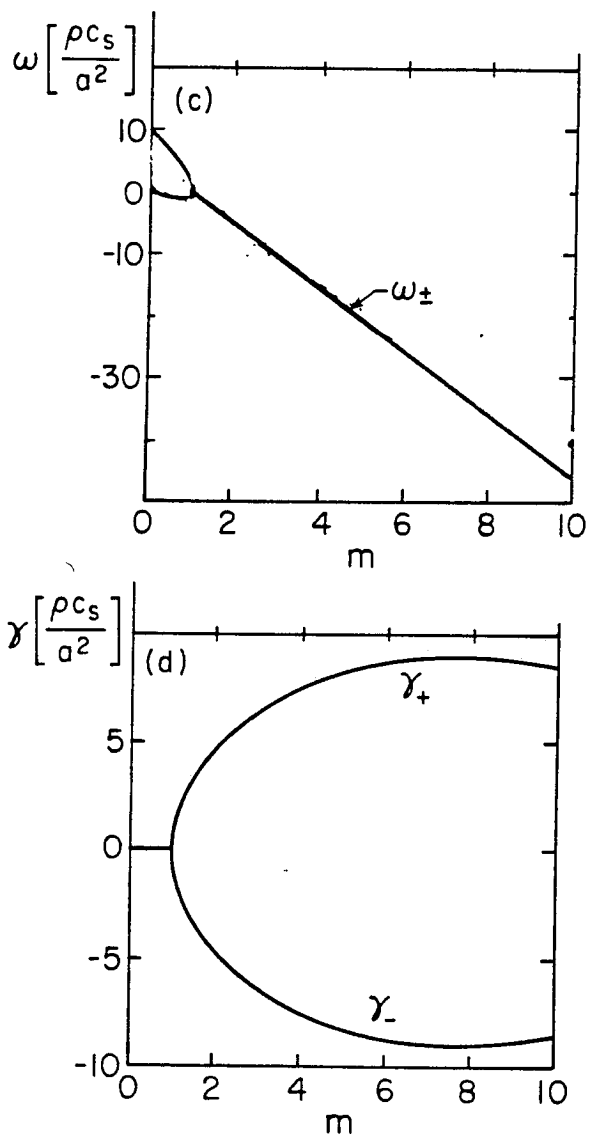


Fig.3.8 The real frequencies and the growth rates for different  $(m,0)$  modes, where  $\hat{\Omega} = -4, T_i/T_e = 1, b/a = 3, \hat{g} = -1$ . Note the FLR stabilizing effect for large  $m$  modes.

### III.3.A. The mechanism of the instability and the stability boundary

Obviously from equation (III.40) we can see that the stability property of the system for the normal mode  $(m,n)$  perturbation is determined by the quantities  $\Omega, g/a, \omega_{*i}$ , and  $\nu_{m,n}$  which represent the rotation, the curvature, the FLR effect, and the boundary effect respectively. To investigate these effects more closely, let us study the determinant of the quadratic dispersion relation (III.34)

$$\begin{aligned} \Delta &= B^2 - 4AC \\ &= -\left\{4m^2\nu_{m,n}\left(\Omega^2 + \frac{g_0}{a}\right) - [2m\Omega + \omega_{*i}(1 - \nu_{m,n})]^2\right\} \end{aligned} \quad (III.41)$$

$$= -4m^2\left\{(\nu_{m,n} - 1)\left[\left(\Omega + \frac{\omega_{*i}}{2m}\right)^2 - \nu_{m,n}\frac{\omega_{*i}^2}{4m^2}\right] + \frac{\nu_{m,n}g_0}{a}\right\} \quad (III.42)$$

By observation of the equation (III.41) and (III.42) we can draw following conclusions.

- (1). *The centrifugal force destabilization.* Formally, the first term of equation (III.41) is the driven term of the instability. Recognizing that the first part of this term comes from the centrifugal force drift and the second part from the gravity drift, we can see that the role played by the gravity depends on its sign. If  $g < 0$  (the good curvature), it always stabilizes the system; if  $g > 0$  (the bad curvature), it always destabilizes the system. Since  $\Omega^2 > 0$ , independent of the rotation direction of the plasma, hence the centrifugal force due to the rotation play the same role as the bad

curvature, it always destabilizes the system.

(2). *The role of the Coriolis force.* The second term of (III.41) is a stabilizing term which comes from the Coriolis force drift and the FLR. Since this term combines both effects together and plays the role of stabilization, the Coriolis force plays a subtle role in the process. The Coriolis charge separation enhances the FLR stabilizing effect or reduces it depending on the direction of plasma rotation. When the plasma rotates in the direction of the electron diamagnetic direction ( $\Omega > 0$ , corresponding to the inward equilibrium electric field case), the Coriolis term adds with the FLR term; when the plasma rotates in the ion diamagnetic drift direction ( $\Omega < 0$ , corresponding to the usual outward equilibrium electric field in the confinement devices), the Coriolis term and the FLR terms cancel each other and the stabilizing effect reduced. This implies that the plasma rotates in positive  $\hat{\theta}$  direction is more stable than it rotates oppositely with the same rotation rates.

(3). *The stabilization of FLR is not absolute.* From the same argument about the second term of (III.41), we can easily find that, unlike the MHD interchange instability driven by unfavorable curvature only, there is not the absolute FLR stabilizing effect for the instability of rotating plasma. Because when there is no rotation in the plasma the equation



(III.41) reduce to

$$\Delta = -\{4m^2\nu_{m,n}g/a - \omega_{*i}^2(\nu_{m,n} - 1)^2\},$$

the only term showing effects to reduce or suppress the instability caused by the bad curvature is the FLR term, in this sense we may call this FLR stabilizing effect absolute. But in the case of the rotating plasma, the stabilizing effect is shown by the whole term of  $[2m\Omega + \omega_{*i}(1 - \nu_{m,n})]^2$ , when  $\Omega < 0$ , but  $2m|\Omega| > \omega_{*i}(1 - \nu_{m,n})$  it is the Coriolis force part which contributes the main stabilizing effect and the FLR tries to reduce it.

(4). *The stability boundary and the most stable case.* As we mentioned above, the instability of the rotating plasma is the result of the competition between several effects. whether the plasma is stable or unstable depends on what region of the relevant parameters its equilibrium state lie in. From equation (III.42), set  $\Delta = 0$  we have

$$\Omega = \frac{\omega_{*i}}{2m} \pm \left\{ \nu_{m,n} \left( \frac{\omega_{*i}^2}{4m^2} - \frac{g_0}{(\nu_{m,n} - 1)a} \right) \right\} \quad (III.44)$$

From (III.44) setting  $b/a$  and either one of  $\frac{g_0}{a}$  and  $\frac{\omega_{*i}}{2m}$  fixed we can get the stability boundary for rotation versus gravity and rotation versus FLR effect respectively. these are drawn in Fig.3.9-3.10 for several low  $m$  modes. From equation (III.42) we can immediatly see that for given

$\frac{g_0}{a}$  and  $\frac{\omega_{*i}}{2m}$  the most stable state of rotation is when

$$\Omega + \frac{\omega_{*i}}{2m} = 0$$

because this condition gives the minimum of  $|\Delta|$ . Also we want to mention that if there is no FLR effect and gravity term, then from (III.42) the rotating plasma is unstable for any normal mode  $(m,n)$  no matter how slow and in which direction the plasma rotates, only after the FLR effect and the good curvature effect joining the process there is possibility of existence of the stability window or stability boundary.

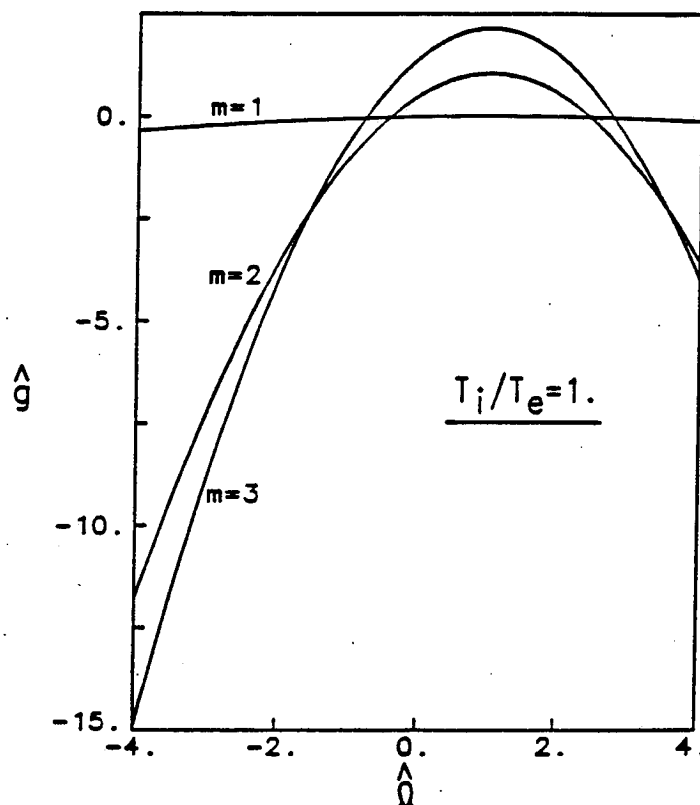


Fig.3.9 The stability boundary in  $\hat{\Omega} - \hat{g}$  plane for modes (1,0), (2,0) and (3,0). Below the boundary curve is the stable region, above the boundary curve is unstable region. Other parameters are  $T_i/T_e = 1$ ,  $b/a=3$ . Notice the boundary curve are not symmetric about  $\Omega=0$ , positive rotation state is more stable. the unit of frequency is the same as previous Figs.

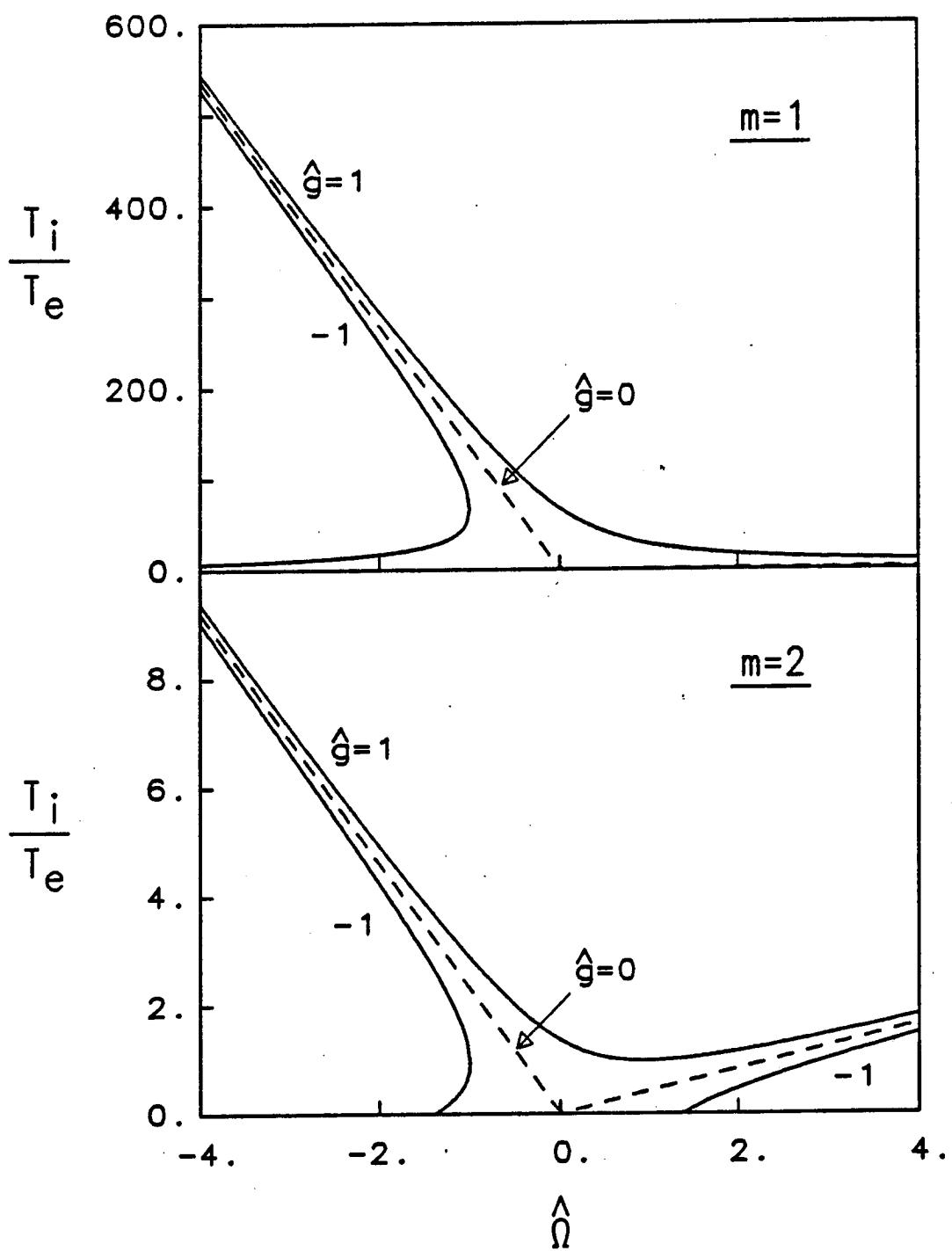


Fig.3.10 The stability boundary in  $T_i/T_e - \hat{\Omega}$  plane where  $\hat{g}$  fixed and  $b/a=3$  for (1,0) mode and (2,0) mode. Compare two figures can see  $m=1$  mode is hard been FRL stabilized when  $\Omega < 0$ . The curve of the boundary for good curvature case in the negative  $\Omega$  region shows the competition between Coriolis force stabilizing effect and FLR effect.

### III.3.B. The wall effect

The conducting wall boundary effect nontrivially enters into the stability analysis of the rotating plasma as we can see from the terms related with  $\nu_{m,n}$  in the equations (III.35)-(III.42) and influences the values of the oscillation frequency and growth rate of different modes. Since it winds up with the FLR term and the centrifugal-gravity term in the expressions of  $\gamma^{(m,n)}$  and there is no explicit analytical expression of  $\nu_{m,n}(\frac{b}{a})$  or  $f_{m,n}(\frac{b}{a})$  available, the analytic analysis of the wall effect seems impossible. However by knowing that  $\nu_{m,n} = 2n + m + f_{m,n}(\frac{b}{a})$  and  $f_{m,n}(\frac{b}{a})$  is a monotonous decreasing function of  $\frac{b}{a}$  we are able to figure out how the growth rate  $\gamma^{(m,n)}$  is changing when the boundary is moving from the infinity towards the plasma. Suppose we fix all other parameters and change the boundary distance from the plasma center, then from equation (III.40)

$$\begin{aligned} \frac{d\gamma^{(m,n)}}{d(b/a)} &= \frac{d\nu_{m,n}}{(b/a)} \frac{d\gamma^{m,n}}{d\nu_{m,n}} \\ &= \frac{m^2}{4\gamma^{(m,n)}\nu_{m,n}^3} \frac{d\nu_{m,n}}{d(b/a)} \left\{ 2\left(\Omega + \frac{\omega_{*i}}{2m}\right)^2 - \nu_{m,n} \left[ \left(\Omega + \frac{\omega_{*i}}{2m}\right)^2 + \frac{\omega_{*i}^2}{2m^2} + 2\frac{g_0}{a} \right] \right\} \end{aligned} \quad (III.45)$$

If we suppose  $g_0 \geq 0$  then for the mode  $(m,n)$  with  $m \geq 2, n \geq 0$  the equation gives positive value, it means that for those modes the growth rates is a monotonous increasing function of the boundary distance. That implies that when the boundary moves towards the plasma it stabilizes the system. The only exception is the  $(1,0)$  mode. Since  $\nu_{1,0} = 1 + f_{1,0}(b/a) \geq 1$ , until the boundary reach the location

where

$$\nu_{1,0} = 2 \left[ 1 - \frac{\frac{\omega_{*i}^2}{2} + \frac{g_v}{2a}}{(\Omega^2 + \frac{\omega_{*i}}{2})^2 + \frac{\omega_{*i}^2}{2} + \frac{g_v}{2a}} \right], \quad (III.46)$$

the expression (III.43) gives negative value, which means when the boundary moves towards the plasma until reaching the characteristic point determined by equation (III.46) it destabilizes the system. After pass this point it stabilizes. At this points the growth rate of (1,0) mode takes its maximum value. In Fig. 3.11 we give the graphs of the growth rates  $\gamma^{(m,n)}$  for modes (1, 0), (2, 0) and (3, 0) versus  $\frac{b}{a}$ . From it the peculiar wall effect on the (1,0) mode can seen clearly. As the wall comes from infinity to the plasma, instead stabilizing this mode as it did for other modes, it destabilizes the (1,0) mode until  $\frac{b}{a}$  reaches the value of about 1.8.

$T_i/T_e=1 \quad \hat{\Omega}=-4 \quad \hat{g}=0 \quad n=0$   
 ROTATING FRAME

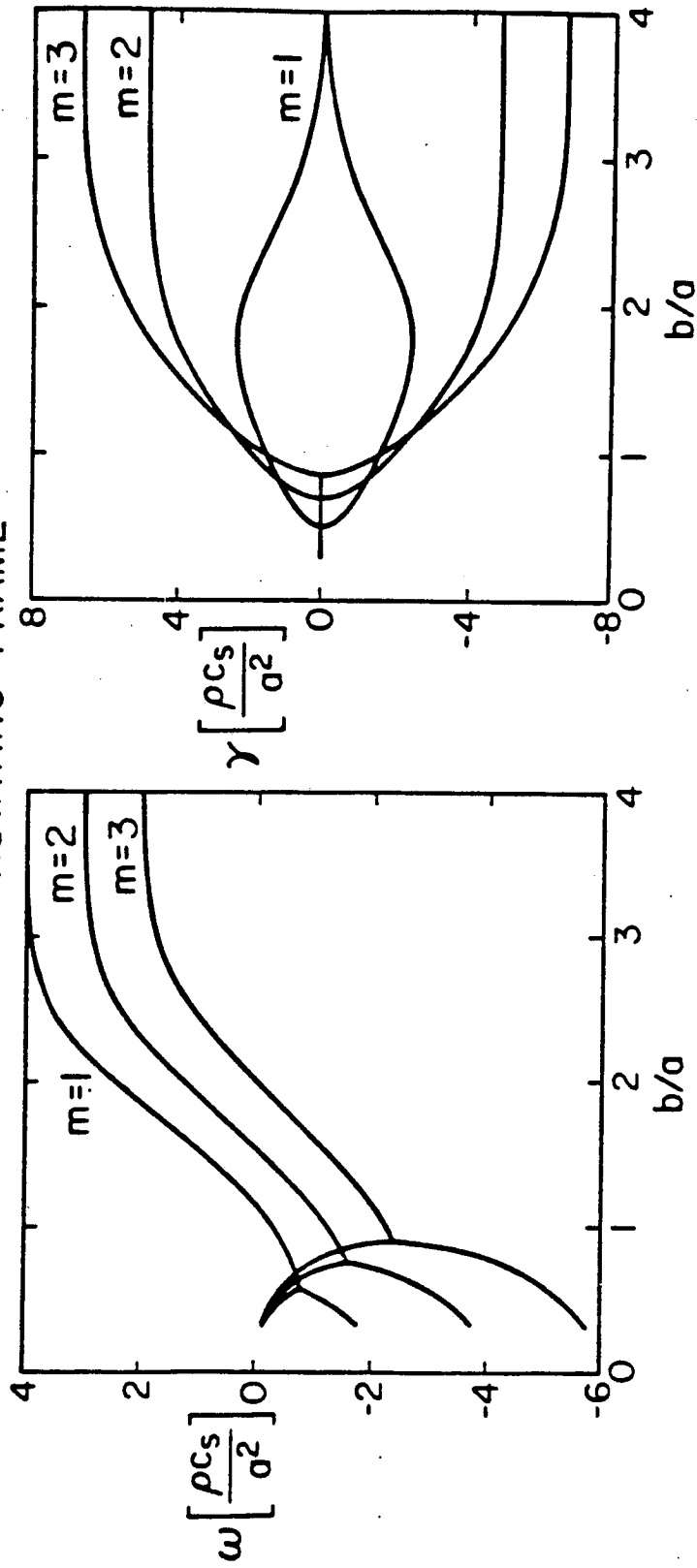


Fig.3.11 The real frequencies and growth rates for first three  $m$  modes change with the relative distance of the conducting wall  $b/a$ . Other parameters are fixed,  $T_i/T_e = 1, \hat{\Omega} = -4, \hat{g} = 0$ . Notice the different behavior of  $(1,0)$  mode.

### III.3.C. The limiting cases

As we mentioned in the beginning of this section that in the corresponding limits, our results will reduce to the results obtained by others. Here are three interesting limiting cases.

- (1) If we set  $\Omega = 0$ ,  $\frac{b}{a} = \infty$ . Then the eigenvalue  $\nu_{m,n} = 2n + m$ . Instituting these expressions into the dispersion relation (III.33) the results given by Mikhailovskii [1977] are recovered.
- (2) Substitute  $g = 0$ ,  $\frac{b}{a} = \infty$  hence  $\nu_{m,n} = 2n + m$  into the dispersion relation (III.33) then calculate the frequency and the growth rate for mode (m,n), we find all the results given by Rosenbluth et al [1962] and Berge [1966]. In these limiting case, since  $\nu_{1,0} = 1$ , (1,0) mode become marginal stable.
- (3) If we set  $g=0$  in our equation, and keep  $b/a$  finite then results given by Rognlin are recovered.

### III.4 The Instability Due To The Shear of The Rotation Frequency

Different from the analysis in the previous section where the instability of the plasma is driven by centrifugal force and the bad curvature, in this section we study the the instability driven by the shear of the plasma rotation frequency which resembles the Kelvin-Helmholtz instability in the shear flow of the ordinary hydrodynamics. As the equation (III.9) shows, the sheared rotation brings into the linear stability equations several more terms than the uniform rotation case hence it makes the the problem more difficult to solve analytically. In general, the numerical methods need to be employed. For the purpose of revealing the basic features of shear rotation caused instability in an analytic way, we have to simplify the equilibrium profiles. Similar to the analytic treatment of sheared flow instability for a vortex sheet [Drazin and Reid 1981], we limit our model to three limiting cases (see Fig. 3.12), where the first two cases corresponding to the situations for which the plasma rotation frequency experiences an abrupt change in a very narrow layer, but the density either keeps constant or also changes abruptly over this layer; the third case allows finite width of the the rotation shear but keeps density profile constant. Unlike the treatment for plane parallel sheared flow case, in our analysis the cylinder geometry is kept.



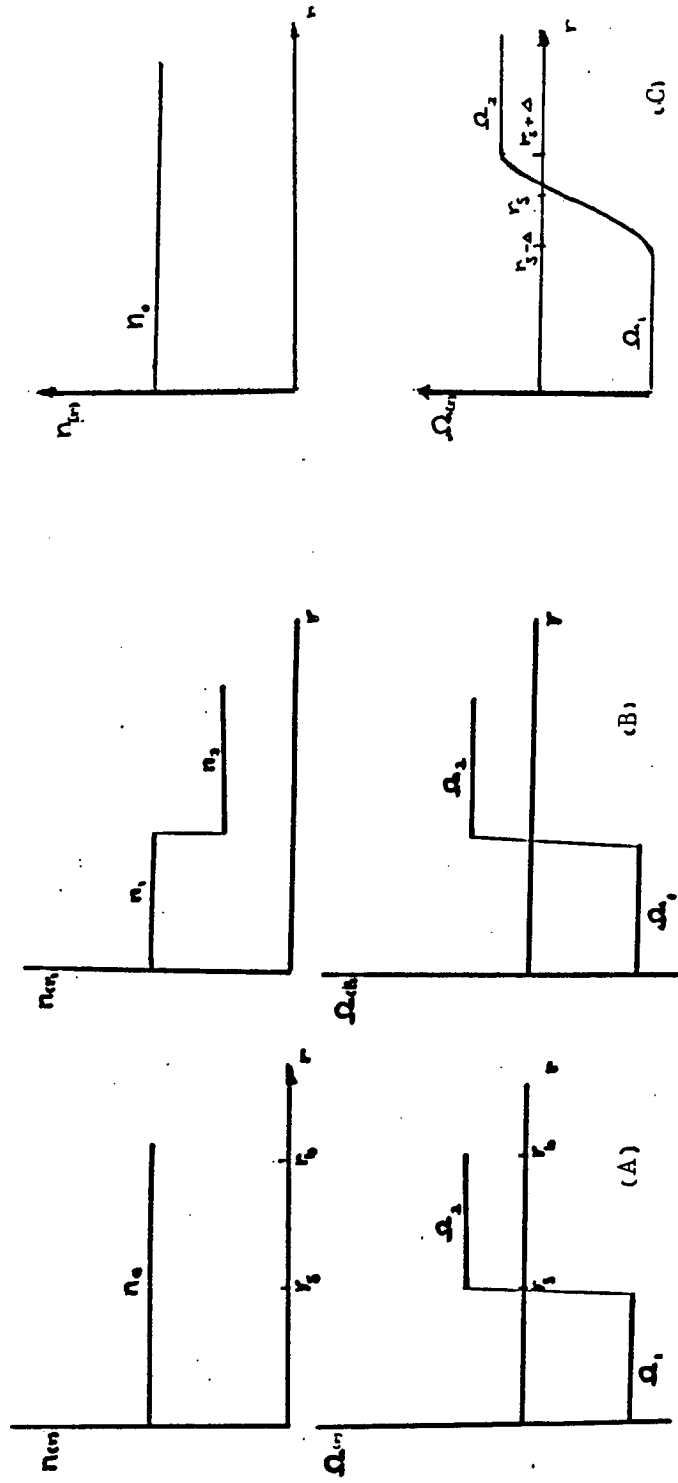


Fig.3.12 The equilibrium density and rotation frequency profiles correspond to subsections III.4.A,B,C.

### III.4.A The constant density and abrupt sheared rotation case

As the simplest model we suppose the equilibrium density of the plasma is a constant  $n_o(r) = N$  and the rotation frequency has a abrupt change over a narrow layer around some position  $r_s$  between the plasma center and the boundary  $r_b$ , i.e.

$$\Omega(r) = \begin{cases} \Omega_1, & (0 < r < r_s); \\ \Omega_2, & (r_s < r < r_b). \end{cases}$$

as shown in Fig.3.12 (A). Substitute this equilibrium profile into equation (III.10), for both regions  $r_b > r > r_s$  and  $0 < r < r_s$ , the equation is

$$\frac{d^2 \xi_m}{dr^2} + \frac{3}{r} \frac{d\xi_m}{dr} + \frac{1-m^2}{r^2} \xi_m = 0. \quad (III.47)$$

Readily we obtain the solutions

$$\xi_m^{(1)} = Ar^{m-1} \quad (0 < r < r_s), \quad (III.48)$$

$$\xi_m^{(2)} = Br^{-(m+1)} + Cr^{m-1} \quad (r_s < r < r_b).$$

From the boundary condition at  $r = r_b$  and the continuity condition of displacement  $\xi_m$  at  $r_s$

$$\xi_m^{(1)}(r)|_{r_s} = \xi_m^{(2)}(r)|_{r_s} \quad (III.49)$$

the coefficients A, B, C are determined as

$$\begin{aligned} A/B &= -r_b^{-2m}, \\ C/B &= r_s^{-2m} - r_b^{-2m}. \end{aligned} \quad (III.50)$$

Integrating equation (III.10) over the narrow layer  $r_s - \epsilon \geq r \geq r_s + \epsilon$  then taking the limit  $\epsilon \rightarrow 0$ , and using the relations (III.50) we have the dispersion relation

$$(m-1)(\omega - m\Omega_1)^2 + (m+1)(1+\delta)(\omega - m\Omega_2)^2 = 0 \quad (III.51)$$

where

$$\delta = \frac{(r_s/r_b)^{2m}}{1 - (r_s/r_b)^{2m}}$$

is a factor showing the outer boundary effect in the dispersion relation, when the outer boundary tends to  $\infty$ ,  $\delta = 0$ .

Solve equation (III.51) respect to  $\omega$  we have

$$\begin{aligned} \omega_r &= \frac{(m-1)\Omega_1 + (m+1)(1+\delta)\Omega_2}{2(1 + \frac{m+1}{2m}\delta)}, \\ \gamma_m &= \frac{\sqrt{(m^2-1)(1+\delta)} |\Omega_2 - \Omega_1|}{2(1 + \frac{m+1}{2m}\delta)} \end{aligned} \quad (III.52)$$

The equation (III.52) clearly shows that the rotation with an abrupt shear drive the plasma system unstable. Except for  $m=1$  mode, all the modes are unstable with the growth rate proportional to the strength of the rotation shear  $|\Omega_2 - \Omega_1|$ . The feature of this kind of the instability is very different from that driven by centrifugal force which closely depends on the density gradient. Equation (III.52) also shows that the finite boundary effect on the instability through the factor  $\frac{\sqrt{1+\delta}}{1 + \frac{m+1}{2m}\delta}$  when  $r_b \rightarrow \infty$  this factor becomes 1, and we have

$$\omega_r = \frac{1}{2}[(m-1)\Omega_1 + (m+1)\Omega_2], \quad \gamma_m = \frac{\sqrt{m^2-1}}{2} |\Omega_2 - \Omega_1| \quad (III.53)$$

[Horton and Liu 1984]. The growth rate increases monotonically with  $m$  but is limited by the validity of the sharp jump of scale  $\Delta r_s$  at  $r_s$  by  $m/r_s \leq 1/\Delta r_s$ . The FLR limit on  $m$  is given in the next subsection.

Compare (III.53) with the hydrodynamic results for two horizontal parallel infinite streams of different velocities  $U_1, U_2$  separated by a vortex sheet in a homogeneous inviscid fluid

$$\omega = \frac{k}{2}(U_1 + U_2) \pm i\frac{k}{2}(U_1 - U_2) \quad (III.42)$$

where  $k$  is the wave number [Drazin and Reid 1981], we see that the rotation shear caused plasma instability has similarity with the one caused in inviscid fluid by the sheared flow with  $k \rightarrow m/r_s$  and  $U \rightarrow r_s\Omega$ .

#### III.4.B The case when both the density and the rotation frequency have abrupt change

Although the results given in subsection III.4.A reveals the basic features of the instability driven by the shear rotation, the model is too idealized for some physical problems.

We consider the following model profiles which includes the density variation along with the variation of rotation frequency of the plasma.

$$n(r) = \begin{cases} n_1, & (0 < r < r_s) \\ n_2, & (r_s < r < r_b) \end{cases} \quad (III.55)$$

$$\Omega(r) = \begin{cases} \Omega_1, & (0 < r < r_s) \\ \Omega_2, & (r_s < r < r_b) \end{cases} \quad (III.56)$$

as shown in Fig. 3.12 (B).

Completing the similar procedure as in the previous subsection, we obtain the dispersion relation

$$(1 + 2\delta\alpha_2)\omega^2 - 2[(m+1)\alpha_2\Omega_2 + (m-1)\alpha_1\Omega_1 + (m^2-1)\kappa(\alpha_2-\alpha_1) + 2m\delta\alpha_2\Omega_2]\omega + m(m+1)\alpha_2\Omega_2^2 + m(m-1)\alpha_1\Omega_1^2 + 2m^2\delta\alpha_2\Omega_2^2 + m(m^2-1)\kappa(\Omega_1+\Omega_2)(\alpha_2-\alpha_1) = 0 \quad (III.57)$$

where

$$\alpha_1 = \frac{n_1}{n_1 + n_2}, \quad \alpha_2 = \frac{n_2}{n_1 + n_2},$$

$$\delta = \frac{(r_s/r_b)^{2m}}{1 - (r_s/r_b)^{2m}}, \quad \kappa = \frac{\rho_i \omega_{ci}}{2r_s}.$$

The parameter  $\delta$ , as in equation (III.52), enters the analysis to represent the influence of the outer boundary. At once we can see that, since  $\frac{r_s}{r_b} < 1$ , this wall effect can be considerable for low  $m$  modes provided the shear layer is not too close to the center of the plasma, but for high  $m$  modes it has very small influence, i.e. the higher modes hardly notice the wall. The parameter  $\kappa$  represent FLR effect and it is decreasing with the increase of the distance of the shear layer from the plasma center.

Solve the dispersion relation (III.57), one obtains

$$\omega_r = \frac{1}{1 + 2\delta\alpha_2} [(m+1)\alpha_2\Omega_2 + (m-1)\alpha_1\Omega_1 + (m^2-1)\kappa(\alpha_2-\alpha_1) + 2m\delta\alpha_2\Omega_2] \quad (III.58)$$

$$\gamma_m = \frac{1}{1+2\delta\alpha_2} \left\{ -[(m+1)\alpha_2\Omega_2 + (m-1)\alpha_1\Omega_1 + (m^2-1)\kappa(\alpha_2-\alpha_1) + 2m\delta\alpha_2\Omega_2]^2 + (1+2\delta\alpha_2)m[(m+1)\alpha_2\Omega_2 + (m-1)\alpha_1\Omega_1^2 + 2m^2\delta\alpha_2\Omega_2^2 + (m^2-1)\kappa(\Omega_1+\Omega_2)(\alpha_2-\alpha_1)] \right\}^{\frac{1}{2}}$$

(III.59)

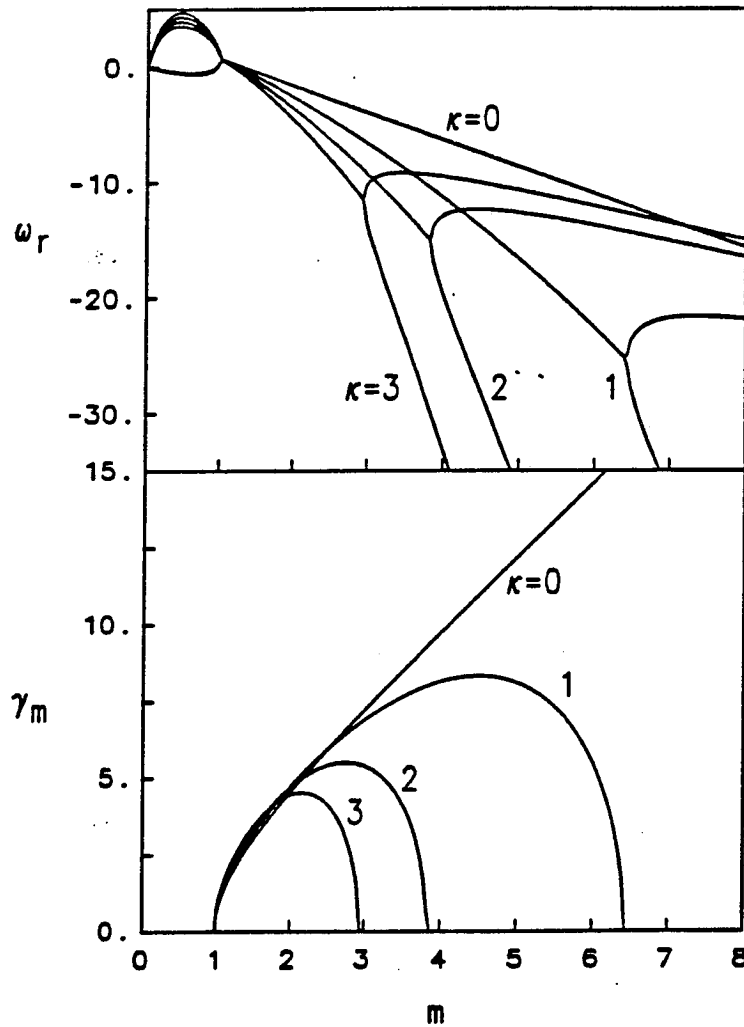


Fig.3.13 The real frequencies and growth rates for different  $m$  mode calculated from Eqs.(III.58-59). The corresponding parameters are  $\alpha_1 = 2/3, \alpha_2 = 1/3, \Omega_1 = -4, \Omega_2 = 1, r_s/r_b = 1/3, \kappa = 0, 1, 2$ , respectively. Notice the FLR stabilizing effect for large  $m$  modes.

In Fig. 3.13 we give the graphs of the real frequency and the growth rate versus mode numbers for a set of typical parameters.

To see the mechanism of the instability we discuss the sufficient condition for instability

$$\gamma^2 > 0.$$

explicitly it gives

$$\begin{aligned} & \alpha_1 \alpha_2 [(m+1)\Omega_2 - (m-1)\Omega_1]^2 + (m-1)\alpha_1 \Omega_1^2 - (m+1)\alpha_2 \Omega_2^2 \\ & + 2m\delta [\alpha_1 \alpha_2 (m-1)(\Omega_1 - \Omega_2)^2 + \alpha_2 (\alpha_1 - \alpha_2) \Omega_2^2] > \kappa (m^2 - 1) (\alpha_2 - \alpha_1)^2 \times \\ & \times [\kappa (m^2 - 1) + m(\Omega_2 - \Omega_1) + 2 \frac{(\alpha_1 \Omega_1 - \alpha_2 \Omega_2)}{\alpha_1 - \alpha_2} + 2m\delta \frac{\alpha_2}{\alpha_1 - \alpha_2} (\Omega_1 - \Omega_2)]. \quad (III.60) \end{aligned}$$

The inequality (III.60) looks messy but the physics meaning of it is quite clear. The first term in the left hand side represents the Kelvin-Helmholtz excitation of the instability. This term is always destabilizing and it is essentially proportional to the shear of the equilibrium rotation. The second and the third terms in the left hand side represent the net centrifugal force excitation acting on the layer from both sides of it, in fact, it is the integrated form of the centrifugal force term in equation (III.9) which is proportional to  $\Omega^2 \frac{dn_o(r)}{dr}$ . A Rayleigh-Taylor type instability would be excited if the inner region is more dense or it rotates faster than the outer region. The fourth term in the left hand side represents the finite outer boundary effect on the instability, for this model this term is positive,

it destabilizes the system. Since  $m=1$  mode is stable in this model problem, so the finite outer boundary plays the same role as it does in the Rayleigh-Taylor type instability discussed in Section III.3. The right hand side which is proportional to  $\kappa$  is the stabilizing term; it represents the FLR effect modified by other parameters. From the dependence of this term on mode number  $m$  we see that the FLR stabilizing effect will dominate for the higher  $m$  modes, the graphs in Fig 3.13 shows this tendency.

Compare the results given in this subsection and the results in last subsection, we see that the jump of the density profile brings more physics into the problem; the most important effects it brings is that the instability in this section is no longer pure Kelvin-Helmholtz type instability, but is a mixture of two types of instabilities. Remember that the Rayleigh-Taylor type instability is closely connected with density gradient and the finite density jump over a very narrow layer is a limiting form of the existence of density gradient, this mixture seems understandable. One word needs to be added, when  $\alpha_1 = \alpha_2$ , the results in this subsection reduces automatically to the results of the last subsection.



### III.4.C The problem of constant density profile with finite width layer of the rotation frequency variation

In the last two subsections we treated the two simplest cases of the sheared rotation instability problem and found that the instability caused by the sheared rotation plasma has remarkable similarity with the instability of inviscid parallel shear flow. To study this analogy deeper, in this subsection we show that under certain conditions our linear stability equation is mathematically equivalent to the linear instability equation of the shear flow in inviscid fluid, hence the method and the existing results of the latter can be applied to the plasma problem too. Suppose the plasma is homogeneous,  $n_r = n_o = \text{constant}$  and through a finite width layer the rotation frequency has a continuous variation such as

$$\Omega(r) = \begin{cases} \Omega_1, & (0 < r < r_s - \Delta) \\ f(r), & (r_s - \Delta < r < r_s + \Delta) \\ \Omega_2, & (r_s + \Delta < r) \end{cases} \quad (III.61)$$

as shown by Fig. 3.12 (C), where  $2\Delta$  is the width of the layer, it is finite compare with the wave length of the perturbation but we suppose that

$$\frac{\Delta}{r_s} \ll 1. \quad (III.62).$$

Since  $\omega_{*i} = 0$  everywhere, the equation (III.9) reduces to

$$\nabla_{\perp}^2 \delta\phi_m = 0 \quad (III.63)$$

outside of the layer, i.e. when  $0 < r < r_s - \Delta$ , or  $r > r_s + \Delta$ . and

$$\nabla_{\perp}^2 \delta\phi_m + \frac{m \frac{d}{dr} \left[ \frac{1}{r} \frac{d}{dr} (r^2 \Omega(r)) \right]}{r(\omega - m\Omega(r))} \delta\phi_m = 0 \quad (\text{III.64})$$

inside the layer, i.e. for  $r_s - \Delta < r < r_s + \Delta$ .

By using the narrowness condition of the layer (III.62) we can further reduce the equation (III.64) to

$$\frac{d^2 \delta\phi_m}{dx^2} - k^2 \delta\phi_m + \frac{d^2 V / dx^2}{\omega/k - V} \delta\phi_m = 0 \quad (\text{III.65})$$

where

$$k = \frac{m}{r_s}, \quad V = r\Omega(r) = rf(r), \quad \text{and} \quad \frac{d}{dx} = \frac{d}{dr}.$$

Equation (III.65) is exactly the same equation as the equation for the perturbation of plane-parallel flow of a perfect fluid [Lin 1966]. In hydrodynamics the equation (III.65) was studied thoroughly and two theorems of the necessary condition of instability for the flow satisfying this equation with the boundary conditions

$$\delta\phi_m(r)|_{r=r_s-\Delta} = \delta\phi_m(r)|_{r=r_s+\Delta} = 0$$

were formulated as the Rayleigh's inflection-point theorem and the Fjortoft's theorem [Drazin and Reid 1981 pp.133].

Although

$$\delta\phi_m(r) = 0 \quad \text{for} \quad r < r_s - \Delta, \quad \text{and} \quad r > r_s + \Delta$$

satisfied the equation (III.63) hence the above mentioned theorems can be applied to our problem, for solving our eigenvalue equation their help is limited. But the mathematical identity of the sheared rotation problem with the well-studied hydrodynamic problem gives us great opportunity to use the existing results. If we take

$$V(r) = rf(r) = \frac{\Omega_1 + \Omega_2}{2} + \frac{\Omega_2 - \Omega_1}{2}(r - r_s)$$

and consider the boundary conditions at  $r=0$  and  $r \rightarrow \infty$  for equation (III.63), our problem is equivalent to a special case of the unbounded shear flow problem solved by Chandrasekhar [1962]. From his solution we can readily get the dispersion relation

$$\omega^4 - \frac{1}{\nu^2}(2\nu^2 - 2\nu + 1 - e^{-2\nu})\omega^2 + \frac{1}{\nu^2}[1 - e^{-\nu} - \nu]^2 = 0 \quad (III.66)$$

where  $\nu = 2m\Delta/r_s$ . Solve (III.66) respect to  $\omega$  we find for  $\frac{2m\Delta}{r_s} > 1.2785$  the mode is stable, otherwise it is unstable. In Fig.3.14 we give a graph of the perturbed  $\mathbf{E} \times \mathbf{B}$  flow with  $\frac{m\Delta}{r_s} = 0.64$  observed in the rotating frame with  $\Omega = \frac{\Omega_1 + \Omega_2}{2}$ .

PERTURBED  $\vec{E} \times \vec{B}$  FLOW  
IN SHEARED LAYER

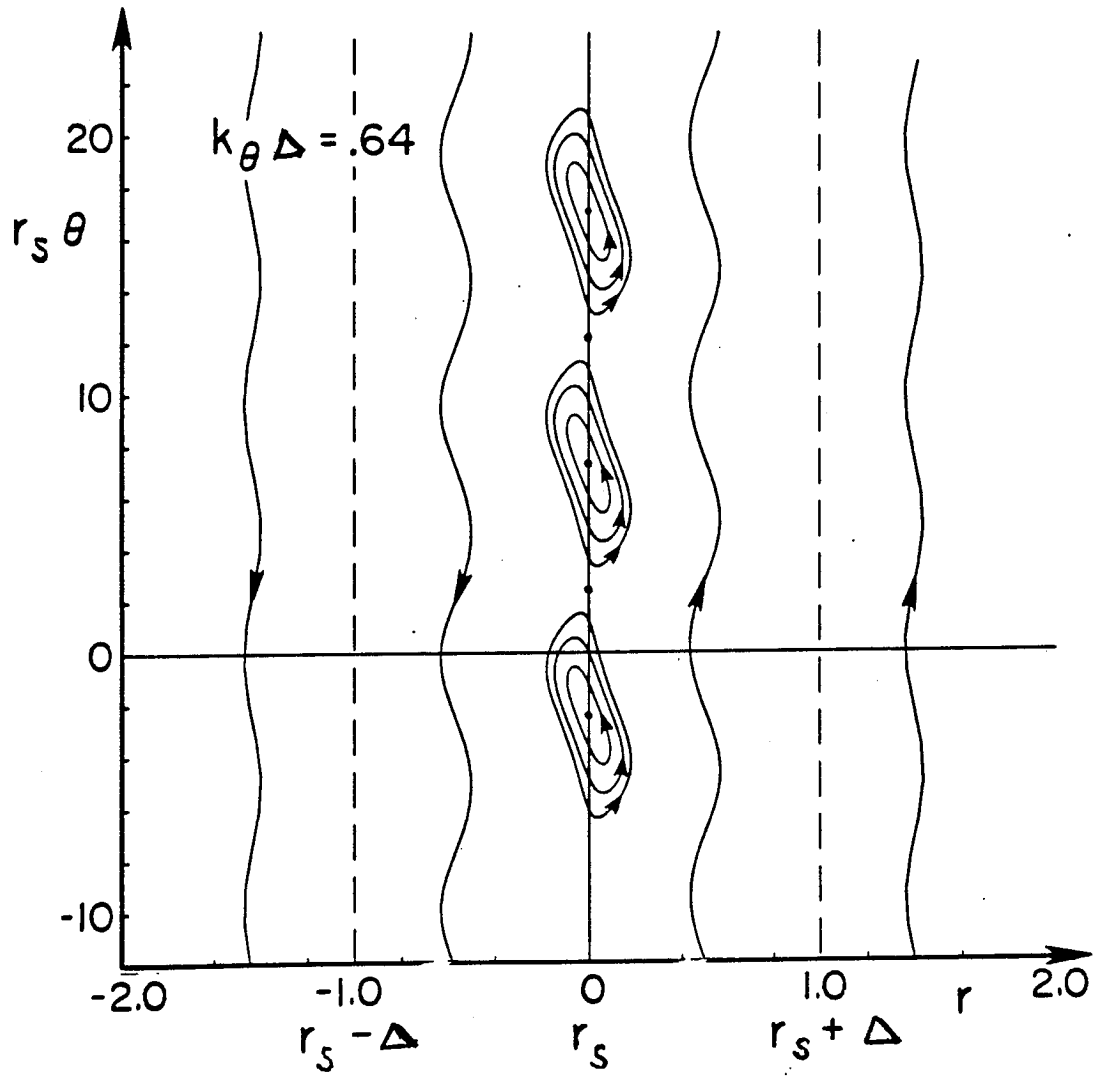
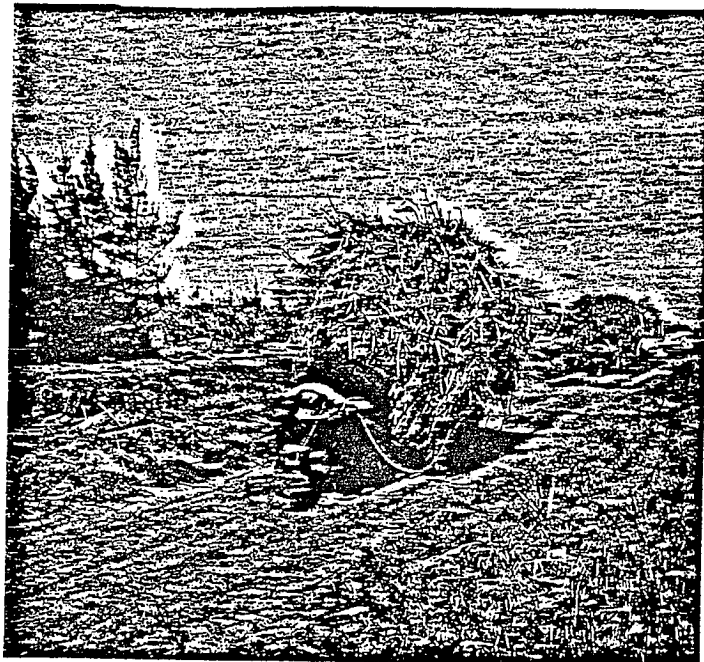


Fig.3.14 The perturbed  $\vec{E} \times \vec{B}$  flow seen from the frame rotating with  $\Omega = (\Omega_1 + \Omega_2)/2$  at  $r_s$ .

*Highly piled, is the firewood stable?*



**Chapter IV**  
**TRAPPED PARTICLE MODE WITH PASSING ELECTRONS**  
**AND ROTATION SHEAR IN THE CENTRAL CELL**  
**OF TANDEM MIRROR**

**Introduction**

In this chapter we present an application of the linear stability analysis for the rotating plasma-the rotation driven trapped particle mode in the central cell of the Tandem Mirror devices.

The low frequency fluctuations with low azimuthal mode numbers and rotating in the ion diamagnetic direction with speeds near the equilibrium  $\mathbf{E} \times \mathbf{B}$  drift velocity are observed in numerous tandem mirror experiments and have attracted considerable attention. In reference [Horton and Liu, 1984] Horton and Liu suggest the possibility that the low  $m$  rotation driven drift modes may be responsible for the fluctuations. The conventional FLR-MHD, rigid rotor modes studied by Freidberg and D'Ippollito [Freidberg And D'Ippollito, 1983] for the axisymmetric tandem mirror are stable at the low plasma pressure in the experiments where the modes are observed. The flute-like drift modes called trapped particle modes by Rosenbluth [ Rosenbluth, 1982] and Berk et al [Berk et al, 1983] are driven unstable by the plasma pressure gradient acting across the unfavorable curved magnetic field at the ends of the central cell, and also are another candidate for

the observed low  $m$  oscillations.

In this chapter we extend the rotationally driven drift model of Horton and Liu to include the effects of the passing electron population and the effect of differential rotation in the equilibrium. The drift modes have frequencies greater than the ion transit frequency and less than the electron transit frequency over the length of the central cell. To keep the analysis simple, we use the hydrodynamic description of the system, i.e. we use the FLR ion fluid equation for ion and two component electron fluid equations for trapped and passing electrons respectively.

The stability analysis is carried out first for the uniformly or rigidly rotating plasma which permits the exact solution and second by using a shooting method eigenvalue code to determine the modes of general radial profiles with different rotation.

The eigenvalue analysis allows consideration of profiles which have free energy from both radial density gradients and sheared rotation. Our numerical results on a sheared rotation profile shows, contrary to a simple free energy argument, that a mildly sheared rotation flow can be a stabilizing effect. The stability may arise from the fact that the interchange of plasma pressure from the inner high pressure region to the outer low pressure region is inhibited by the differential rotation. The free energy in the sheared rotation is released by a different kind of interchange mode working on the radial mixing of the angular momentum gradient rather than the pressure gradient. Since the dynamics represented by the eigenfunctions of the

pressure gradient modes and of the sheared flow modes are rather different, there are more stable plasma configurations with both monotonically decreasing density and rotation rate profiles.

In Section IV.1 we derive the linear stability equation by a way similar to what we did in Chapter II and III, but modified by including the contribution of the passing electrons. In Section IV.2 we investigate the stability of uniformly rotating plasma with a Gaussian density profile and a linear gravity. It turns out that we can find an analytic solution of the stability equation, hence we are able to present the analytic formulas for the threshold and cutoff passing electron ratio as a function of rotation frequency, effective gravity, the relative wall distance, and the ion-to-electron temperature ratio. In Section IV.3 we present the numerical study of stability with the shooting code which reproduces the analytic results and shows the stabilizing effect of mildly sheared rotational profiles. In Section IV.4 we present the summary and conclusions.



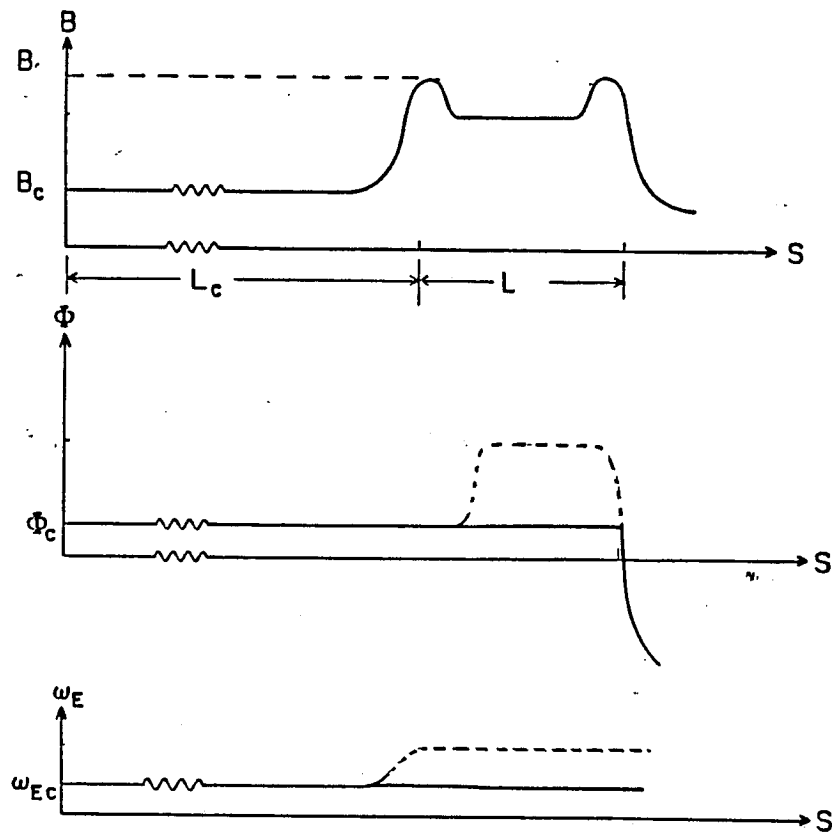


Fig.4.1 Axial variation of magnetic field, ambipolar potential  $\Phi_0$ , and  $\mathbf{E} \times \mathbf{B}$  rotation frequency  $\Omega$  about midplane of a model tandem mirror configuration.

## VI.1 Derivation of Trapped Particle Mode Equation From Hydrodynamic Equations

In this section we derive the equation of trapped particle mode from the hydrodynamic equations with the finite ion gyroradius stress tensor in the ion fluid and a two-component electron fluid consisting of trapped and passing components in a cylinder model of the axisymmetric tandem mirror. The two-component electron fluid model has been used for trapped particle modes by Rosenbluth [Rosenbluth, 1982]. The analysis shows that this hydrodynamic description gives a good simplified description of the modes compared with that given by the Vlasov description recently presented by Kesner and Lane [Kesner and Lane, 1985]. The hydrodynamic description given here is valid for modes with frequencies greater than the ion-transit frequency and less than the electron-transit frequency. We restrict consideration here to the electrostatic approximation.

To derive the linear stability equation, we use an equilibrium model of three cells tandem mirror system. The axial variation of electromagnetic field, equilibrium electrostatic potential and the  $\mathbf{E} \times \mathbf{B}$  rotation frequency is shown in Fig.4.1. This model simple tandem mirror system is composed of three parts. A relatively long central cell of length  $L_c$ , with the plasma having uniform or nonuniform rotational frequency there depending on the radial variation of the electrostatic potential. This region has an unfavorable field line curvature. At each end of

the central region are magnetic or electrostatic plugs which are characterized by good curvature, which we referred to simply as plugs. this region can in practice be quite complex being made up of quadrupole coil sets, choke coils and coils for thermal barriers. However, for our theoretical model, we will avoid these complexities and consider the plug regions as axisymmetric single mirrors that are nearly square well in shape as shown in Fig.4.1. Besides having a favorable curvature, these cell have positive electrostatic potential with respect to the central cell and the plasma there has different rotation frequency than the plasma in the central cell (see the dashed line in Fig.4.1), and this axial shear of rotation frequency can be another source of instability [Lee and Catto, 1981;Byers and Cohen, 1985;Berk and Lane, 1985]. But for simplicity of mathematical treatment, here we suppose the potentials are the same in plugs and in the central cell (see solid line in Fig.4.1).

#### IV.1.A Ion hydrodynamic equations

As we mentioned earlier that we treat the ion fluid with account of the FLR effect, i.e. we take the FLR ordering. By the same procedure as we presented in Chapter II, we obtain the ion fluid continuity equation up to order  $\epsilon^3$  by iteration as

$$\frac{\partial n_i}{\partial t} + \frac{c}{B}[\phi, n_i] - \frac{c}{\omega_{ci}B} \nabla \cdot \left\{ n_i \frac{\partial}{\partial t} \nabla \phi + \frac{cn_i}{B} [\phi, \nabla \phi] \right\}$$

$$+\frac{cT_i}{eB}[n_i, \nabla\phi] - \frac{1}{\omega_{ci}}[n_i, U] = 0. \quad (IV.1)$$

where all the notations have the same definitions as in Chapter I.

Completing the linearization procedure as in Chapter III for normal modes, we have the linearized equation of (IV.1) for the fluctuation component with azimuthal mode number  $m$  as

$$-i(\tilde{\omega})\delta n_{im} - i\frac{cm}{Br}\frac{\partial n_o}{\partial r}\delta\phi_m + \nabla \cdot \{\delta(n_i \mathbf{V}_i)\}_m^{(3)} = 0 \quad (IV.2)$$

where

$$\begin{aligned} \nabla \cdot \{\delta(n_i \mathbf{V}_i)\}_m^{(3)} = & i\frac{c}{\omega_{ci}B} \left\{ \nabla \cdot [n_o(\tilde{\omega} - \omega_{*i})\nabla\delta\phi_m] + \frac{2m\Omega}{r}\frac{dn_o}{dr}\delta\phi_m \right. \\ & + m\frac{d\Omega}{dr}\frac{d}{dr}(n_o\delta\phi_m) + \frac{m}{r}\frac{d}{dr}\left[\frac{1}{r}\frac{d}{dr}(r^2\Omega)\right]n_o\delta\phi_m \\ & \left. - \frac{cT_i}{eB}\frac{m}{r}\frac{d}{dr}\left(\frac{1}{r}\frac{dn_o}{dr}\right)\delta\phi_m - \frac{Bm}{cr}(r\Omega^2 - g)\delta n_{im} \right. \\ & \left. + \frac{T_i m}{er}\frac{d}{dr}\left[\frac{1}{r}\frac{d}{dr}(r^2\Omega)\right]\delta n_{im} + \frac{T_i}{e}r\frac{d\Omega}{dr}\frac{d}{dr}\left(\frac{1}{r}\delta n_{im}\right) \right\} \end{aligned} \quad (IV.3)$$

#### IV.1.B The electron fluid equations

Following Rosenbluth [Rosenbluth, 1982] we describe the electron fluid by  $n = n_e^t + n_e^p$ , where  $n_e^t$  is the density of electrons trapped in the central cell and  $n_e^p$  is the density of electrons passing through the central cell to the plugs or end cells.

Neglecting the collisional mixing between the two electron components we have

$$\frac{\partial n_e^{t,p}}{\partial t} + \nabla \cdot (n_e \mathbf{V}_e)^{t,p} = 0 \quad (IV.4)$$

The trapped electron component  $\mathbf{E} \times \mathbf{B}$  drifts with the local potential of the central cell, hence

$$(n_e \mathbf{V}_e)^t = \frac{cn_e^t}{B} \hat{\mathbf{z}} \times \nabla \phi - \frac{cT_e}{eB} \hat{\mathbf{z}} \times \nabla n_e^t \quad (IV.5)$$

and the passing component  $\mathbf{E} \times \mathbf{B}$  drifts with an average potential obtained from averaging the electrostatic potential  $\phi$  over the central cell plasma (where the characteristic parameters are  $L_c$ -the central cell length,  $B_c$ - the magnetic field strength in the central cell and  $n_c$ -the density of corresponding component in the central cell) and the plug plasma (where the corresponding parameters are  $L_p, B_p, n_p$ ). The precise definition and the calculation of the electron averaging-operator requires the use of kinetic equations. Here we follow Rosenbluth [Rosenbluth, 1982] by taking the simple approximation that

$$\hat{L}\phi = \langle \bar{\phi} \rangle = \left\langle \frac{1}{\tau} \int \frac{ds}{v_{\parallel}} \phi_{cs} \right\rangle \simeq \frac{L_c \phi_c}{L_c + L_p} \quad (IV.6)$$

In Ref. [Horton and Liu, 1984] a similar approximation is made by introducing the constant eigenvalue  $\lambda$  of the bounce-averaging operator  $\hat{L}$ , however, no attempt is made to evaluate  $\lambda$  in terms of the central cell and plug parameters there.

In addition to the convective change in the trapped electron density given by

$$\delta n_e^p = -\frac{mc}{r\tilde{\omega}B} \frac{dn_{oe'}^p}{dr} \delta \bar{\phi}, \quad (IV.7)$$

there is an adiabatic change arising from the rapid transit motion given by

$$\delta n_{e||}^p = \frac{n_{oe}^p e(\delta\phi - \delta\bar{\phi})}{T_e} \quad (IV.8)$$

as well known from kinetic theory, when we give the equations (IV.7-8) the assumption of no axial dependence for the equilibrium electrostatic potential is used. The total passing electron density fluctuation is

$$\delta n_e^p = n_{oe}^p \frac{e(\delta\phi - \delta\bar{\phi})}{T_e} - \frac{mc}{r\tilde{\omega}B} \frac{dn_{oe}^p}{dr} \delta\bar{\phi} \quad (IV.9)$$

and the trapped electron density fluctuation is

$$\delta n_e^t = -\frac{mc}{r\tilde{\omega}B} \frac{dn_{oe}^t}{dr} \delta\phi. \quad (IV.10)$$

#### IV.1.C The Radial Eigenvalue Equation

For low frequency drift modes the electrostatic potential is governed by the condition of quasineutrality

$$n_i = n_e^t + n_e^p \quad (IV.11)$$

Evaluating the fluctuating part of equation (IV.11) with equations (IV.2) and (IV.9-10) yields

$$-\frac{mc}{r\tilde{\omega}B} \frac{dn_o}{dr} \delta\phi + \frac{\nabla \cdot \delta(n_i \mathbf{V}_i)_m^{(3)}}{i\tilde{\omega}} = -\frac{mc}{r\tilde{\omega}B} \frac{dn_{oe}^t}{dr} \delta\phi - \frac{mc}{r\tilde{\omega}B} \frac{dn_{oe}^p}{dr} \delta\bar{\phi} + \frac{en_{oe}^p}{T_e} (\delta\phi - \delta\bar{\phi}). \quad (IV.12)$$

Using  $n_o^i = n_{oe}^t + n_{oe}^p$  and equation (IV.3) for the term  $\nabla \cdot \delta(n_i \mathbf{V})_i^{(3)}$  yields the radial mode equation

$$\begin{aligned} & \frac{c^2 m_i}{B^2 e} \left\{ \nabla \cdot [n_o (\tilde{\omega} - \omega_{*i}) \nabla \delta \phi_m] + m \frac{d\Omega}{dr} \frac{d}{dr} [n_o (1 - \frac{\omega_{*i}}{\tilde{\omega}}) \delta \phi_m] \right. \\ & + [(2m\Omega + \frac{m^2(\Omega^2 + g/r)}{\tilde{\omega}} - \frac{m^2 c T_i}{\tilde{\omega} B e r^2} \frac{d}{dr} (r^2 \frac{d\Omega}{dr})) (\frac{1}{r} \frac{dn_o}{dr}) + \frac{m}{r} n_o \frac{d}{dr} (\frac{1}{dr} \frac{d}{dr} (r^2 \Omega)) \\ & \left. + \frac{1}{r} \frac{d}{dr} (n_o \omega_{*i}) \right] \delta \phi_m \left\} - (\frac{mc}{rB} \frac{dn_{oe}^p}{dr} + \frac{en_{oe}^p}{T_e} \tilde{\omega}) (\delta \phi_m - \langle \delta \bar{\phi}_m \rangle) = 0. \quad (IV.13) \end{aligned}$$

Equation (IV.13) includes a term of the average of the fluctuating potential with mode number  $m$ ,  $\langle \delta \bar{\phi}_m \rangle$ , which we need to model in order to make the equation mathematically tractable. For modes that are essentially flute-like in the central cell with the fluctuating potential dropping to a small value in the plug the bounce average can be approximated quite well as

$$\hat{L} \delta \phi_m = \langle \delta \bar{\phi}_m \rangle = \lambda \delta \phi_m \cong \frac{L_c}{L_c + L_p} \delta \phi_m. \quad (IV.14)$$

which gives

$$1 - \lambda \cong \frac{L_p}{L_c + L_p} \ll 1. \quad (IV.15)$$

For strong mirror ratio  $R = B_p/B_c$  at the ends of the central cell, assuming essentially mirror confinement for the bulk of the electrons, then the density of the passing electrons is small with

$$\frac{n_{oe}^p}{n_{oe}} \cong \frac{1}{2(R+1)} \cong \frac{B_c}{B_p} \ll 1. \quad (IV.16)$$

Taking estimates (IV.14-16) into account, the term representing the charge separation from the passing electrons in equation (IV.13) may be written as

$$\left(\frac{mc}{rB} \frac{dn_{oe}^p}{dr} + \frac{en_{oe}^p}{T_e} \tilde{\omega}\right) (\delta\phi_m - \langle \delta\bar{\phi}_m \rangle) = \frac{en_{oe}}{T_e} \left(\frac{n_{oe}^p}{n_{oe}}\right) \left(\frac{L_p}{L_c + L_p}\right) (\tilde{\omega} - \omega_{*e}) \delta\phi_m \quad (IV.17)$$

where we assume that

$$\omega_{*e} = \omega_{*e}^p \equiv -\frac{mcT_e}{reB} \left(\frac{d \ln n_{oe}^p}{dr}\right). \quad (IV.18)$$

Introducing a dimensionless parameter  $A_p$  measuring the ratio of the charge separation from the passing electrons to that from the polarization current gives

$$A_p = \left(\frac{2n_{oe}^p}{n_o}\right) \left(\frac{a^2 \omega_{ci}^2 m_i}{T_e}\right) \left(\frac{L_p}{L_c + L_p}\right) = 2\eta_p \left(\frac{a^2}{\rho_s^2}\right) \left(\frac{L_p}{L_c + L_p}\right) \simeq \frac{a^2 B_c L_p}{\rho_s^2 B_p L_c}, \quad (IV.19)$$

where  $a$  is the perpendicular length scale of the plasma,  $\eta_p = n_{oe}^p/n_o$  - the ratio of passing electron population, and  $\rho_s^2 = \frac{T_e}{m_i \omega_{ci}^2}$ .

By using equations (IV.18-19) we rewrite equation (IV.13) as

$$\begin{aligned} & \nabla \cdot [n_o (\tilde{\omega} - \omega_{*i}) \nabla \delta\phi_m] + m \frac{d\Omega}{dr} \frac{d}{dr} [n_o (1 - \frac{\omega_{*i}}{\tilde{\omega}}) \delta\phi] \\ & + [(2m\Omega + \frac{m^2(\Omega^2 + g/r)}{\tilde{\omega}}) \frac{1}{r} \frac{dn_o}{dr} - \frac{mn_o \omega_{*i}}{r^2 \tilde{\omega}} \frac{d}{dr} (r^2 \frac{d}{dr} (\Omega))] \quad (IV.20) \\ & + \frac{mn_o}{r} \frac{d}{dr} [\frac{1}{r} \frac{d}{dr} (r^2 \Omega)] + \frac{1}{r} \frac{d}{dr} (n_o \omega_{*i}) - \frac{2A_p n_o}{a^2} (\tilde{\omega} - \omega_{*e}) \delta\phi_m = 0. \end{aligned}$$

Equation (IV.20) in fact is the equation (III.9) modified by adding a passing electron term. With proper boundary conditions, such as  $\delta\phi_m(r)|_{r=0} \simeq r^m$  and



given  $\delta\phi(r)$  or  $\frac{d\delta\phi_m(r)}{dr}$  at the boundary  $r=b$ , the equation (IV.20) determines the spectrum of eigenvalues for given radial profiles of  $n_o$ ,  $\phi_o$  (hence  $\Omega(r)$ ) and the explicit form of fictitious gravity  $g(r)$ .

In the limit in which the density gradients are weak compared with the potential gradients, equation (IV.20) reduces to

$$\nabla^2 \delta\phi_m + \frac{m}{r} \frac{d}{dr} \left[ \frac{1}{r\tilde{\omega}} \frac{d}{dr} (r^2 \Omega) - \frac{2A_p}{a^2} \right] \delta\phi_m = 0, \quad (IV.21)$$

where the  $\frac{1}{\tilde{\omega}}$  term describes the interchange of vorticity  $\chi(r) = \frac{d(r^2 \Omega)}{dr} = \frac{d(rV_\theta)}{dr}$ . For the case  $\frac{d\chi}{dr} \neq 0$  there is a restoring tendency of the perturbed flow discussed in subsection **IV.3.B** of this chapter.

Here, as in section **III.2**, we introduce the linear Lagrangian displacement  $\xi_m(r)$  defined by

$$\xi_m(r) = \frac{mc}{r\tilde{\omega}B} \delta\phi_m(r) \quad (IV.22)$$

and rewrite the first-order ion density perturbation as

$$\delta n_{im} = -\xi_m \frac{dn_o}{dr}. \quad (V.23)$$

The nonlinear Lagrangian displacement was analyzed in Ref. [Liu et al, 1985].

Substituting equation (IV.22) into equation (IV.20) yields

$$\frac{1}{r} \frac{d}{dr} \left[ r^3 n_o \tilde{\omega} (\tilde{\omega} - \omega_{*i}) \frac{d\xi_m}{dr} \right] + [(1 - m^2) n_o \tilde{\omega} (\tilde{\omega} - \omega_{*i})$$

$$+(\omega^2 + \frac{m^2 g}{r})r \frac{dn_o}{dr} - \frac{2A_p n_o r^2 \tilde{\omega}(\tilde{\omega} - \omega_{*e})}{a^2} \xi_m = 0. \quad (IV.24)$$

The boundary conditions on  $\xi_m(r)$  are  $\xi_m(r)|_{r \rightarrow 0} \simeq r^{m-1}$  and given  $\xi_m(r)|_{r=b}$  or  $\frac{d\xi_m(r)}{dr}|_{r=b}$ . For the  $A_p = 0$  case, equation (IV.24) reduces to the Rosenbluth-Simon equation for flute mode in a cylindrical plasma.

Although not as obvious, the mode equation (IV.20) and (IV.24) can be regarded as the generalization of the equations in Ref. [Horton and Liu, 1984] for electron drift waves in a rotating plasma as given, for example, in equation (21) of Horton and Liu. identifying the axial eigenvalue  $\lambda$  from the electron bounce averaging operator in equation (21) of their paper with  $A_p$  given in this chapter through the relation  $1 - \lambda = 2\alpha^2 A_p$  ( $\alpha = \rho_s/a$ ) then the equation (24) in that paper is the same as the equation (IV.20) in this section. For large  $A_p$  values,  $A_p \simeq 1/2\alpha^2$ , the passing electron contribution dominates and give rise to an electron drift wave with  $\tilde{\omega} \simeq \omega_{*e}/(1 + 2\alpha^2 \nu_{m,n})$  which is the drift dispersion relation with  $k_{\perp}^2 \rho_s^2 \rightarrow 2\alpha^2 \nu_{m,n}$  from the radial eigenvalue problem. The electron dissipation  $i\delta_e(k)$  retained in that paper but neglected in this chapter, drives the electron drift wave unstable.

## IV.2 Analytic Solutions for Solid Body Rotation with Passing Particles

Here we derive and analyze the dispersion relation for solid body rotation  $\Omega = \text{constant}$ , the Gaussian density profile and linear gravity

$$n_o(\mathbf{r}) = n_o \exp(-r^2/a^2) \quad \text{and} \quad g(\mathbf{r}) = g_o r/a$$

as we did in section III.3. The eigenvalue Eq.(IV.20) reduces to the same equation as (III.27)

$$\frac{d^2}{dr^2} \delta\phi + \left( \frac{1}{r} - \frac{2r}{a^2} \right) \frac{d\delta\phi}{dr} + \left( \frac{2}{a^2} \nu - \frac{m^2}{r^2} \right) \delta\phi = 0 \quad (IV.25)$$

where we define the eigenvalue  $\nu$  by

$$\begin{aligned} \nu(\omega, m, A_p, g_o/a, T_i/T_e) = & - \frac{1}{\tilde{\omega}(\tilde{\omega} - \omega_{*i})} \left[ m^2 (\Omega^2 + \frac{g_o}{a}) \right. \\ & \left. + \tilde{\omega} (2m\Omega + \omega_i^*) + A_p \tilde{\omega} (\tilde{\omega} - \omega_e^*) \right]. \end{aligned} \quad (IV.26)$$

Notice that here  $\nu$  is different from the one given by equation (3.28) by adding a term from charge separation by passing electrons. Following the same procedure as in section III.3, the solution of Eq.(IV.25) is given by the Whittaker function  $W_{p,q}(x)$  with

$$\delta\phi_{m,n}(r) = A_m \frac{a}{r} \exp(r^2/a^2) W_{p,q}(r^2/a^2) \quad (IV.27)$$

where  $p = (\nu_{m,n} + 1)/2$  and  $q = m/2$ , or equivalently in the confluent hypergeometric function as the equation (III.32)

$$\delta\phi_{m,n}(r) = A_{m,n} (r/a)^m {}_1F_1\left(\frac{m}{2} + 1 - \nu_{m,n}, m + 1; \frac{r^2}{a^2}\right).$$

The eigenvalues, which are determined by boundary conditions  $\delta\phi_{m,n}(b) = 0$ , are

$$\nu_{m,n}(b/a) = m + 2n + f(b/a)$$

the same as (III.34).

The dispersion relation following from Eq.(IV.26) is

$$A\tilde{\omega}^2 + B\tilde{\omega} + C = 0 \quad (IV.28)$$

where

$$\begin{aligned} A &= \nu_{m,n} + A_p \\ B &= 2m\Omega + \omega_{*i}(1 - \nu_{m,n}) - A_p\omega_{*e} \\ C &= m^2(\Omega^2 + \frac{g_o}{a}) \end{aligned} \quad (VI.29)$$

Equation (VI.31) is related to Eq.(25) of the Ref.[Horton and Liu, 1984] by re-interpreting the meaning of the axial eigenvalue parameter  $\lambda$  in that work in terms of the passing electron parameter  $A_p$  defined in Eq.(IV.19).

The quadratic Eq.(IV.28) gives instability for  $C > 0$  driven by the centrifugal force of rotation. The stabilization arises from  $B \neq 0$  due to the charge separation from the Coriolis force, the finite Larmor radius effect and the axial motion of the passing electrons. The passing electron contribution has the opposite sign to the finite Larmor radius effect whereas the Coriolis force effect can reinforce either the passing electron ( $\Omega < 0$ ) or the finite Larmor radius effect ( $\Omega > 0$ ).

The effective gravity  $g_o$  may be due to the ponderomotive force either from radio frequency fields or from the curvature of the magnetic field lines. For the case

where  $g$  is dominated by the curvature of the axisymmetric magnetic field lines we remove the scaling of  $g$  by introducing  $g_o = (v_s^2 a/L^2)\hat{g}$  with the dimensionless  $\hat{g}$  given by

$$\hat{g} = \frac{3L^2}{2} \frac{\int_1^2 \left( \frac{1}{B^2} \frac{dB}{dz} \right)^2 dz}{\int_1^2 \frac{dz}{B^2}} \quad (IV.30)$$

which is order unity in terms of the gyroradius and aspect ratio scaling. The maximum value of  $\hat{g}$  is given by the infinite parabolic mirror field  $B = B_o(1 + z^2/L^2)$  and where  $\hat{g} = 3/4$  [Horton, 1981].

In this analytic model the frequency and growth rate are functions of the six dimensionless parameters:  $m$ ,  $\hat{\Omega}$ ,  $\hat{g}$ ,  $A_p$ ,  $\frac{b}{a}$ ,  $\frac{T_i}{T_e}$ , and units of frequency are  $c_s \rho_s / a^2$ .

The dimensionless frequency and the dimensionless growth rate given by the quadratic dispersion relation (IV.28) in the laboratory frame are

$$\begin{aligned} \omega &= m\hat{\Omega} + \frac{m}{\nu_{m,n} + A_p} [A_p - \hat{\Omega} - \frac{T_i}{T_e}(\nu_{m,n} - 1)] \\ \gamma &= \frac{m}{\nu_m + A_p} [(\nu_{m,n} + A_p)(\hat{\Omega}^2 + \hat{g}) - (\hat{\Omega} + \frac{T_i}{T_e}(\nu_{m,n} - 1) - A_p)^2]^{1/2} \end{aligned} \quad (IV.31)$$

respectively.

The discriminant determining stability (in the dissipationless limit) is given by

$$\Delta = B^2 - 4AC = 4m^2 \left\{ \left[ \hat{\Omega} + \frac{T_i}{T_e}(\nu_{m,n} - 1) - A_p \right]^2 - (\hat{g} + \hat{\Omega}^2)(\nu_{m,n} + A_p) \right\}. \quad (IV.32)$$

The stabilizing condition as

$$A_p^2 - A_p \left[ \hat{\Omega}(\hat{\Omega} + 2) + \hat{g} + 2 \frac{T_i}{T_e} (\nu_{m,n} - 1) \right] - [(\nu_{m,n} - 1) \left( \hat{\Omega} - \frac{T_i}{T_e} (\nu_{m,n}^{1/2} + 1) \right) (\hat{\Omega} + \frac{T_i}{T_e} (\nu_{m,n}^{1/2} - 1) + \nu_{m,n} \hat{g})] \geq 0 \quad (IV.33)$$

For given  $m$ ,  $\hat{\Omega}$ ,  $\hat{g}$ , we can determine critical  $A_p$  for stability. We find a good approximation for the critical density above which the mode is stable in the absence of electron dissipation

$$(A_p)_{crit} \equiv A_p^s \simeq \hat{\Omega}(\hat{\Omega} + 2) + \hat{g} + 2 \frac{T_i}{T_e} (\nu_{m,n}(b/a) - 1). \quad (IV.34)$$

The region of stability determined by (IV.33) is shown in Fig.4.2-4.

We discuss the different effects on stability as follows.

#### A. Effect of Passing Electrons

For low rotational speeds there is in general both a critical or threshold value  $A_p^c$  and a cutoff value  $A_p^s$  for the passing electron density. For unstable modes  $A_p^c < A_p < A_p^s$ . For  $A_p$  below threshold  $A_p^c$  the stable region in  $\hat{\Omega}$  is determined by finite Larmor radius effects through  $(T_i/T_e)(\nu_{m,n} - 1)$  and the value of  $\hat{g}$ .

For reference parameters we take  $\hat{g} = 0$  which implies just enough rf stabilization to balance the bad axisymmetric curvature or very weak bad curvature and  $b/a = 3$ . The stable windows for  $m = 1$  and  $m = 2$  are shown in Fig 4.2(a-b). For  $m = 1$ , Fig.4.2(a) seems give a stable window  $-2 < \hat{\Omega} < 0$ . But carefull treatment shows that for  $A_p \ll 1$ , the stable window is located in  $0 < \hat{\Omega} < 2$  which consistent with what we found in section IV.3.[see Fig.4.2(b)]. For  $m = 2$

the window  $-0.2 < \hat{\Omega} < 2.0$  is destabilized for  $A_p > A_p^c \simeq 1$  and stabilized for  $A_p > A_p^s \simeq 3.0$ . For  $|\hat{\Omega}| > 1$  the system is unstable for all  $A_p$  below  $A_p^s$  where  $A_p^s$  is given by Eq. (IV.34).

For  $\hat{g} = +1$ , a typical value for an axisymmetric system with no rf stabilization, there are unstable regions for all  $\hat{\Omega}$  for  $0 < A_p < 2$  for the  $m = 1$  mode and for  $0 < A_p < 4$  for the  $m = 2$  as shown in Fig.4.3.

For  $\hat{g} = -1$  corresponding to a strongly quadrupole or rf stabilized system the  $m = 1$  mode has a stable window for  $-2.7 < \hat{\Omega} < +1.2$  for all  $A_p$  as shown in Fig.4.4. The  $m = 2$  mode is stable for  $-\infty < \hat{\Omega} \leq 1$  for all  $A_p$ .

#### B. Effect of the Ratio of the Wall-to-Plasma Radius

Now we consider the effect of varying the wall-to-plasma radius ratio  $b/a$ . Decreasing  $b/a$  may be viewed as the relaxation of the original plasma profile from the instabilities or from other transport processes. In the analytic model used here there is an edge or wall plasma density given by  $n(b)/n(0) = \exp(-b^2/a^2)$ . For the values of  $b/a = 3, 2, 1$  the edge-to-central density ratios are  $10^{-4}$ , .02 and .37, respectively.

We use  $\hat{g} = 0$  and  $\hat{\Omega} = -4$  as the reference values for varying the plasma-to-wall radius. In Fig.4.5 we show the effect of decreasing  $b/a$ . As the wall is brought into the plasma, the  $m = 1$  growth rate increases as  $(\nu_{1,0}(b/a) - 1)^{1/2}$  whereas the finite Larmor radius stabilization increases as  $(T_i/T_e)(\nu_{1,0}(b/a) - 1)$ . For small  $b/a$  first the  $m = 3$  and finally the  $m = 2$  mode become stabilized; however, the  $m = 1$

mode remains unstable for smaller  $\frac{b}{a}$ . The effect of the wall-to-plasma radius on the threshold passing electron density is shown by comparing Fig.4.6 for  $b/a = 1$  with Fig 4.3 for  $b/a = 3$ . The  $A_p$  required for stabilization of the  $m = 1$  mode increases from  $A_p(b/a = 3) = 2$  to  $A_p(b/a = 1) = 10$ .

Thus we find that as  $b/a$  decreases from 3 to 1 the finite Larmor radius effects opens up a stable window for  $-2 < \hat{\Omega} < 2.5$  and  $A_p < A_p^c \sim 4$  but for  $\hat{\Omega} < -2$ , typical of tandem mirror rotations, there is a substantial increase in the  $A_p$  required for stability,  $A_p > A_p^s(b/a)$ , with decreasing  $b/a$ .

The result of varying  $b/a$  has an important implication for the quasilinear evolution of the system. As the quasilinear relaxation take place, the plasma radius becomes a function of time  $a(t)$  and increases toward  $b$ . The stability analysis implies that in the final stages of evolution only the  $m = 1$  mode is unstable and that there may be a marginally stable quasilinear steady state for  $a(t \rightarrow \infty) \simeq b$ . In this final state the plasma is poorly confined with  $n(b)/n(0) \simeq 1/3$  for the Gaussian density model.

### C. Effect of Varying the Quadrupole RF Fields

The effect of varying the quadrupole or rf fields is parameterized by the value of  $\hat{g}$ . Changing the system from a strongly unfavorable effective gravity  $\hat{g} = +1$  to a strongly favorable effective gravity  $\hat{g} = -1$  is shown by comparing Figs 4.3 and 4.4. or Figs.4.6 and 4.7. For  $\hat{g} = +1$  the system is unstable to  $m = 1$  and  $m = 2$  modes for all  $\hat{\Omega}$  unless the passing electron density parameter  $A_p$  exceeds



the cutoff value  $A_p > A_p^s$ . For strongly favorable  $\hat{g}$  there is a stable rotational window for  $|\hat{\Omega}| \leq 1$  for  $m = 1$  and  $m = 2$  for all values of  $A_p$ .

For faster rotational speeds  $\hat{\Omega}^2 > |\hat{g}|$  the value of  $\hat{g}$  is of secondary importance compared with the values of  $A_p$  and  $b/a$  in determining the stability of the system.

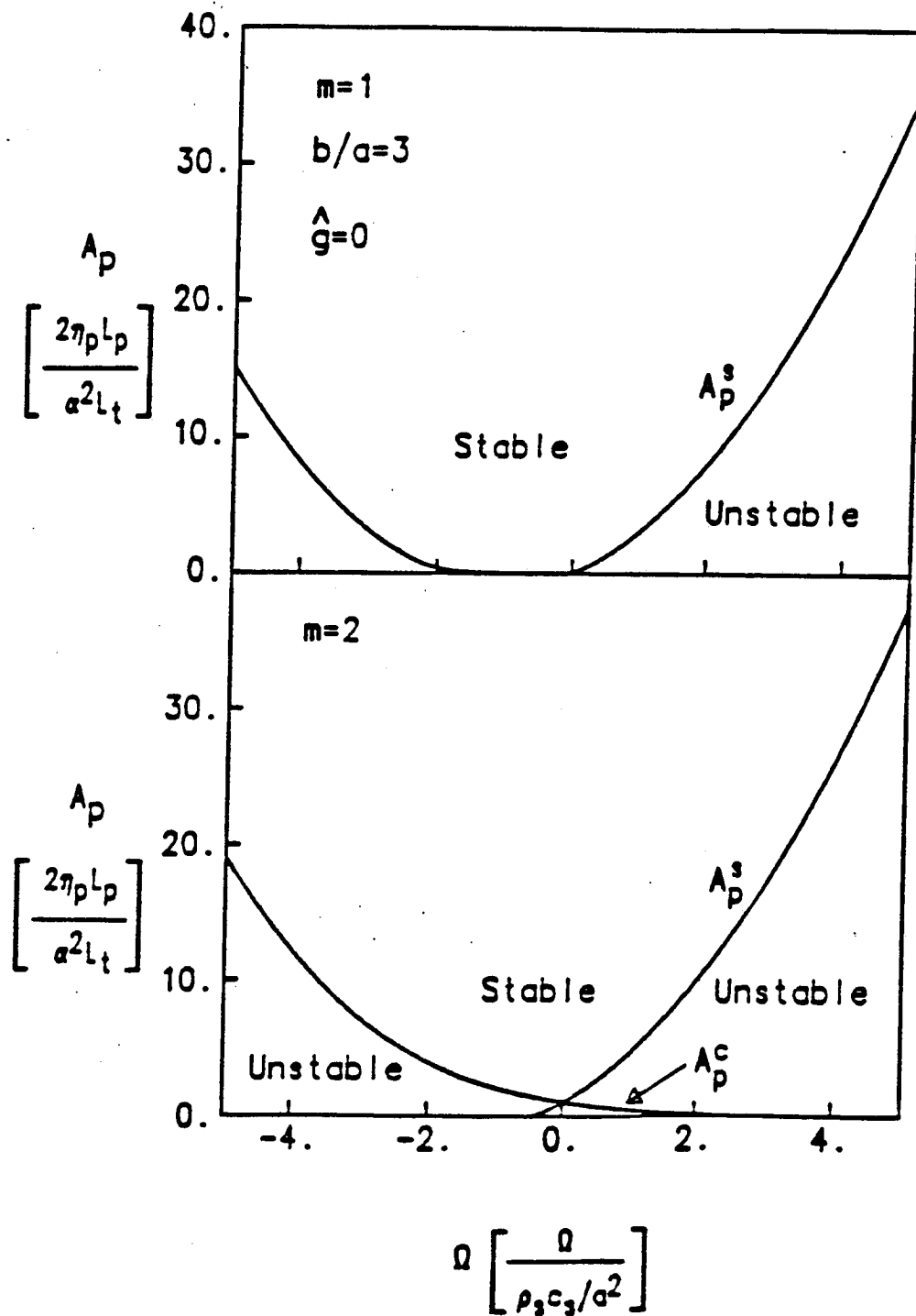


Fig.4.2(a) The stability boundaries in the plane representing passing particle density,  $A_p$ , and solid body rotation frequency,  $\hat{\Omega}$ , with  $T_i/T_e = 1$ ,  $\hat{g} = 0$ ,  $b/a = 3$ , and  $m = 1.2$ .

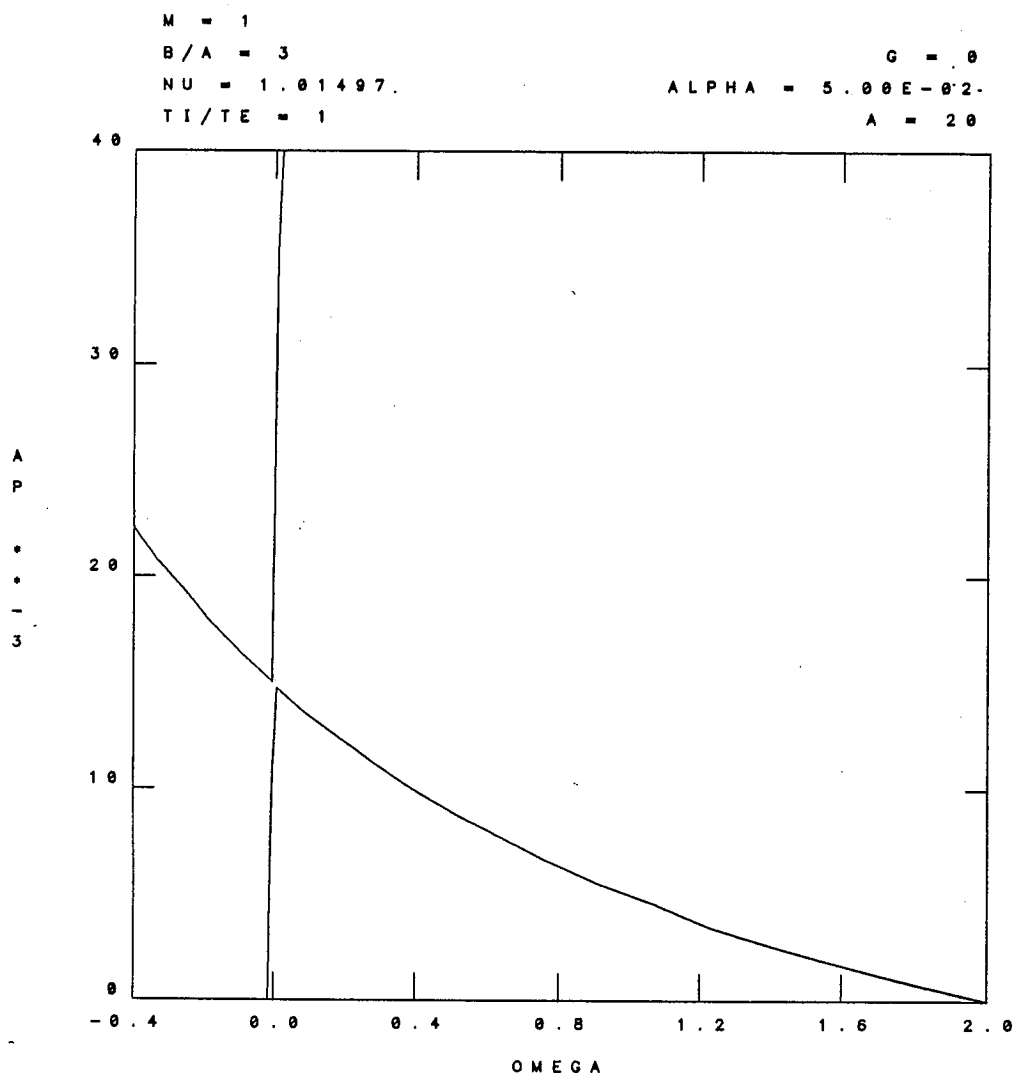


Fig.4.2(b) The details of stability boundary for  $m = 1$ ,  $A_p \ll 1$ , magnification =  $1 \times 10^3$  compared with Fig.4.2(a). Notice the consistency with Fig.3.5.

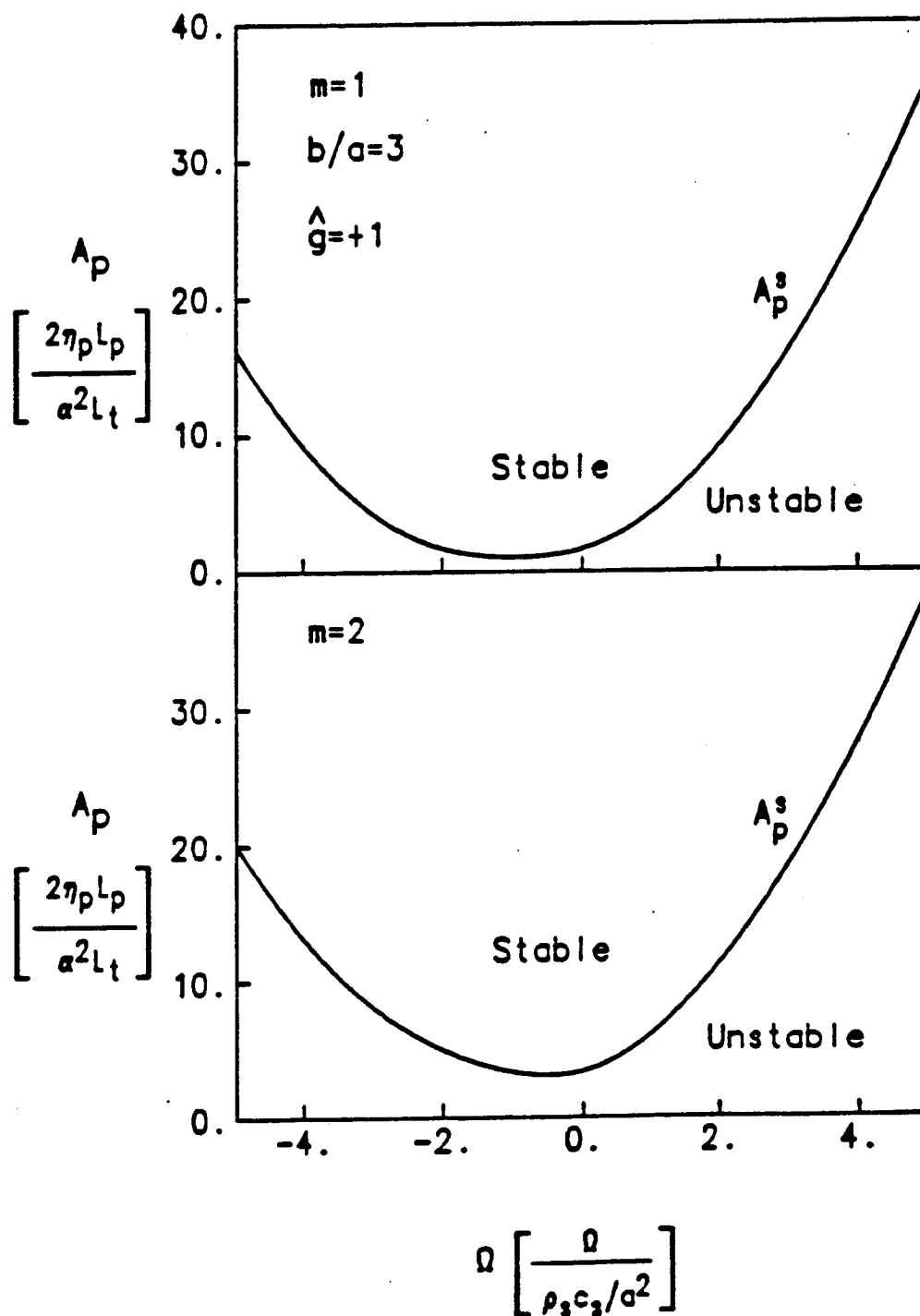


Fig.4.3 The same as Fig.4.2(a) with a unfavorable radial well,  $\hat{g} = +1$ .

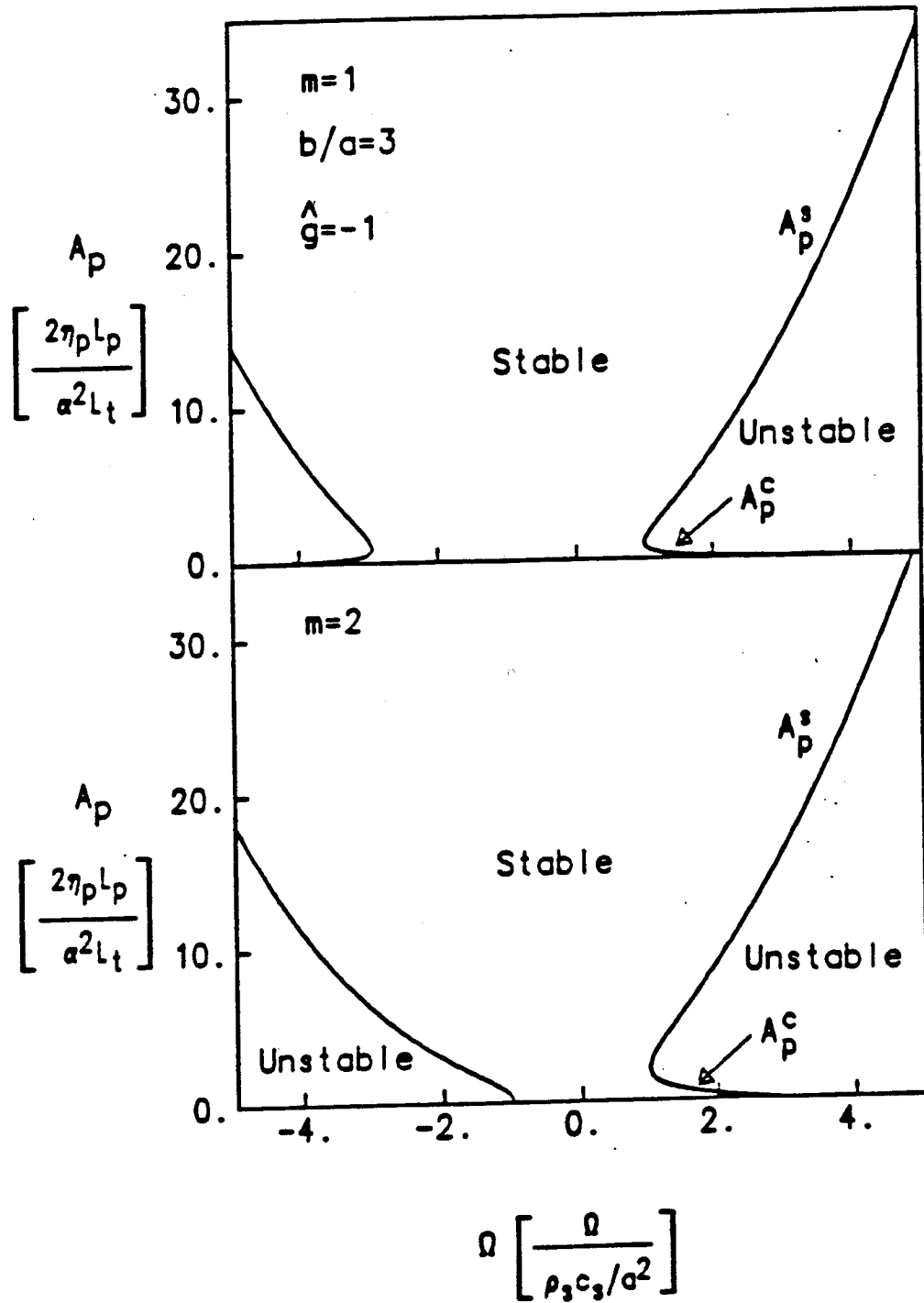


Fig.4.4 The same as Fig 4.2(a) with a favorable radial well,  $\hat{g} = -1$ .

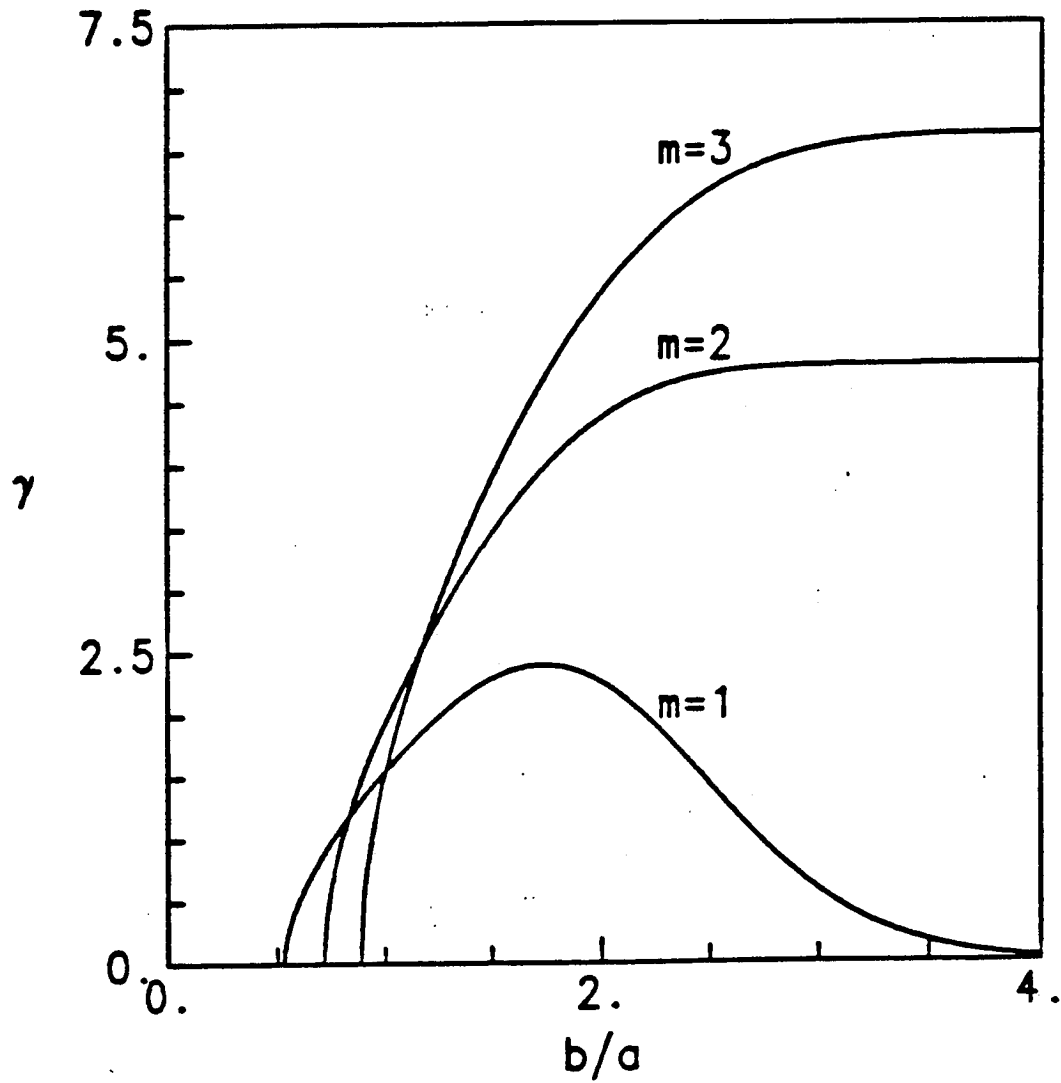


Fig.4.5 The variation of the low- $m$  growth rates with wall-to-plasma radius ratio,  $b/a$ , for solid body rotation,  $\hat{\Omega} = -4$ , and Gaussian density profile.

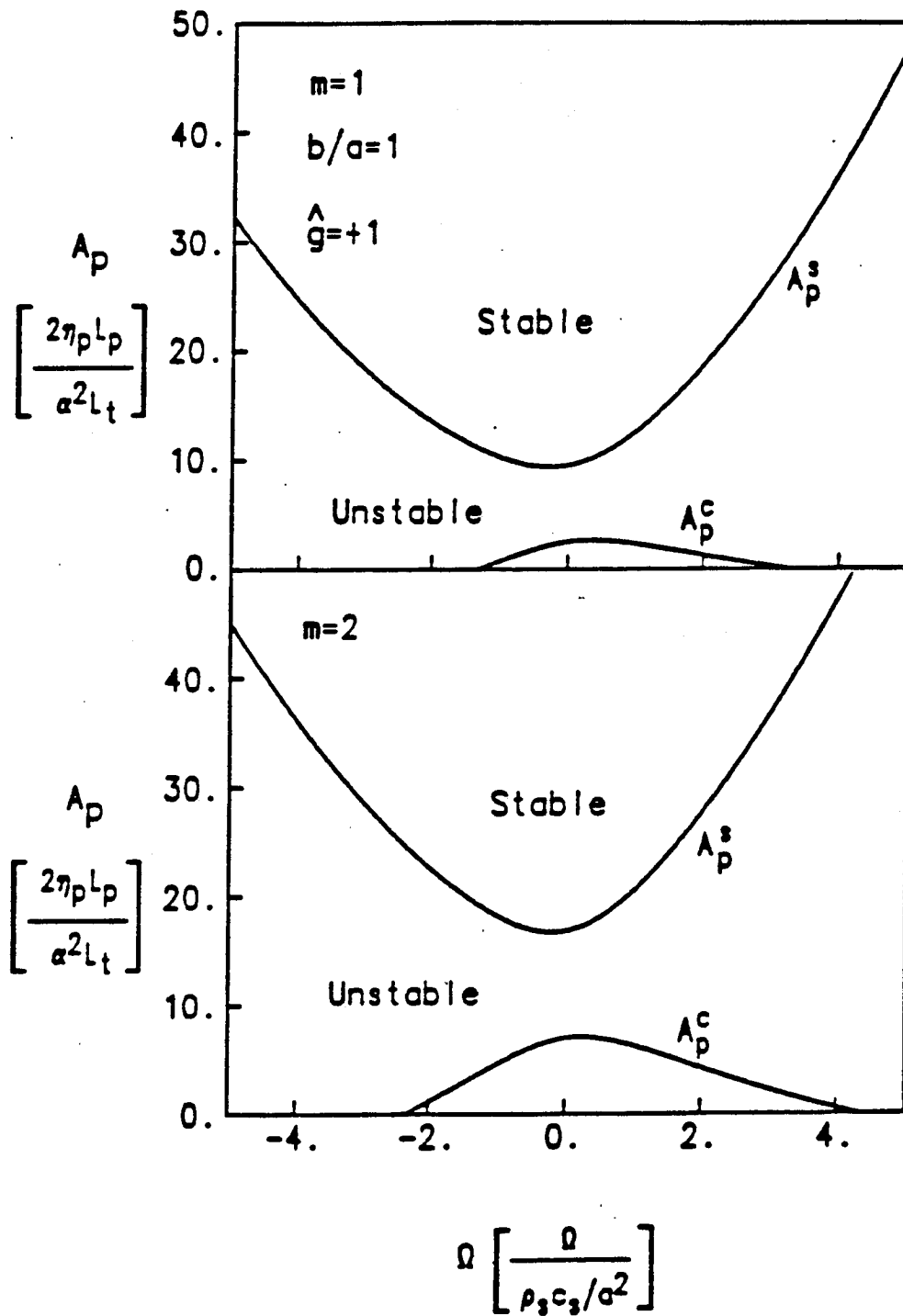


Fig.4.6 The same as Fig.4.3 with  $\hat{g} = +1$ , but  $b/a = 1$ .

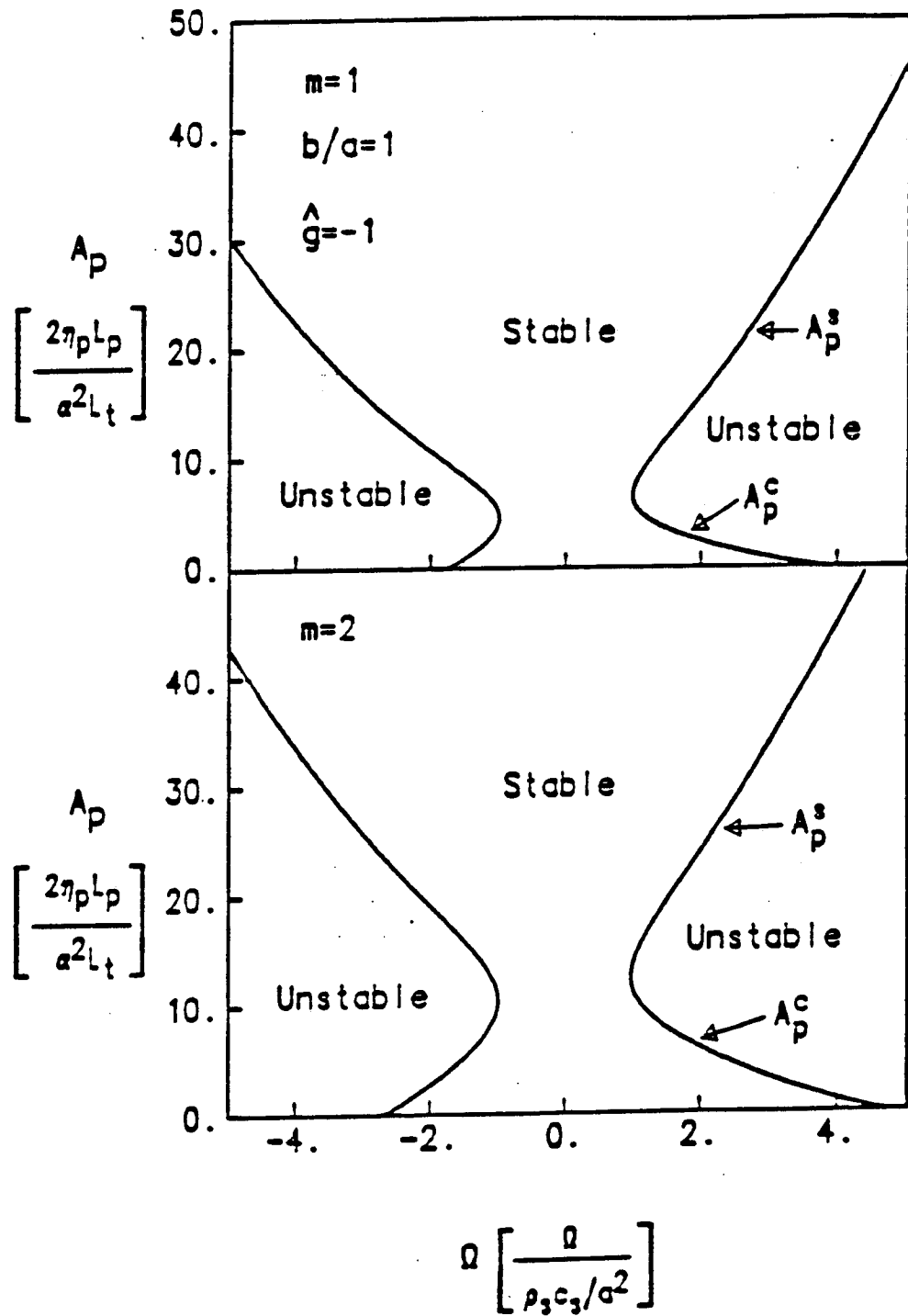


Fig.4.7 The same as Fig.4.4 with  $\hat{g} = -1$ , but  $b/a = 1$ .



### IV.3 Differential Rotation and Passing Particles

For general profiles of density and potential that evolve from background transport processes the stability analysis must be performed numerically. In this section we use the well-known shooting method to find the eigenvalues and wavefunctions from Eq.(24). In this study we restrict consideration to the simple boundary condition  $\delta\phi_m(r = b) = 0$ .

The profiles used in the study are Gaussian and parabolic for the density

$$n_g(r) = n_o \exp(-r^2/a^2) \quad (IV.35)$$

$$n_p(r) = n_o(1 - r^2/b^2) \quad (IV.36)$$

and the inverse tangent for the rotational speed

$$\Omega(r) = c_1 \tan^{-1} \left( \frac{r - r_1}{\Delta} \right) + c_2 \quad (IV.37)$$

where  $c_1$  and  $c_2$  are given in terms of the central rotation frequency  $\Omega_o = \Omega(r = 0)$  and the edge rotation frequency  $\Omega_b = \Omega(r = b)$  by

$$c_1 = \frac{\Omega_b - \Omega_o}{\tan^{-1} \left( \frac{b - r_1}{\Delta} \right) + \tan^{-1} \left( \frac{r_1}{\Delta} \right)} \quad (IV.38)$$

$$c_2 = \Omega_o + c_1 \tan^{-1} \left( \frac{r_1}{\Delta} \right)$$

The constant  $\Delta$  is a parameter controlling the steepness of the rotation frequency variation. The potential  $\phi_o(r)$  and rotational  $\Omega(r)$  profiles used in the study are shown in Fig. 4.8.

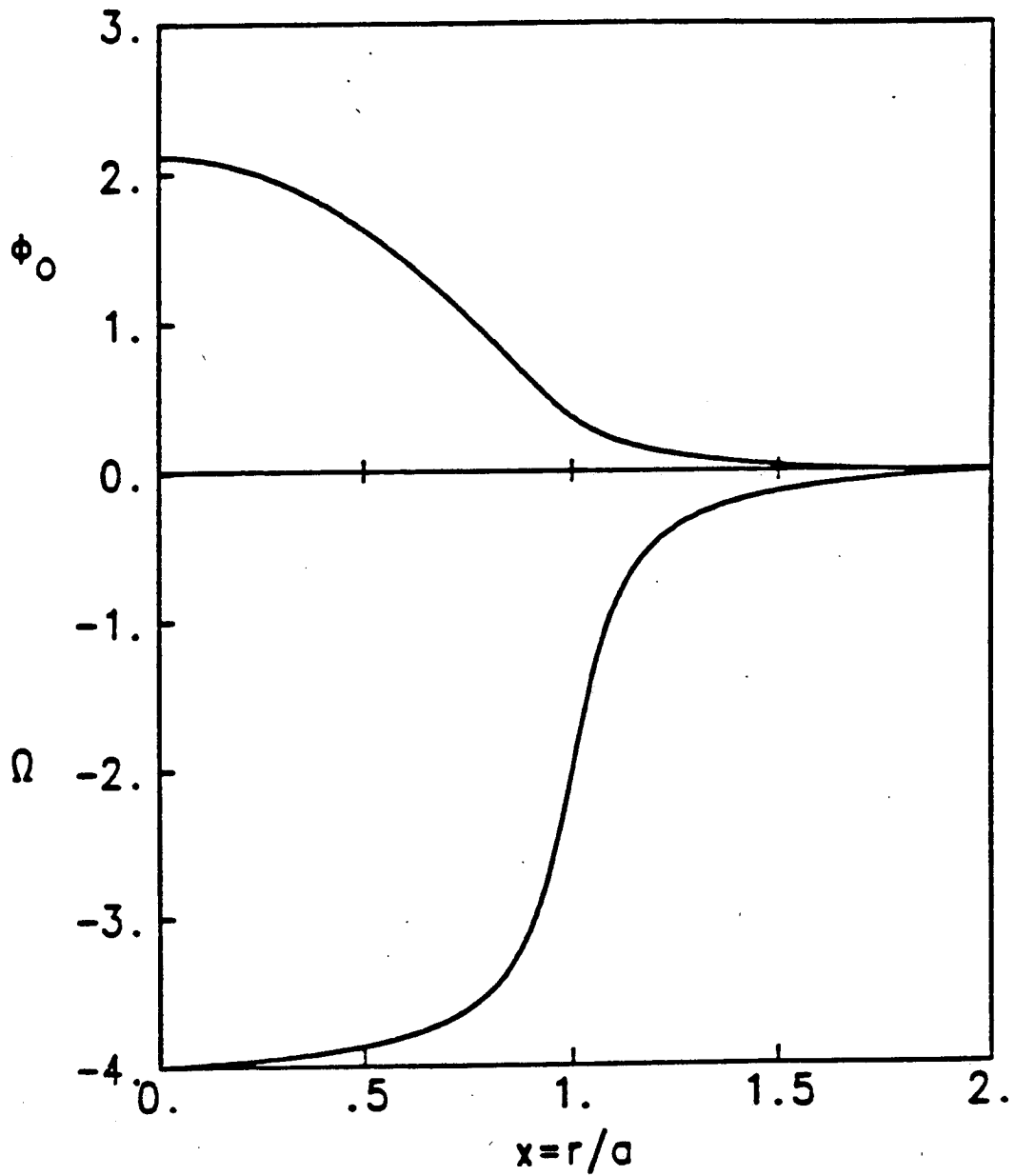


Fig.4.8 Typical profiles of the equilibrium potential and the sheared rotational frequency,  $\hat{\Omega}(x)$ , used in the study of differential  $\mathbf{E} \times \mathbf{B}$  rotation. Here, the on-axis rotation rate is  $\hat{\Omega}_o = -4$ , the edge rotation is  $\hat{\Omega}_b = 0$ ,  $\Delta/a = 0.1$ ,  $r_1/a = 1$ .

The accuracy of the eigenvalue solver is tested by taking the limit  $\Omega_b = \Omega_o$  which gives  $c_1 = 0$  and  $\Omega(r) = \Omega_o = \text{constant}$  and comparing the results with the analytic solutions given in Eq. (IV.34) for a Gaussian density profile.

#### A. Differential Diamagnetic Drifts

For the parabolic density profile (IV.39) the absolute value of the diamagnetic drifts  $\omega_{*i,e}(r)$  are strongly increasing functions of radius. In this subsection we keep the  $\mathbf{E} \times \mathbf{B}$  rotation rigid at  $\Omega = \Omega_o$  and show that the change from a Gaussian to a parabolic density profile is stabilizing for comparable mean density gradients. (As usual in changing a profile, an exact comparison is not meaningful since it depends on choosing some arbitrary constraints.) the decreased growth rate is expected from the local approximation since the dispersion of the wave frequency  $\omega_{*i,e}(r)$  with radius weakens coherence of the modes. For the parabolic density we note that although  $\omega_{*i,e}(r) \rightarrow \infty$  as  $r \rightarrow b$  the function  $n(r)\omega_{*i,e}(r)$  in Eq.(24) remains finite for  $0 \leq r \leq b$ .

The unstable modes in the spectrum  $m = 1 - 10$  are shown in Fig. 4.9. The width of the unstable spectrum is limited by FLR effects which are enhanced by the radial dispersion from  $\omega_{*i,e}(r)$ .

In the presence of  $\omega_{*i,e}(r)$  the modes develop radially outgoing and incoming wave components given by  $k_r = (2i)^{-1}(\delta\phi_m^* \partial_r \delta\phi_m - \delta\phi_m \partial_r \delta\phi_m^*)$  which, in contrast, is zero for for the  $\omega_{*i,e} = \text{constant}$  Gaussian profile. The wave function for the parabolic profile is peaked closer to the plasma in radial position than the

Gaussian wavefunction consistent with the local approximation. The change in the wavefunction is shown in Fig. 4.10 (a), (b), which compares the  $m = 1, 2, 3$  modes for the parabolic and Gaussian profiles and gives their respective frequencies and growth rates. The preferred stability of the parabolic profile suggests that quasilinear relaxation may drive the system toward states with variations in  $\omega_{*i}(r)$  subject to the constraints imposed by particle sources and sinks.

### B. Differential $\mathbf{E} \times \mathbf{B}$ Rotation

For the Gaussian density profile with constant  $\omega_{*i,e}$  we decrease the magnitude of the speed of rotation of the outer plasma by varying  $\Omega_b$ . A smaller  $\Omega_b$  than  $\Omega_o$  is observed in the experiments [Hooper et al, 1983], and may result from collisional ion viscosity in the edge plasma or charge exchange collisions with the higher edge neutral density component.

In Fig. 4.11(a) we show the  $m = 1$  growth rate as a function of decreasing edge plasma rotation speed  $\Omega_b$ . With the central plasma rotating at  $\Omega_o = 2\omega_{*i}(\hat{\Omega} = -4$  for  $T_i = T_e$ ) the solid body growth rate is  $\gamma_1 \simeq 2[\rho_s c_s / a^2]$  for  $A_p \leq 2$  as given by Eq.(IV.34) and shown in Fig. 4.11(a) at  $\Omega_b = \Omega_o$ . As the edge speed drops to zero the growth rate decreases for all  $A_p$ .

Figure 4.11(b) shows the same parameter variation for the  $m = 2$  mode which has the solid body growth rate  $\gamma_2 \simeq 4[\rho_s c_s / a^2]$  for  $\Omega_b = \Omega_o$ . Again the growth rate decreases as  $\Omega_b$  approaches zero.

Changing to a parabolic density profile combines the stabilizing effects of

$\omega_*(r)$  and  $\Omega(r)$  and is shown in Fig. 4.12(a) for  $m = 1$  and Fig. 4.12(b) for  $m = 2$ .

A possible explanation of the stabilizing effect of the differential rotation on the interchange instability driven by the centrifugal force acting on the density gradient is the change in the topology of the eigenfunction. As the interchange of the plasma from  $\delta n = -\xi \partial n_o / \partial r$  takes place to release the energy density

$$\delta W = \frac{1}{2} m_i \delta n r \Omega^2 \xi = -\frac{1}{2} m_i r (\partial n_o / \partial r) \Omega^2 \xi^2$$

the tongues of displaced plasma are wrapped back in azimuthal angle (entrained) which decreases the amount of interchanged plasma. Mathematically, the falling behind or entrainment of the tongues is given by the phase shift that the eigenfunction develops from the dispersion in  $\tilde{\omega} = \omega - m\Omega(r)$ .

We take the wave function  $\delta\phi_m(r)$  as real in the interior of the plasma and write  $|\delta\phi_m| \cos[m\theta - \omega t + \beta(r)]$  for the phase shift arising from the complex wavefunction  $\delta\phi_m(r) = |\delta\phi_m| \exp[i\beta(r)]$  for  $r > 0$ . Although it is not possible to derive a formula for  $\beta(r)$  we can estimate the value of  $\beta$  by integrating Eq.(IV.20) across the resonant layer defined by  $Re(\omega) = m\Omega(r_m)$  while neglecting  $\beta(r)$  in all terms except the second derivative term. These approximations lead to

$$\frac{d\delta\phi_m}{dr} = \frac{d}{dr} |\delta\phi_m| + i |\delta\phi_m| \frac{d\beta}{dr} \simeq \frac{F_m |\delta\phi_m|}{\omega - m\Omega(r)} \quad (IV.39)$$

for  $r$  sufficiently near the resonance  $\Omega(r_m) = Re(\omega/m)$ . Integrating through the resonance gives  $\beta = \pi F_m / m |d\Omega/dr|$  where  $F_m$  is a constant. This simple calcula-

tion of  $\beta$  is useful for understanding the origin of  $\beta$ , but the value of  $\beta$  is computed from the  $\arg[\delta\phi_m(r)]$ .

The change in the topology of the wavefunctions is shown in Fig. 4.13 and Fig. 4.14, which gives the contours of constant  $\phi(r, \theta, t) = \phi_o(r) + |\delta\phi_m(r)|\cos[m\theta + \beta(r) - \omega t]$  for a typical 25th wave. The spiraling of the tongues of plasma develops in the vicinity of the resonant layers. In contrast for solid body rotation the wavefunction is purely real ( $\beta \equiv 0$ ) and the tongues or arms are pure radial displacements with symmetry about the radial axes of the arms at  $\theta_n = 2\pi n/m$  with  $n = 1, 2, \dots, m$ .

A dynamical picture of the stability effect of the differential rotation follows from the vorticity theory of instability given by Lin [Lin, 1966]. In this argument the flow  $V_\theta = r\Omega$  is decomposed into sum of vortex filaments and the interchange of a strong and weak vortex filament is shown to result in a perturbed flow that restores the original configuration provided the gradient of the vorticity does not vanish. In our problem the effective vorticity is  $\zeta = N \frac{d(rV_\theta)}{dr}$  which follows from the stability analysis of equation (IV.21) and the condition is equivalent to

$$F = \frac{d\zeta}{dr} \neq 0.$$

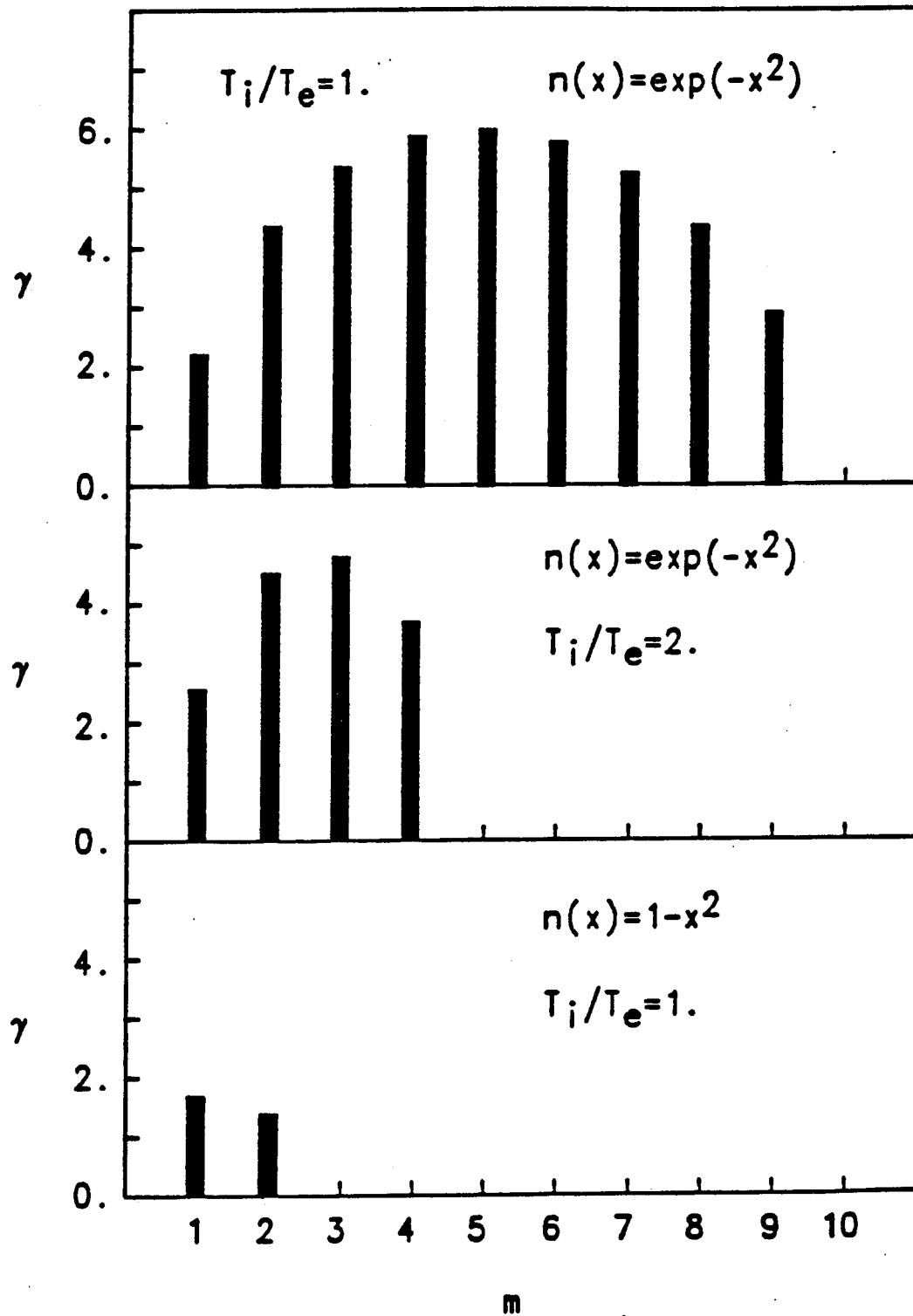


Fig.4.9 Low-m spectra for solid body rotation,  $\hat{\Omega} = -4$ , Gaussian density profile with  $T_i/T_e = 1, 2$ , and the parabolic density profile with  $T_i/T_e = 1$ .

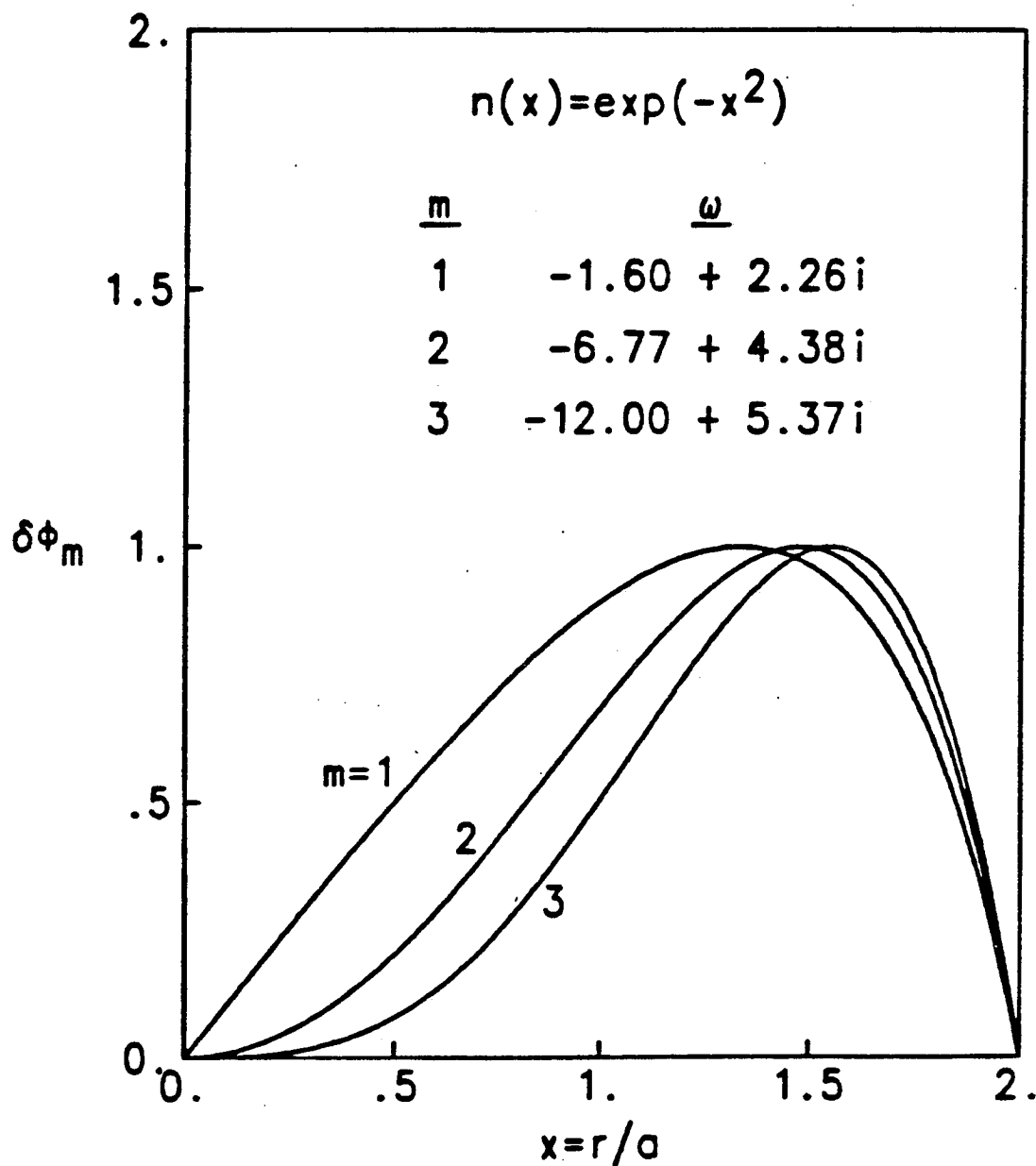


Fig.4.10(a) The wave functions vs.  $x = r/a$  for  $m = 1, 2, 3$ , with solid body rotation,  $\hat{\Omega} = -4$ ,  $T_i/T_e = 1$ , and a Gaussian density profile. The imaginary parts of the wave functions vanish.



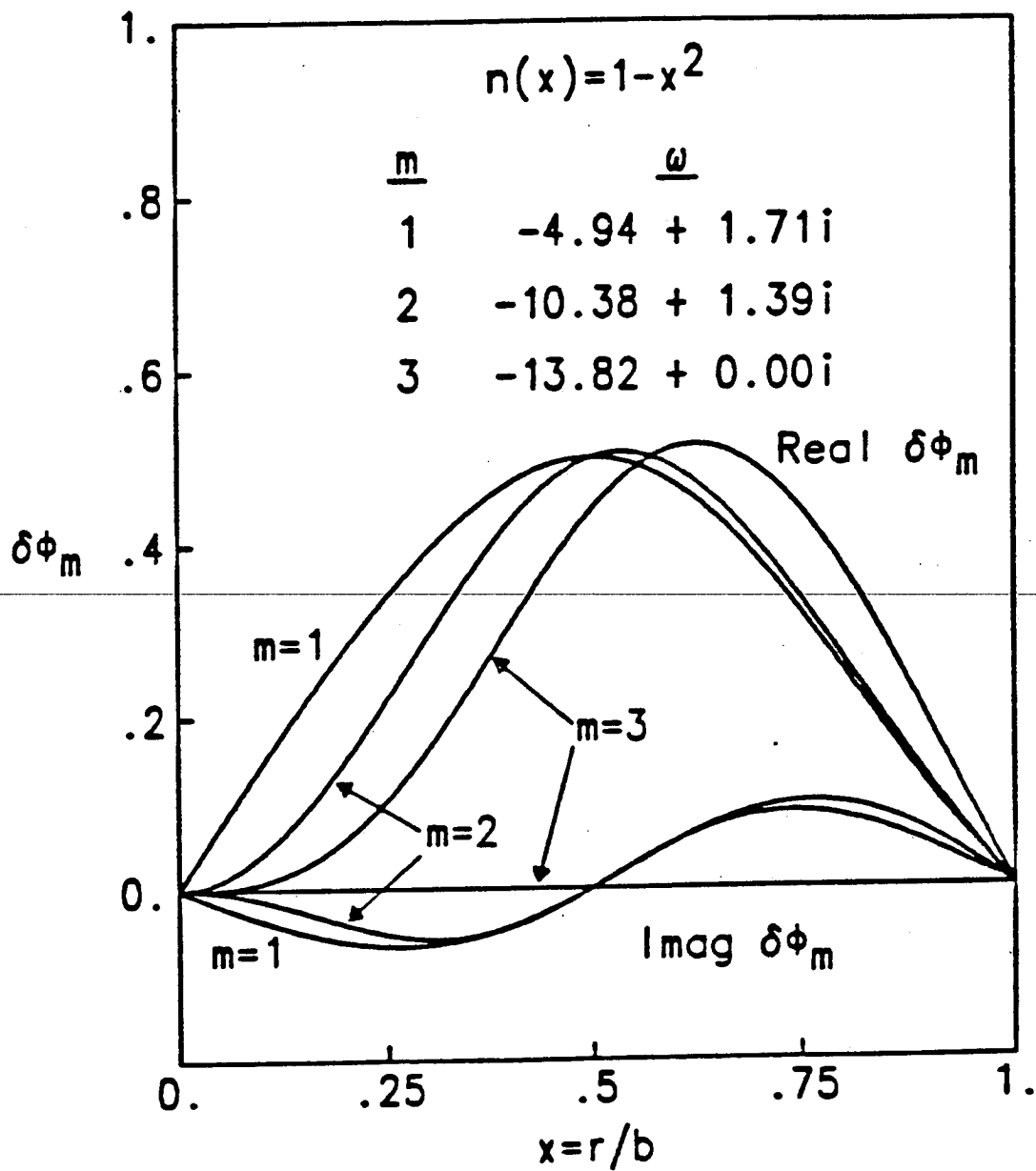


Fig.4.10(b) The real and imaginary parts of the wave functions vs.  $x = r/b$  for  $m = 1, 2, 3$ , with solid body rotation,  $\hat{\Omega} = -4$ ,  $T_i/T_e = 1$ , and a parabolic density profile.

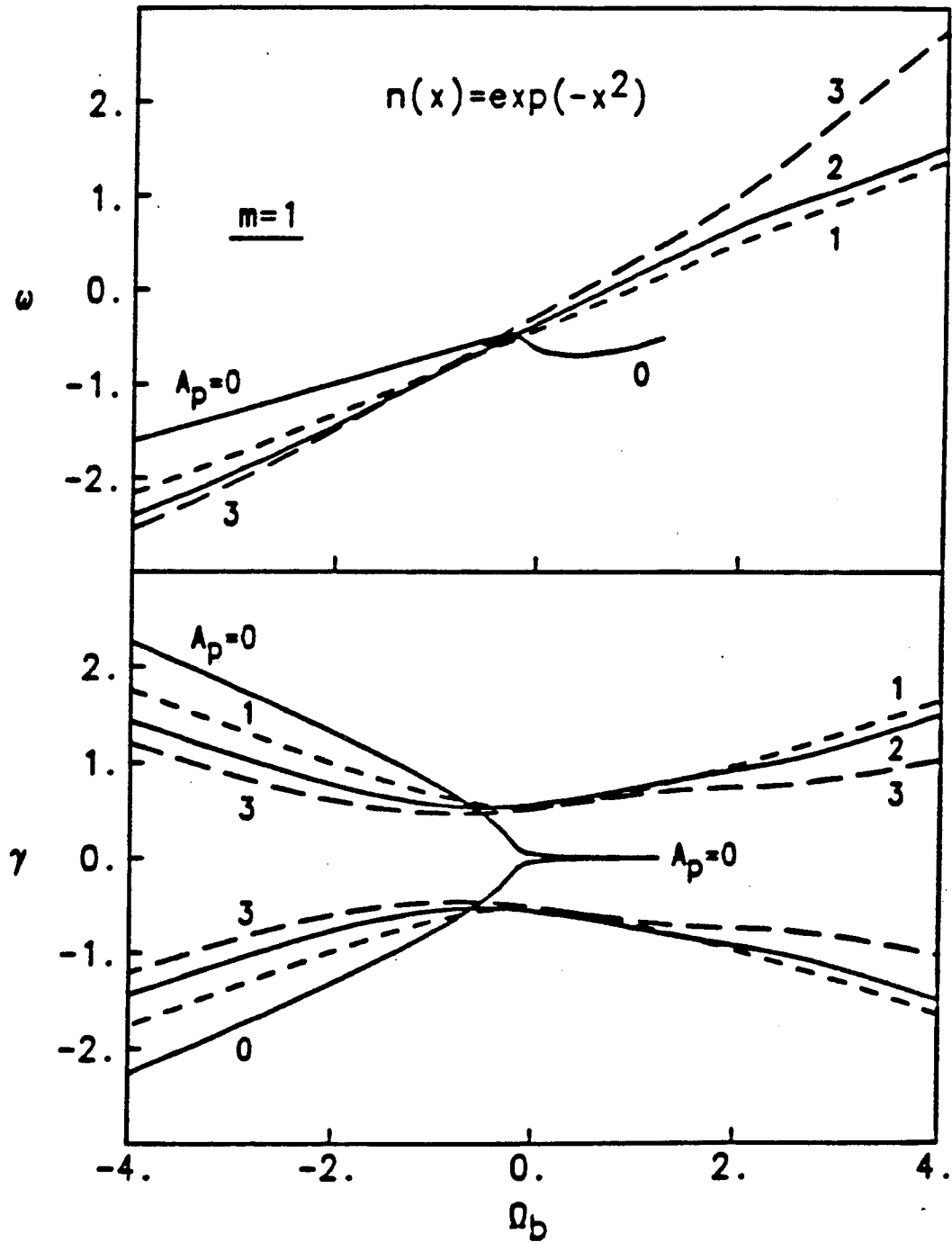


Fig.4.11(a) The real and imaginary frequencies versus the edge plasma rotation frequency,  $\hat{\Omega}_b$ , for the  $m = 1$  mode and varying  $A_p$ . The density profile is a Gaussian with  $b/a = 2$ ,  $\Delta/a = 0.1$ ,  $r_1/a = 1$ , and  $T_i/T_e = 1$ . The central rotation rate is  $\hat{\Omega}_o = -4$ , so that  $\hat{\Omega}_b = -4$  corresponds to solid body rotation.

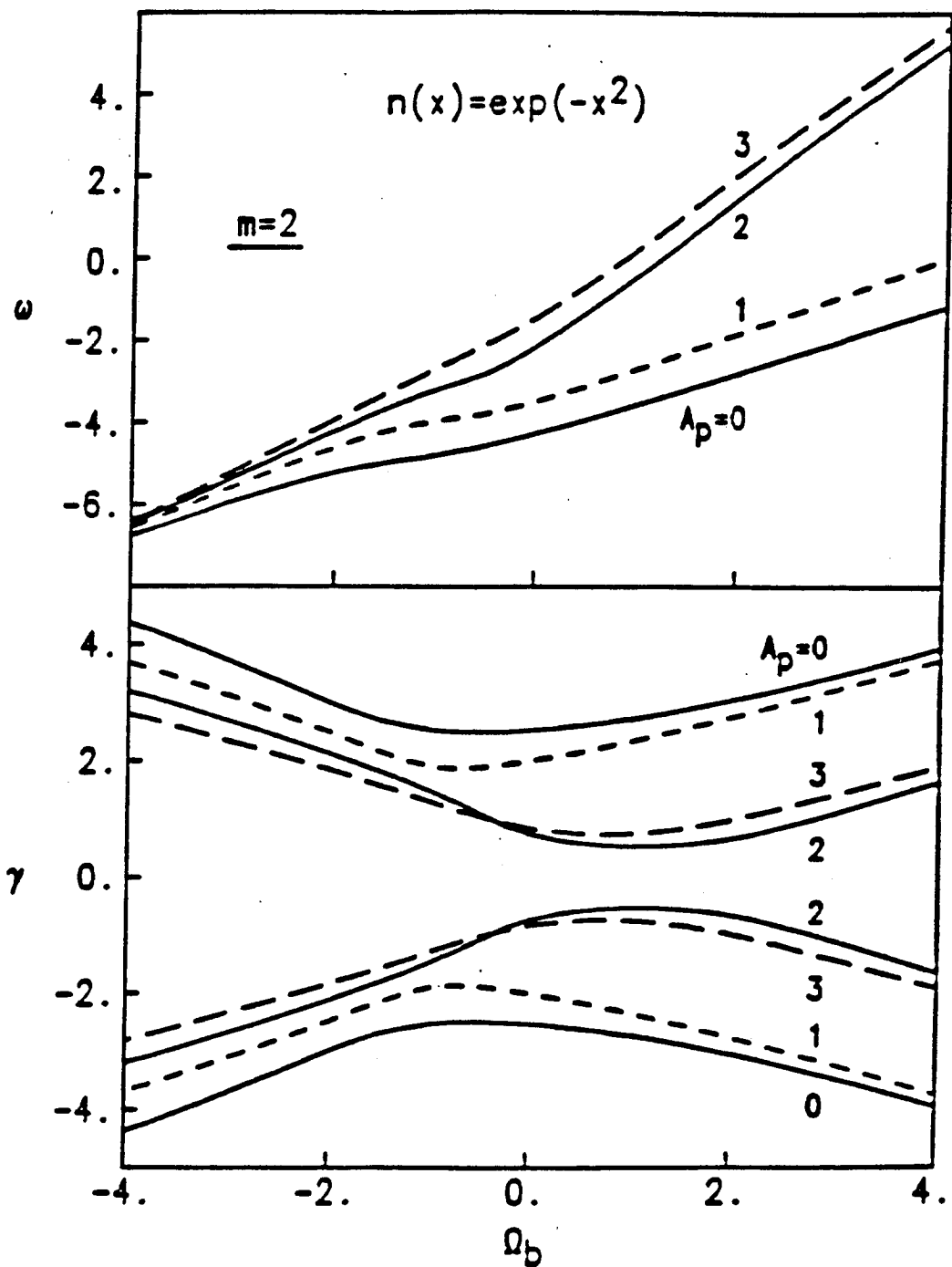


Fig.4.11(b) The same as Fig.4.11(a) for the  $m = 2$  mode.

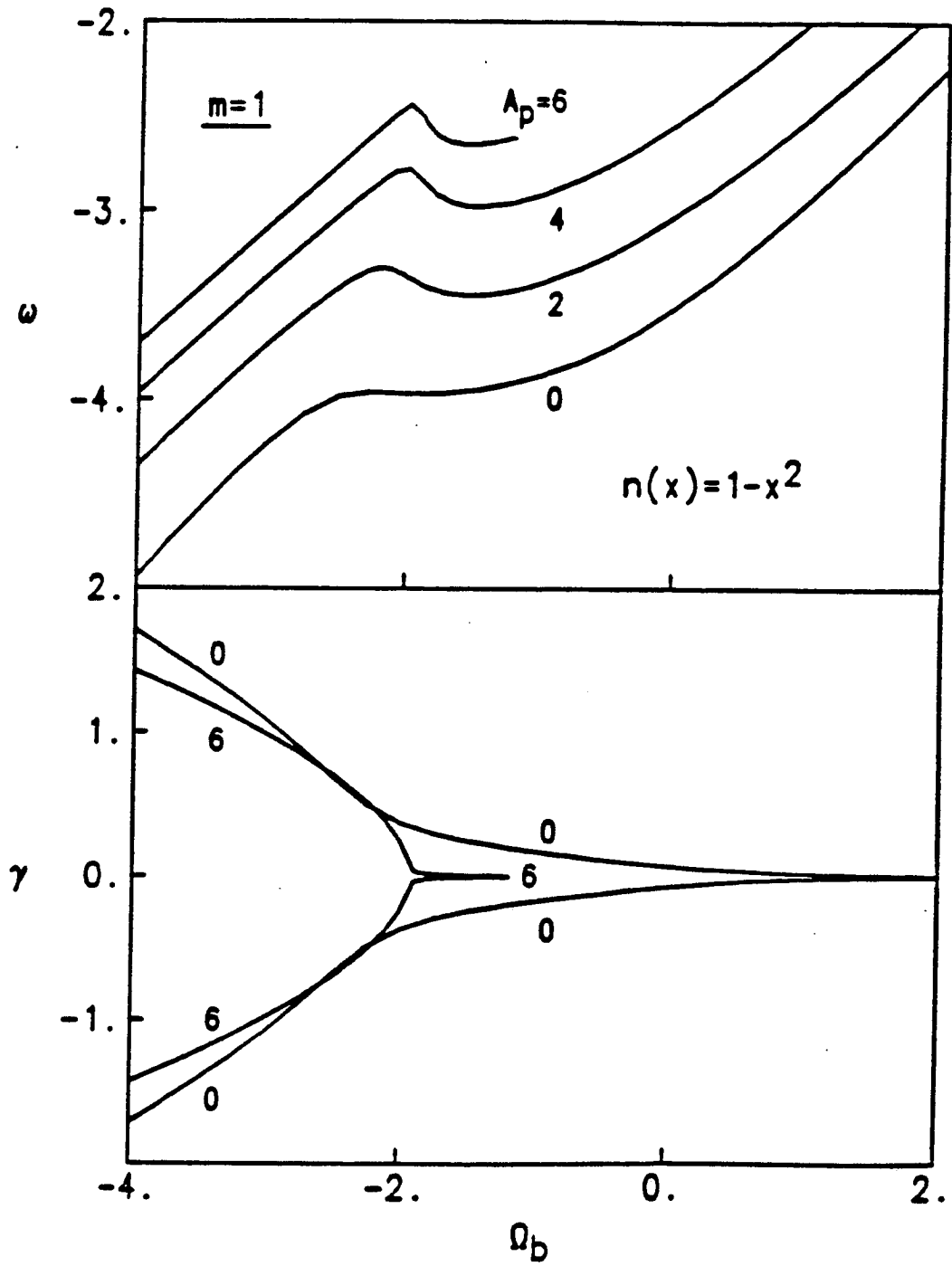


Fig.4.12(a) The same as Fig.4.11(a) for a parabolic density profile,  $m = 1$  mode. The shear parameters here are scaled to the plasma radius,  $\Delta/b = 0.1$  and  $r_1/b = 0.5$ .

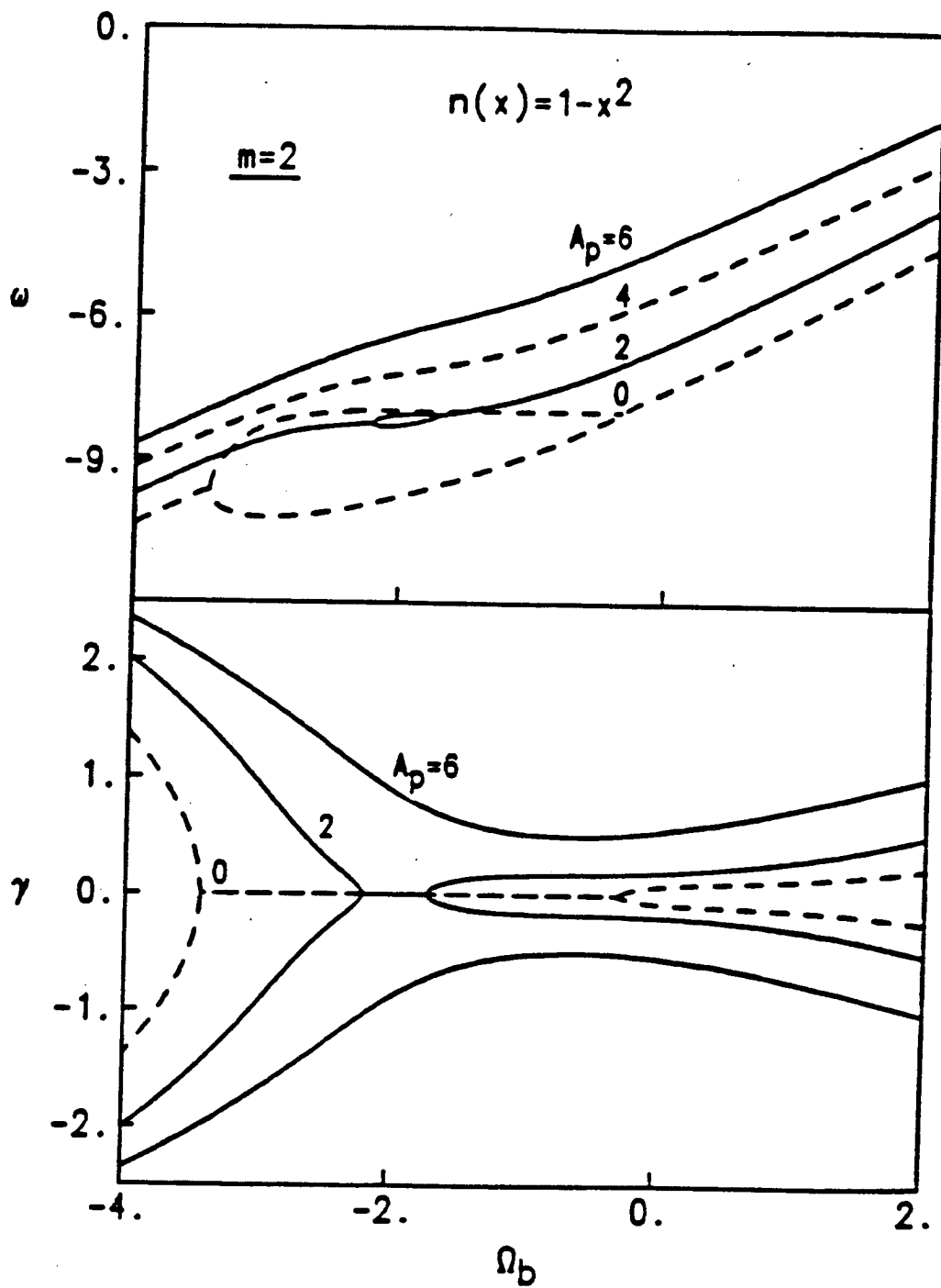


Fig.4.12(b) The same as Fig.4.12(a) for the  $m = 2$  mode.

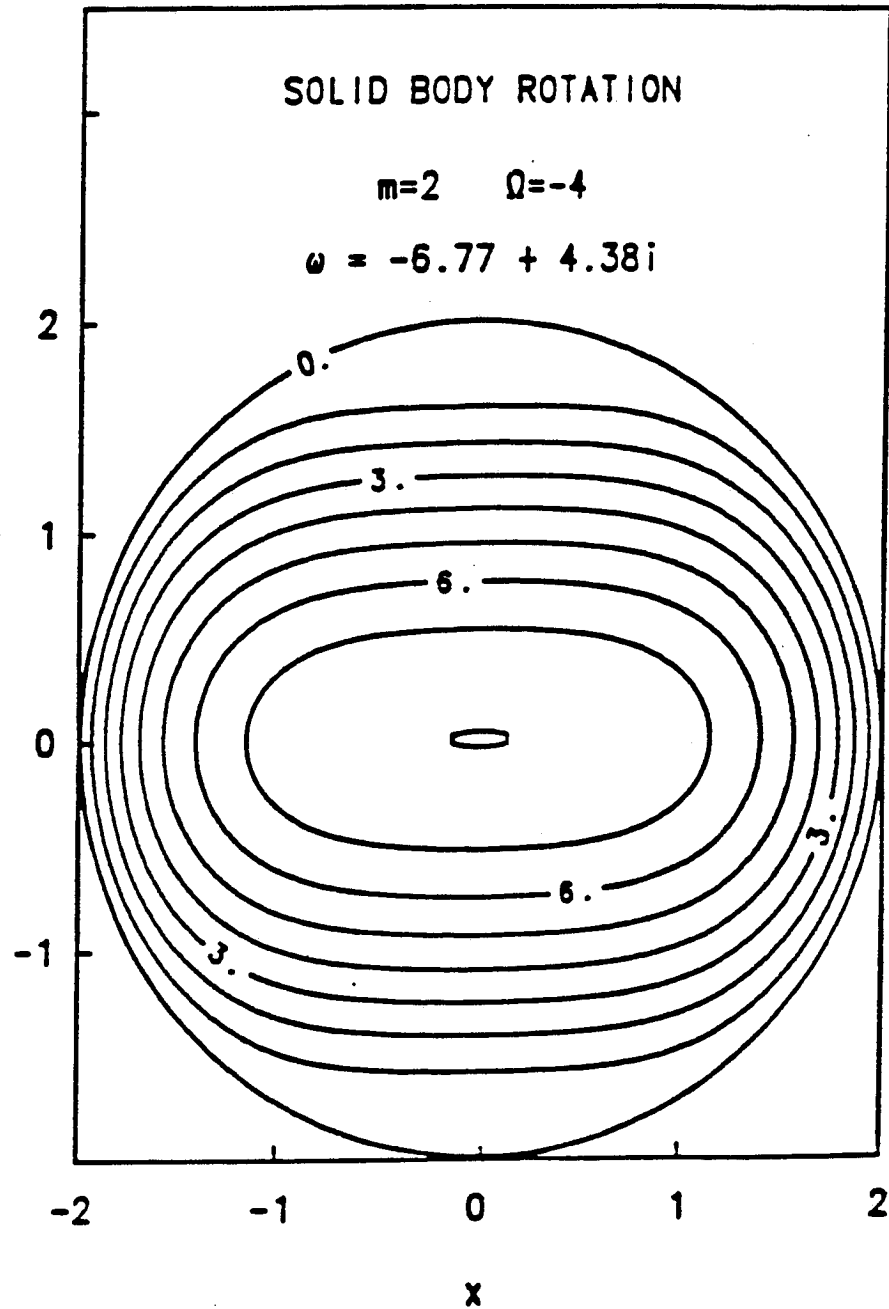


Fig.4.13 The contours of constant potential in the laboratory frame which are the instantaneous flow lines of the (clock-wise)  $\mathbf{E} \times \mathbf{B}$  guiding-center motion. Shown is the  $m = 2$  mode of the solid body rotating plasma for a Gaussian density profile. The amplitude of the perturbation is taken as  $\max(\delta\phi_m) = 0.25\phi_0(r = 0)$ .

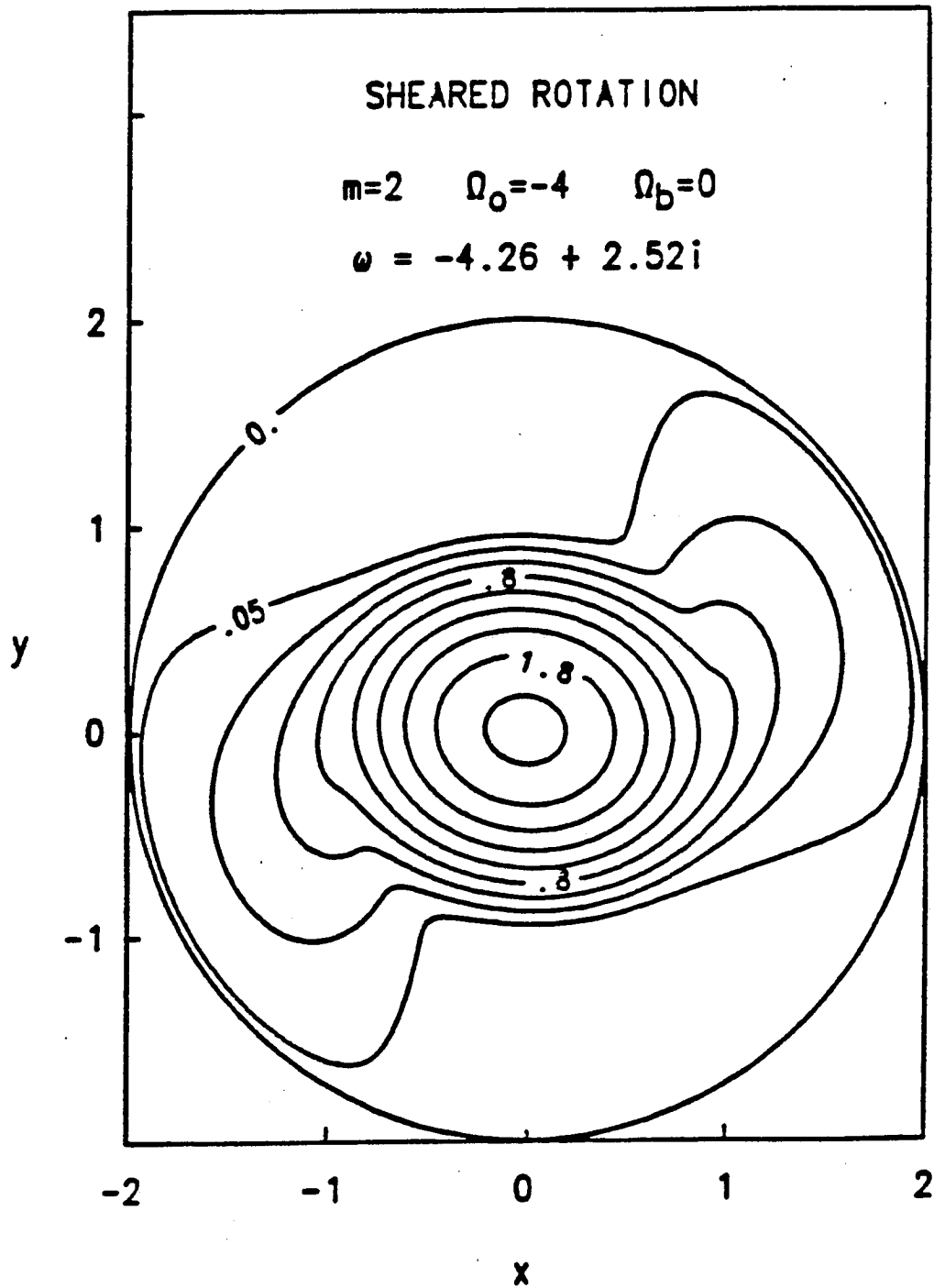


Fig.4.14 The same as Fig.4.13 for a differentially rotating plasma. The rotational profile is as shown in Fig.4.8.

#### IV.4 Summary and Conclusion

In this chapter we analyze the trapped particle mode stability of the rotating plasma including the effects of differential  $\mathbf{E} \times \mathbf{B}$  rotation, sheared diamagnetic drifts and the role of passing electrons in stabilizing the rotational instabilities of a tandem mirror system. The basic stability equation for the system is derived from the ion and electron hydrodynamic equations with a two component electron fluid description introduced by Rosenbluth describing the trapped and passing electron dynamics. The mode equation contains the finite ion Larmor radius, the Coriolis force and the passing electrons as sources of charge separation that influence the stability of the centrifugal force driven interchange mode.

The stability analysis shows that solid body rotation with a Gaussian density profile, which allows analytic solution, is substantially more unstable than the profiles with differential rotation with  $\mathbf{E} \times \mathbf{B}$  and diamagnetic drifts.

For sufficiently strong shear the radial gradient of the angular momentum will drive a different type of instability; however, below the onset of the sheared flow instabilities the change in the topology of the interchange wave function, as shown in Fig. 4.13-4.14, produced by the differential flows reduces the effectiveness of the density gradient or pressure gradient driven interchange instability.

The critical passing electron density required for stability  $A_p^s$  is given approximately by Eq.(IV.34) which agrees well with the exact results given in Figs. 4.2-4.4, 4.6-4.7.



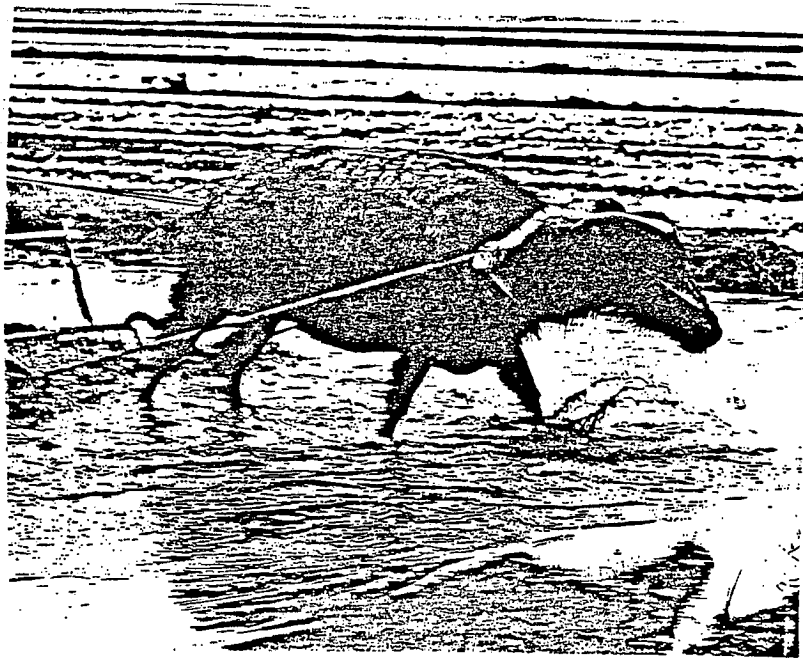
The stability analysis shows that there are a number of combinations of differential flows and passing electron density values that produce stable system when electron dissipation is neglected.

In the low  $m$  modes example considered it is shown that the growth rate begins to increase from the free energy in the sheared rotation only after the flow becomes reversed at radial boundary. Similarly the introduction of differential rotation in the diamagnetic drift frequencies by a broader density profile distorts the wave function and substantially reduces the growth rates. For example the change to a parabolic density profile gives the growth rate spectrum shown in Fig. 4.9 which has  $\gamma_m$  monotonically decreasing with  $m$  and only  $m = 1$  and  $m = 2$  modes unstable for  $T_i = T_e$ .

Stabilization by large  $A_p > A_p^s$  tends to push the wave frequency in the laboratory toward zero which is detrimental for plasma confinement since the  $m = 2$  asymmetries of the laboratory plasma then resonate with the wave.

In conclusion we suggest that a plasma starting in with constant  $\Omega$  and  $\omega_{*i,e}$  profiles will tend to be strongly unstable and would evolve through the quasilinear relaxation as contained by background transport processes towards more stable configurations with substantial differential rotation in the profiles.

*The water buffalo walks, vortices follow, .....*



chapter V  
NONLINEAR MOTION  
- THE SOLITARY VORTEX SOLUTION

**Introduction**

In the previous two chapters we analyzed the linear instability of the rotating plasma and its application to the central cell plasma of the Tandem Mirror devices. In this chapter we study the nonlinear motion of the rotating plasma by solving the nonlinear equations derived in Chapter II. We show that under certain conditions our nonlinear equations can have an analytical solution which is similar to the solitary vortex solution first obtained in the study of nonlinear Rossby waves [Larichev and Reznik 1976]. The solitary vortices have attracted considerable attention in the study of planetary atmosphere dynamics and oceanography, and, in past few years, the number of articles about the solitary vortex solution in magnetically confined plasma is rapidly growing and their potential importance is gradually being acknowledged.

In this chapter we will show that a low  $\beta$ , inhomogeneous, rotating plasma column immersed in a constant axial magnetic field can exhibit solitary vortex solutions as well. These vortices take the form of a shielded dipole, the vorticity falling off exponentially at large distances. They travel in the azimuthal direction with a constant velocity. We obtain the relation between the velocity, the core

size of the vortex dipole, and various system parameters, which we refer to as the nonlinear dispersion relation by analogy with the corresponding relation between linear phase velocity and wavenumber. The nonlinear dispersion relation shows that the velocities of the vortices and the phase speeds of the linear modes occupy complementary regions of parameter space. This complementarity also holds true for most one-dimensional soliton systems, as well as the other cases for which solitary vortex solutions are known.

The arrangement of this chapter as follows: In Section V.1, we give a brief historical summary of this topic and present the usual mathematical method for obtaining this kind of solution from a typical nonlinear equation—the single layer quasigeostrophic equation. In section V.2, we reduce the nonlinear equations of rotating plasma to the proper form for obtaining the solitary vortex solution. In section V.3, we give the solitary flute-vortex solution of the rotating plasma and nonlinear dispersion relation of the solution. In section V.4 the solitary flute-vortex solution modified by small amount of passing electrons is analyzed. In section V.5, we give a discussion of the properties of the vortices obtained in section V.3, and finally in section V.6, we give the summary and conclusions of this chapter.

## V.1 A brief historical summary

In 1976 an exact solitary vortex solution was obtained by Larichev and Reznik for nonlinear Rossby waves. Soon after that the solution was applied to explaining the atmospheric blocking [Flierl 1980] and in oceanography it was used as a model for gulf stream rings [Flierl et al 1980]. In 1979 Hasegawa et al discussed the analogy between the nonlinear drift wave equation in magnetically confined plasma and the nonlinear Rossby wave equation [Hasegawa et al 1979]. In 1982 Meiss and Horton solved the the nonlinear equation describing electron-drift and ion acoustic waves in presence of magnetic shear and obtained the two-dimensional solitary wave solution [ Meiss and Horton 1983]. Later, Pavlenko and Petviashvili reported that for a coupled nonlinear equations describing the flute motion of the inhomogeneous magnetically confined plasma with a transverse gravity field a solitary vortex solution for the density and electric potential perturbations were obtained[Pavlenko and Petviashvili, 1983].

Since then, growing number of papers about the solitary wave solutions for drift waves, flute-interchange and other modes in magnetically confined plasma has been published [Taniuti and Hasegawa 1982; Mikhailovskii et al, 1984; Petviashvili and Pogutse, 1984; Shukla et al, 1985; Hazetine et al, 1985; Horton et al, 1985].

At the same time as theoretical workers are predicting the solitary vortices

from their equations, laboratory experiments have confirmed the existence of these vortices in the rotating shallow fluid [Antipov et al 1982,1983; Antonova et al 1983; Flierl et al 1983]. In the experiment of Antipov-group the results favored monopolar vortices (they also observed the dipolar ones); while other two groups observed quite stable dipolar vortices. In numerical experiments, the robustness in strong interactions of the solitary vortex solutions for the nonlinear drift wave or Rossby wave equation has been indicated [Makino et al 1981; McWilliams and Zabusky 1982; Zabusky and McWilliams 1982]. Recently Laedke and Spatschek proved that for certain special cases the solitary vortex solution of the nonlinear Rossby equation is linear stable [Laedke and Spatschek 1985].

As well as study of the solitary dipolar vortices, there is another direction to attack the problem. Recognizing the analogy between Rossby waves in the atmosphere of planet and the drift waves in magnetically confined plasma, Petviashvili derived a nonlinear equation describing the nonlinear Rossby waves on a planet which is similar to the equations he derived for drift waves in a plasma [Petviashvili 1977; 1980; 1983]. From his equation an anticyclone solution- a single monopole vortex which rotates oppositely to the global rotation of the planet atmosphere is obtained. As we mentioned moments ago, the experiments of Antipov group seems favored to his monopole solution. According to this theory and the results of the rotating shallow fluid experiments, Nezlin suggested that Jupiter's Great Red Spot and the largest anticyclonic vortices in the atmospheres of other

giant planets are Rossby solitons [Nezlin 1984]. Horton and Meiss collaborated with Zabusky also studied the solitary monopole solution of the nonlinear drift wave equation from a view of a macro-charge source, and proposed that the wake field produced by a macro-charge travelling above certain speed is captured to form the "wakeless" monopole vortex [Horton et al 1985].

Based on above mentioned facts we can see that although much remain to be done, the feature of the solitary vortices is attractive and it could reasonably be expected that solitary vortices will play as essential a role in two-dimensional fluids as the classical soliton does in the one-dimensional case [Mikhailovskii et al 1984].

Since no matter how different the physics is discussed, the published works on solitary vortices with dipole structure always obtain finally the same nonlinear equation which allows the solution, and the procedure for obtaining the solution often referred by many authors as "standard procedure" and omitted in in their text; here we show this procedure in some detail. The author of this thesis should mention that the remain materials in this section is not his original work; most the material here used due to the authors who pioneered this topic of study [Larichev and Reznik 1976; Flier et al 1980; Meiss and Horton 1983].

As the typical equation we take the single layer quasigeostrophic equation in geophysical context first derived by Charney for the Rossby wave in a rotating

neutral fluid [Charney 1948]

$$\frac{\partial}{\partial t}(\nabla^2\psi - \psi) + \frac{\partial}{\partial y}\psi + [\psi, \nabla^2\psi] = 0 \quad (\text{V.1})$$

where  $\psi = \psi(x, y, t)$  is the stream function which related to the velocity field  $\mathbf{v}(x, y, t)$  by  $\mathbf{v} = \hat{\mathbf{z}} \times \nabla\psi$ . In plasma physics equation (V.1) also called the Hasegawa-Mima equation describes the drift wave without dissipation .

To seek a stationary solution of equation (V.1), we set

$$\psi = \psi(x, y - ut) = \psi(x, y') \quad (\text{V.2})$$

where  $u$  is a constant represents the propagating speed of the perturbation in the  $y$  direction. Substituting (V.2) into equation (V.1) yields

$$-u \frac{\partial}{\partial y'}(\nabla^2\psi - \psi) = \frac{\partial}{\partial y'}\psi + [\psi, \nabla^2\psi] = 0 \quad (\text{v.3})$$

By using the property of Poisson bracket equation (V.3) can be written as

$$[\psi - ux, \nabla^2\psi - \psi - x] = 0 \quad (\text{V.4})$$

The solution of equation (V.4) is

$$\nabla^2\psi - \psi - x = F(\psi - ux) \quad (\text{V.5})$$

where  $F(z)$  is arbitrary function of  $z$ . Our purpose is to seek a localized solution of the equation (V.1), so when  $y \rightarrow \infty$  we require that  $\psi \rightarrow 0, \nabla^2\psi \rightarrow 0$ . This implies that

$$F(z) = \frac{z}{u} \quad (\text{V.6})$$



hence the equation (V.5) becomes

$$\nabla^2 \psi - \left(1 + \frac{1}{u}\right) \psi = 0. \quad (\text{V.6})$$

In a polar coordinates  $r, \theta$  where

$$r^2 = x^2 + y'^2, \theta = \arctan \frac{y'}{x},$$

the solution of equation (V.6) which meets the localization requirement is

$$\psi_1 = \sum_{n=1}^{\infty} D_n K_n(kr) \sin n\theta + \sum_{n=0}^{\infty} E_n K_n(kr) \cos n\theta \quad (\text{V.8})$$

where

$$k^2 = \frac{u+1}{u} \quad (\text{V.9})$$

and  $K_n$  is the  $n$ -th order McDonald function,  $D_n, E_n$  are constant coefficients.

We notice that the linear form of the function  $F(z)$  (V.6) is required by the localization condition of the solution and it holds for any region with streamlines which extend to infinity in  $y$ . But for the region where the streamlines are closed  $\nabla^2 \psi$  still can be any arbitrary function of  $\psi - ux$ . For simplicity, we choose a dipole solution by keeping only one term in (V.8)

$$\psi_1(r, \theta) = E_1 K_1(kr) \cos \theta \quad (\text{V.10}).$$

For this choice of the solution, if  $E_1 u > 0$ , there is a special closed streamline in the frame comoving with the wave. On that line the stream function of the comoving frame

$$\chi(r, \theta) = \psi(r, \theta) - ur \cos \theta = 0, \quad (\text{v.11})$$

where  $r=a$ , and  $a$  is related with the constant  $u$  and  $E_1$  by relation

$$\frac{1}{au} K_1\left(\sqrt{\frac{u+1}{u}} a\right) = \frac{1}{E_1} \quad (\text{V.12}).$$

If  $E_1 u < 0$ , the solution (V.10) is singular at the origin and all the streamlines are closing at this singular point.

The physical requirements for finiteness of vorticity and energy lead us to choose the solution (V.9) with  $E_1 u > 0$ . And we consider (V.9) as the solution of equation (V.5) in the outer region where  $r = \sqrt{x^2 + (y - ut)^2} \geq a$ .

In the inner region where  $r < a$ , we still have the freedom to choose the form of  $F(z)$  provided the choice can meet the requirements of matching both  $\psi$  in both region and its first few order derivatives on the border line  $r=a$ , and guarantying the solution is regular. This means that even though we specified the outer solution by taking a dipole solution, the freedom of choice of the form of  $F(z)$  under the just mentioned conditions allows a more general set of the solutions for equation (V.1). Once again, for simplicity (this can be read synonymously with the lack of the author's knowledge about how to treat the general case), we take  $F(z)$  as linear function of  $z$ ,

$$F(\psi - ux) = C + D(\psi - ux) \quad (\text{V.13})$$

where  $C$  and  $D$  are constants. Substituting (V.12) into equation (V.5), and letting  $D = 1 - p^2$  one obtains

$$\nabla^2 \psi + p^2 \psi = C_+ + [(1 + p^2)u + 1]r \cos \theta \quad (\text{V.14})$$

The solution which is regular in the region  $r < a$  can be written as

$$\psi_2(r, \theta) = \frac{C}{p^2} + \frac{1}{p^2}[1 + (p^2 + 1)u]r \cos \theta + \sum_{n=1}^{\infty} A_n J_n(pr) \sin n\theta + \sum_{n=0}^{\infty} B_n J_n(pr) \cos n\theta. \quad (\text{V.15})$$

where  $J_n$  is the  $n$ -th order Bessel function,  $A_n, B_n$  are constant coefficients. We match the solution (V.8) and (V.15) on the border line  $r=a$  by requiring that

- (i). the stream function is continuous:  $\psi_1|_{r=a} = \psi_2|_{r=a}$ ;
- (ii). the velocity  $\hat{z} \times \nabla \psi$  is continuous:  $\hat{z} \times \nabla \psi_1|_{r=a} = \hat{z} \times \nabla \psi_2|_{r=a}$ ;
- (iii). the vorticity is continuous:  $\nabla^2 \psi_1|_{r=a} = \nabla^2 \psi_2|_{r=a}$ .

After matching two solutions, at the end we obtain the solitary vortex solution of equation (V.1) as

$$\psi(r, \theta) = \begin{cases} \left\{ -\frac{k^2 a J_1(pr)}{p^2 r J_1(pa)} + \left(1 + \frac{k^2}{p^2}\right) \right\} ur \cos \theta, & (0 \leq r < a) \\ \frac{K_1(kr)}{K_1(ka)} ua \cos \theta. & (r > a) \end{cases} \quad (\text{V.16})$$

This solution has two free parameters  $u$  and  $a$ , which represent the scale and the propagating speed of the vortex respectively. Two other parameters  $k$  and  $p$  are not independent, they are determined by  $u$  and  $a$  through the equation (V.9) and the relation

$$\frac{1}{\gamma} \frac{J_2(\gamma)}{J_1(\gamma)} = -\frac{1}{\beta} \frac{K_2(\beta)}{K_1(\beta)} \quad (\text{V.17})$$

where  $\gamma = pa$ ,  $\beta = ka$ . Equation (V.17) has an infinite set of roots  $\gamma_n(\beta)$ ,  $n = 1, 2, \dots$ , the first three roots are given graphically by Meiss and Horton [1983].

Several pertinent remarks about this solution follow.

(i). **It is a special solution of the nonlinear equation.** First of all, from infinity of terms of the outer solution (V.1) we only picked the dipole term, this choice gave a closed streamline which is a circle. Second, inside the circle, from many possible choices for the form of the function  $F(z)$  we made an ad hoc assumption of the linear form (V.13) which further limits the solution. Even so, this solution is a nonlinear solution, because the form of  $F(z)$  we chose has a nonvanishing nonlinear term - the advection term  $[\psi, \nabla^2 \psi]$ .

(ii). **It is a coherent solution.** In the rest frame of the vortex, it is a constant dipole. Inside the vortex core  $a$ , the vorticity and velocity are finite; outside the core the strength rapidly decays to zero with the asymptotic form  $r^{-\frac{1}{2}} e^{-kr}$ .

(iii). **There is a complementarity relation between the linear mode phase velocity and the propagating speed of the vortex.** One of the most remarkable properties of this solution is that there is a close relation between the phase velocity of the linear modes of the equation (V.1) and the vortex propagating speed  $u$ , both of them complementarily fill the  $\omega - k$  space. We can show this remarkable feature by consider the relation (V.9) and the dispersion relation of the linear modes of the equation (V.1). Linearizing equation (V.1), assuming a normal mode with form  $e^{i(k_x x + k_y y - \omega t)}$  yields the dispersion relation

$$v_{phase} = \frac{\omega}{k_y} = -\frac{1}{k^2 + 1}. \quad (V.18)$$

From it one can immediately obtain the allowed region for the phase velocity

$$-1 < v_{phase} < 0. \quad (V.19)$$

On the other hand equation (V.9), implies the vortex is localized if

$$\frac{u+1}{u} > 0. \quad (V.20)$$

This leads to the conclusion that

$$u < -1, \text{ or } u > 0. \quad (V.21)$$

Comparing (V.19) and (V.21) we see the complementarity. Due to the fact that the equation (V.9) determines the allowed region for the propagating speed of the vortex just like the dispersion relation of the linear modes determines the phase velocity, we call the relation (V.9) nonlinear dispersion relation of the vortex. It may be useful to mention that all the publications about the dipole-like solitary vortex solution in plasma physics give the identically same solution as (V.17); the differences between them rest on the different nonlinear dispersion relations. So at least formally, we can use the nonlinear dispersion relation as a standard to distinguish the different physics of the vortex solutions. In appendix D of this thesis we list all reported vortex solutions in magnetically confined plasma classified according to their nonlinear dispersion relations.

(vi) **Limiting cases.** As the last remark we like to point out that although the solitary vortex solution presented in this section is a special solution for the

nonlinear Rossby wave equation (V.1) as we argued in remark (i), it includes two famous exact vortex solutions obtained before as limiting cases.

(a) Stern vortex [Stern 1975]. When  $u \rightarrow 0^+$  with  $a$  fixed (so that  $ka \rightarrow \infty$ ), the vortex solution (V.17) becomes Stern vortex

$$\psi_{\text{Stern}} = \begin{cases} 0, & r > a \\ \frac{a^3}{(\gamma_n^\infty)^2} \left( \frac{J_1(\gamma_n r/a)}{J_1(\gamma_n^\infty)} - \frac{r}{a} \right) \cos \theta, & r < a, \end{cases} \quad (\text{V.22})$$

where  $\gamma_n^\infty$  is the  $n$ -th zero of  $J_2(\gamma_n)$ .

(b) Lamb vortex [Lamb 1916; Batchelor 1967]. When  $u \rightarrow 1$  with  $a$  fixed (so that  $ka \rightarrow 0$ ), the solution in (V.17) reduces to the Lamb vortex

$$\psi_{\text{Lamb}} = \begin{cases} \frac{a^2}{r} \cos \theta, & r > a \\ a \left( \frac{r}{a} - \frac{2}{\gamma_n^0} \frac{J_1(\gamma_n^0 r/a)}{J_0(\gamma_n^0)} \right) \cos \theta, & r < a \end{cases} \quad (\text{V.23})$$

where  $\gamma_n^0$  is the  $n$ -th zero of  $J_1(\gamma_n)$ .

## V.2 Reduction of The Nonlinear Equations of rotating plasma

Starting in this section we study the nonlinear motion of the rotating plasma, and particularly the solitary vortex solution of our nonlinear equations. In this section we reduce the nonlinear equations derived in Chapter II to a proper form for pursuit of the vortex solution. We suppose the plasma is rotating uniformly, so we take equations (II.39)-(II.40) as the basic equations.

The analysis of linear instability of uniformly rotating plasma we did in Chapter III shows that when the azimuthal wave mode number  $m$  is small, for example, when  $m \leq 3$  the mode is quite global, but when  $m \geq 4$  the linear modes are basically localized near the edge of the plasma column [see Fig.3.2]. The linear analysis also shows that for low ion temperature  $T_i < T_e$ , i.e.the ion FLR effect is not very strong, the high  $m$  modes have much higher growth rate than low  $m$  global modes. Based on these results we propose that the nonlinear interaction between the local high  $m$  modes at the plasma edge is dominant at a certain stage of the nonlinear evolution. During this stage, we can suppose the characteristic length of the perturbed density and potential is small, i.e.

$$\left| \frac{d \ln \delta n}{dr} \right|^{-1}, \left| \frac{d \ln \delta \phi}{dr} \right|^{-1} \ll r_n = \left| \frac{d \ln n_o}{dr} \right|^{-1}.$$

In this case, equations (II.44) and (II.45) reduce to

$$\frac{\partial \tilde{n}}{\partial t} - \frac{cT_e}{Be} \frac{1}{n_o} \frac{\partial n_o}{\partial r} \frac{\partial \tilde{\phi}}{r \partial \theta} = \frac{cT_e}{Be} [\tilde{n}, \tilde{\phi}] \quad (V.24)$$

$$\begin{aligned} & \frac{1}{\omega_{ci}} \frac{cT_e}{Be} \left( \frac{\partial}{\partial t} + \frac{T_i}{m_i \omega_{ci} n_o} \frac{\partial n_o}{\partial r} \frac{\partial}{r \partial \theta} \right) \nabla^2 \tilde{\phi} - 2 \frac{\Omega}{\omega_{ci}} \frac{cT_e}{Be} \frac{1}{n_o} \frac{\partial n_o}{\partial r} \frac{\partial \tilde{\phi}}{r \partial \theta} \\ & + \frac{1}{\omega_{ci}} (\Omega^2 r + g(r)) \frac{\partial \tilde{n}}{r \partial \theta} = \frac{1}{\omega_{ci}^2} \frac{cT_e^2}{Bem_i} [\nabla^2 \tilde{\phi}, \tilde{\phi} + \frac{T_i}{T_e} \tilde{n}] \end{aligned} \quad (V.25)$$

where  $\tilde{n} = \frac{\delta n}{n_o(r)}$ ,  $\tilde{\phi} = \frac{e\delta\phi}{T_e}$ .

Since the small-sized perturbations are localized around the edge of the plasma the cylindrical geometry of the configuration is less important, and we can use Cartesian coordinates:

$$\begin{aligned} \frac{r}{r_n} & \longrightarrow x \\ \frac{r\theta}{r_n} & \longrightarrow y. \end{aligned}$$

Using a dimensionless time  $\tau$ ,

$$t \frac{\rho_s v_s}{r_n^2} \longrightarrow \tau,$$

equations (V.24), (V.25) become

$$\frac{\partial \tilde{n}}{\partial \tau} + \frac{\partial \tilde{\phi}}{\partial y} = [\tilde{n}, \tilde{\phi}] \quad (V.26)$$

$$\left( \frac{\partial}{\partial \tau} - \frac{T_i}{T_e} \frac{\partial}{\partial y} \right) \nabla^2 \tilde{\phi} + v_c \frac{\partial \tilde{\phi}}{\partial y} + v_g \frac{\partial \tilde{n}}{\partial y} = [\nabla^2 \tilde{\phi}, \tilde{\phi} + \frac{T_i}{T_e} \tilde{n}] \quad (V.27)$$

where

$$v_c = \frac{2\Omega}{\frac{\rho_s v_s}{r_n^2}} = 2\hat{\Omega}$$

$$v_g = \left( \frac{r_n}{\rho_s} \right)^2 \left( \frac{\Omega^2 r_n r}{v_s^2} + \frac{r_n g(r)}{v_s^2} \right) = \hat{\Omega}^2 r / r_n + \hat{g}$$



$v_c$  is Coriolis drift,  $v_g$  represents the centrifugal and gravitational drift. We take the localized value of  $v_g$  as constant in further calculations. Also

$$v_s = \left(\frac{T_e}{m_i}\right)^{\frac{1}{2}}, \quad \rho_s = \frac{v_s}{\omega_{ci}}.$$

The equations (5.26) and (V.27) are the nonlinear equations for which we seek the solitary vortex solution. Before proceeding to the solution it might be worthwhile to mention that:

- (i) Equation (V.26) and (V.27) are very similar to the equations derived by Rahman and Weiland [ 1984 ] for high  $\beta$  plasma, except for the second term of (V.27) which comes from the Coriolis force in the rotating frame. Heuristically, since plasma in toroidal devices experiences poloidal rotation in certain situations, the analysis of our problem may give some insight into that case as well.
- (ii) Compared with the equations given by Pavlenko and Petviashvili [1983], our equations differ from theirs by two terms: the first one is the Coriolis term intrinsic to the rotating frame while the second one is the second nonlinear term in equation (V,27) which they missed by error as pointed out by Mikhailovskii et [1984].

### V.3 Solitary Flute-Vortex In The Rotating Plasma

We seek a stationary solution of (V.26) and (V.27) in the form of

$$\begin{aligned}\tilde{n}(x, y, t) &= \tilde{n}(x, y') \\ \tilde{\phi}(x, y, t) &= \tilde{\phi}(x, y')\end{aligned}\tag{V.28}$$

where  $y' = y - u\tau$ ,  $u = \text{const.}$  is a free parameter.

Substituting (V.28) into (V.26), (V.27), we have

$$\frac{\partial}{\partial y'}(\tilde{\phi} - u\tilde{n}) = [\tilde{n}, \tilde{\phi}]\tag{V.29}$$

$$-(u + \frac{T_i}{T_e})\frac{\partial}{\partial y'}\nabla^2\tilde{\phi} + v_c\frac{\partial\tilde{\phi}}{\partial y'} + v_g\frac{\partial\tilde{n}}{\partial y'} = [\nabla^2\tilde{\phi}, \tilde{\phi} + \frac{T_i}{T_e}\tilde{n}].\tag{V.30}$$

In the remainder of this chapter we drop the tildes on  $n$  and  $\phi$  for convenience.

To solve (V.29), (V.30), we divide the  $x - y'$  plane into two regions

$$\text{Region I: } x^2 + y'^2 < r_o^2$$

$$\text{Region II: } x^2 + y'^2 > r_o^2$$

where  $r_o$  is a constant parameter characterizing the size of the vortex. We look for solutions which satisfy the following conditions:

- (1) In Region I,  $n$  and  $\phi$  must be finite at  $r = (x^2 + y'^2)^{\frac{1}{2}} = 0$ .
- (2) In Region II, when  $r \rightarrow \infty$ ,  $n$  and  $\phi$  must decay to zero.
- (3) On the border between Region I and Region II, where  $r = r_o$ :

- (a) The stream function must be continuous,  $(\phi)_I = (\phi)_{II}$ .
- (b) The velocity field must be continuous,  $\hat{z} \times (\nabla\phi)_I = \hat{z} \times (\nabla\phi)_{II}$ .
- (c) The vorticity must be continuous,  $(\nabla^2\phi)_I = (\nabla^2\phi)_{II}$ .
- (d) The density perturbation must be continuous,  $(n)_I = (n)_{II}$ , where subscripts I, II denote the corresponding quantities in Region I and Region II.

After some algebra very similar to these in Section V.1 we find that to satisfy conditions (1),(2), the simplest solutions  $n$ ,  $\phi$  should satisfy following equations

In Region I ( $r < r_o$ )

$$n = d\phi + (1 - du)x \quad (V.31)$$

$$\nabla^2\phi = -p^2\phi + Cx \quad (V.32)$$

$$C = (v_c + dv_g) + p^2u \quad (V.33)$$

In Region II ( $r > r_o$ )

$$n = \frac{\phi}{u} \quad (V.34)$$

$$\nabla^2\phi = k^2\phi \quad (5.35)$$

$$k^2 = \frac{v_c u + v_g}{u(u + T_i/T_e)}. \quad (V.36)$$

Here  $k, p, d$  and  $C$  also are real constants related by equations (V.33),(V.36).

Solving equations (V.31)-(V.36), and imposing the matching conditions 3(a),(b),(c),(d), we obtain the solutions

$$\phi = \begin{cases} \left[ -\frac{k^2 r_o}{p^2 r} \frac{J_1(pr)}{J_1(pr_o)} + \left(1 + \frac{k^2}{p^2}\right) \right] ur \cos \theta & (r < r_o) \\ ur_o \frac{K_1(kr)}{K_1(kr_o)} \cos \theta & (r > r_o) \end{cases} \quad (\text{V.37})$$

$$n = \begin{cases} \left[ \frac{k^2}{p^2} \frac{u(u k^2 - v_c)}{v_g} \left(1 - \frac{r_o J_1(pr)}{r J_1(pr_o)}\right) + 1 \right] r \cos \theta & (r < r_o) \\ \frac{K_1(kr)}{K_1(kr_o)} r_o \cos \theta & (r > r_o) \end{cases} \quad (\text{V.38})$$

where  $\theta = \tan^{-1} \frac{y'}{x}$ ,  $k$  is a real parameter defined by (V.36). The parameters  $k$  and  $p$  are related by

$$\frac{1}{kr_o} \frac{K_2(kr_o)}{K_1(kr_o)} = -\frac{1}{pr_o} \frac{J_2(pr_o)}{J_1(pr_o)} \quad (\text{V.39})$$

where  $J$ ,  $K$  are Bessel and McDonald functions.

From (V.37)-(V.38) we can see that both  $n$  and  $\phi$  have the form of a vortex pair moving with constant velocity  $u$  in the  $y$  direction, i.e. in the azimuthal direction around the edge of the plasma column. In Fig. 5.2, we give a contour plot of our vortex. The radial size of the core of each vortex is characterized by parameter  $r_o$ , and the strength is a complicated function of two independent free parameters  $u$  and  $r_o$ . In the exterior region ( $r > r_o$ ) the vortices decay to zero as  $e^{-kr}/r^{\frac{1}{2}}$ . All these features are identical to the vortex solution given in the Section V.1 for the nonlinear Rossby wave equation.

#### V.4 Solitary Flute-Vortex Modified By the Passing Electrons In The Rotating Plasma

In this section we briefly present a modified version of the results given in Section V.3. If we consider the rotating plasma in the central cell of the Tandem Mirror and include the charge uncovering effect of small amount of passing electrons in the quasineutrality equation (II.40), and suppose that the plasma rotating is uniform, then equations (II.39)-(II.40) are modified by the passing electron current. After the similar procedure of making equations dimensionless under the same assumptions as we did in Section V.2, the dimensionless nonlinear equations become

$$\frac{\partial \tilde{n}}{\partial \tau} + \frac{\partial \tilde{\phi}}{\partial y} = [\tilde{n}, \tilde{\phi}], \quad (\text{V.40})$$

$$\left(\frac{\partial}{\partial \tau} - \frac{T_i}{T_e}\right) \nabla^2 \tilde{\phi} - A_p \frac{\partial \tilde{\phi}}{\partial \tau} + (v_c - A_p v_{*e}) \frac{\partial \tilde{\phi}}{\partial y} + v_g \frac{\partial \tilde{n}}{\partial y} = [\nabla^2 \tilde{\phi}, \tilde{\phi} + \frac{T_i}{T_e} \tilde{n}], \quad (\text{V.41})$$

where  $A_p$  has the same definition as in Chapter 4 and  $v_{*e}$  is the electron drift velocity other notations have the same definitions given in Section V.2. We notice that including the passing electrons does not modify the continuity equation, (V.40) is exactly the same as (V.26) but the quasineutrality equation is modified. Considering the FLR ordering we used to derive the nonlinear equation the continuity equation is two order lower than the quasineutrality equation, the way by which this small amount of electron modifies the equations is justified.

After repeating every step we did in Section V.3, a vortex solution of equations

(V.40) and (V.41) is obtained. The expression of the solutions is exactly the same as the solution we gave in Section V.3 for  $n$ , and  $\phi$  as we expected. To avoid repetition, we will not write them here. The new physics in this modified flute-vortex solution is shown by the nonlinear dispersion relation which is very different from the one given by equation (V.36)

$$k^2 = \frac{u[v_c + A_p(u - v_{*e})] + v_g}{u(u + \frac{T_i}{T_e})}. \quad (\text{V.42})$$

From this dispersion relation we see that this modified flute-vortex mixes the properties of the rotating flute-vortex and the electron drift vortex. The property of the electron drift vortex is brought in by the passing electrons. This can be seen more clearly in a limiting case. If we let  $A_p \rightarrow 1$ ,  $\frac{T_i}{T_e} \rightarrow 0$ ,  $v_c = V_g \rightarrow 0$ , (no rotation, no gravity, and cold ion plasma), The nonlinear dispersion relation (V.42) becomes the nonlinear dispersion relation for the electron drift vortex [Meiss and Horton 1983]

$$k^2 = \frac{u - v_{*e}}{u}.$$

If we set  $A_p = 0$ , then the dispersion relation (V.36) for rotating flute-vortex appears as one expected.

## V.5 : Properties of the Vortices

In this section we consider (A) the nonlinear dispersion relation, (B) the bounds of propagation speeds, (C) the complementary phase velocities of the linear modes, and (D) the spatial structure of the vortex flows for the vortex solution given in Section V.3.

### V.5.A The Nonlinear dispersion relation

The vortices derived in section 3 are a two parameter family of exact solutions to the field equations. The free parameters are taken either as the core size  $r_o$  and speed  $u$ , or  $r_o$  and exterior scale size  $k$ . Equation (V.36) relates the two alternative choices of parameters  $u$  or  $k$ , conventionally we call it nonlinear dispersion relation. The requirement that the vortex decays to zero in the exterior region constraints the speed  $u$  of the vortices to be within the bounds determined by  $k^2(u) > 0$ , i.e.

$$k^2 = \frac{uv_c + v_g}{u(u + T_i/T_e)} > 0. \quad (V.43)$$

For this reason we find it more convenient to parameterize the vortex as shown in Fig.5.1 with the core size  $r_o$  and exterior decay rate  $k$ .

The solutions are computed by specifying the plasma parameters  $\Omega, g, T_i/T_e$  and  $r_o, k$ . The relation (V.39) which relates  $p$  to  $k$  is solved for the principal branch of  $pr_o = f(kr_o)$  defined by  $\gamma_1 \leq pr_o \leq \gamma_2$  where  $\gamma_1$  is the first nonzero root of  $J_1(x)$  and  $\gamma_2$  is the first root of  $J_2(x)$ . For each  $k$  the two branches of the solutions of equation (V.43) for vortex velocities  $u_{\pm}(k^2, T_i/T_e, v_c, v_g)$  are computed and then

the vortex fields (V.37) and (V.38) are determined.

### V.5.B. Propagation speeds of the vortices

The vortices obtained in Section V.3 can only propagate in certain bands of speeds that are determined by the plasma parameters  $\Omega$ ,  $g$  and  $T_i/T_e$ .

The limits on the vortex propagation bands are determined by inequality (V.43) which is equivalent to the inequalities

$$uv_c + v_g > 0 \quad \text{and} \quad u(u + \frac{T_i}{T_e}) > 0 \quad (\text{V.44})$$

or

$$uv_c + v_g < 0 \quad \text{and} \quad u(u + \frac{T_i}{T_e}) < 0 \quad (\text{V.45})$$

For different directions of plasma rotation the conditions (V.44) and (V.45) give different propagation bands which are shown in Fig.5.3.

#### (i) Inward equilibrium electric field

For radially inward equilibrium electric fields ( $\Omega > 0$ ), zero or bad curvature  $v_c > 0$  and  $v_g > 0$ . The regions of vortex propagation are

$$u > 0 \quad (\text{V.46})$$

and

$$-\frac{T_i}{T_e} > u > -\frac{v_g}{v_c}, \quad \text{if} \quad \frac{T_i}{T_e} < \frac{v_g}{v_c} \quad (\text{V.47})$$

or

$$-\frac{v_g}{v_c} > u > -\frac{T_i}{T_e}, \quad \text{if} \quad \frac{T_i}{T_e} > \frac{v_g}{v_c} \quad (\text{V.48})$$



## (ii) Outward equilibrium electric field

For radially outward equilibrium electric fields ( $\Omega < 0$ ) and bad curvature  $v_c < 0, v_g > 0$ , the vortex propagation bands are

$$-\frac{v_g}{v_c} > u > 0 \quad (\text{V.49})$$

and

$$u < -\frac{T_i}{T_e} \quad (\text{V.50})$$

From equations (V.46–V.50) we see that there is wide region of propagation in the direction of the plasma rotation, but only a limited region in which the vortices may travel in the opposite direction. This behavior of the plasma vortices is similar to the situation observed in the rotating shallow fluid experiments [Antipov et al 1982, 1983; Flierl et al 1983].

### V.5.C The complementary regions of linear modes

In the gaps where vortices do not propagate, the linear wave modes of the system propagate with the phase velocity  $u_p = \omega/(k_y V_{de}) = r\omega/(mV_{de})$ .

Returning to the field equations (V.26) and (V.27) and looking for the linear modes in form of  $e^{(ik_x x + ik_y y - i\omega t)}$ , we obtain the dispersion relation

$$k_{\perp}^2 c_p (c_p + T_i/T_e) + v_c c_p + v_g = 0 \quad (\text{V.51})$$

where  $c_p = \omega/(k_y V_{de})$  and  $k_{\perp}^2 = k_x^2 + k_y^2 > 0$ . Alternatively, one may return to the full radial equations (II.39) and (II.40) and solve for the eigenmodes

$\phi_m(r)e^{(im\theta - i\omega t)}$  for the rigid rotor equilibrium as we did in Section III.3. In this case one also obtains equation (V.51) with  $c_p = a\omega/(mV_{de}), k_\perp^2 \rightarrow \nu(m, n, b/a)$  where  $\nu_{m,n}$  are eigenvalues defined by equation (III.45). The eigenvalues  $\nu_{m,n}$  are discrete and positive definite so that in this case the phase velocities  $c_p$  lie in the continuum between the vortex propagation bands. Thus, equations (V.43) for the vortices and (V.51) for the waves cover all values of external wave number or decay scale as shown in Figs. 5.3.

The wave dispersion relation (V.51) predicts exponential growth for parameters  $\Omega, g, T_i/T_e$  which make a negative discriminant  $B^2 - 4AC < 0$  for the quadratic equation  $Ac_p^2 + Bc_p + C = 0$ , where  $A = k_\perp^2, B = k_\perp^2 T_i/T_e + v_c, C = v_g$ . In the unstable parameter region the phase velocity is  $c_p = -B/2A$ .

#### V.5.D The spatial structure of the vortices

We now consider the variation in the vortex fields with the vortex parameters. We show that the vortices propagating in the electron or ion diamagnetic direction have different behavior (for convenience we call them electron or ion diamagnetic vortex respectively). The ion diamagnetic vortex requires considerably larger energy for excitation than the electron diamagnetic one for comparable vortex parameters  $r_o$  and  $k$ .

As a reference system we consider a plasma column rotating in the ion diamagnetic direction with a speed twice the ion diamagnetic speed,  $\hat{g} = 1$ , and a core size  $1/5$  the density gradient scale length  $r_n$  with  $T_i = T_e = T$ . The speed of

propagation of the two branches is shown in Fig. 5.4. For comparison, we also give a similar Fig. 5.5 for a plasma column rotating in electron diamagnetic direction with the same speed.

For vortices with external scale sizes,  $1/k$ , comparable to the density gradient scale length  $r_n$ , the speeds of propagation are large compared with the diamagnetic drift speeds. Strictly speaking, due to the conditions we gave in the derivation of equations (V.26) and (V.27), our analytic solutions are not valid

for these large vortices. For vortices with small external scale sizes compared to  $r_n$ , the speeds of propagation are close to those of the linear modes of the system. At large  $k$  the speeds approach the limiting speeds as  $1/k^2$ .

In Figs. 5.6 and 5.7 we show the variation of the electron and ion diamagnetic vortex fields with  $k$  for the reference parameters used in Fig. 5.4.

The electron diamagnetic vortex has a maximum of the electrostatic potential at  $r \simeq r_o/2$  with  $e\phi_{max}/T \simeq 2.3r_o/k$  for  $k = k_{\perp}r_n > 1$ . This maximum of the potential is consistent with the mixing length for modes for  $\mathbf{E} \times \mathbf{B}$  convective saturation,  $V_E \simeq V_{de}$  or  $e\phi/T_e \approx 1/(k_x r_n)$ , which we know to apply to drift waves and their turbulent spectra.

The ion diamagnetic vortices have larger electrostatic fields than the electron diamagnetic vortices for comparable  $r_o$  and  $k$  as shown by the comparison of Fig. 5.7 and 5.6. The electrostatic potentials have maxima at roughly  $|e\phi_{max}/T_e| \simeq 12r_o/k$ , and thus have  $|e\phi_{max}| > T_e$  for  $k = k_{\perp}r_n \leq 12r_o$ . The en-

ergy required to excite the ion vortex is large. The polarization of the ion vortex is characteristic of MHD motions with  $|e\phi/T| \gg |\delta n/n|$ . As the exterior scale of the ion vortex decreases, the maximum potential decreases until reaching a minimum value  $|e\phi_{min}/T| \simeq 2$  or  $3r_o$ . The value of  $k$  at which this minimum occurs decreases from  $k \simeq 14.5$  for  $r_o = .05$  to  $k \simeq 6.5$  for  $r_o = 0.3$ . The saturation of  $\phi$  at  $\phi_{min}$  implies that there is minimum excitation energy  $E_{min}$  for creation of an ion diamagnetic vortex.

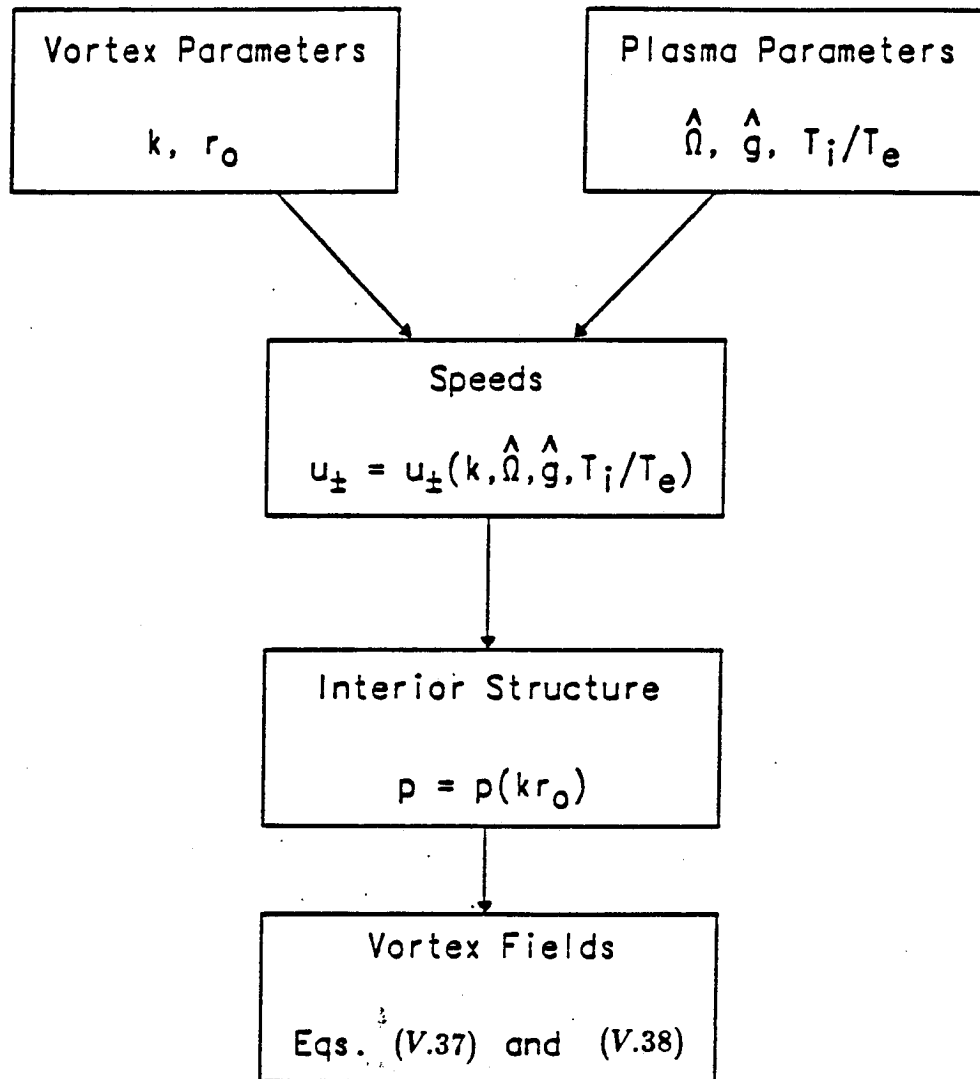


Fig.5.1 Schematic diagram of the parameter representation of the vortices.

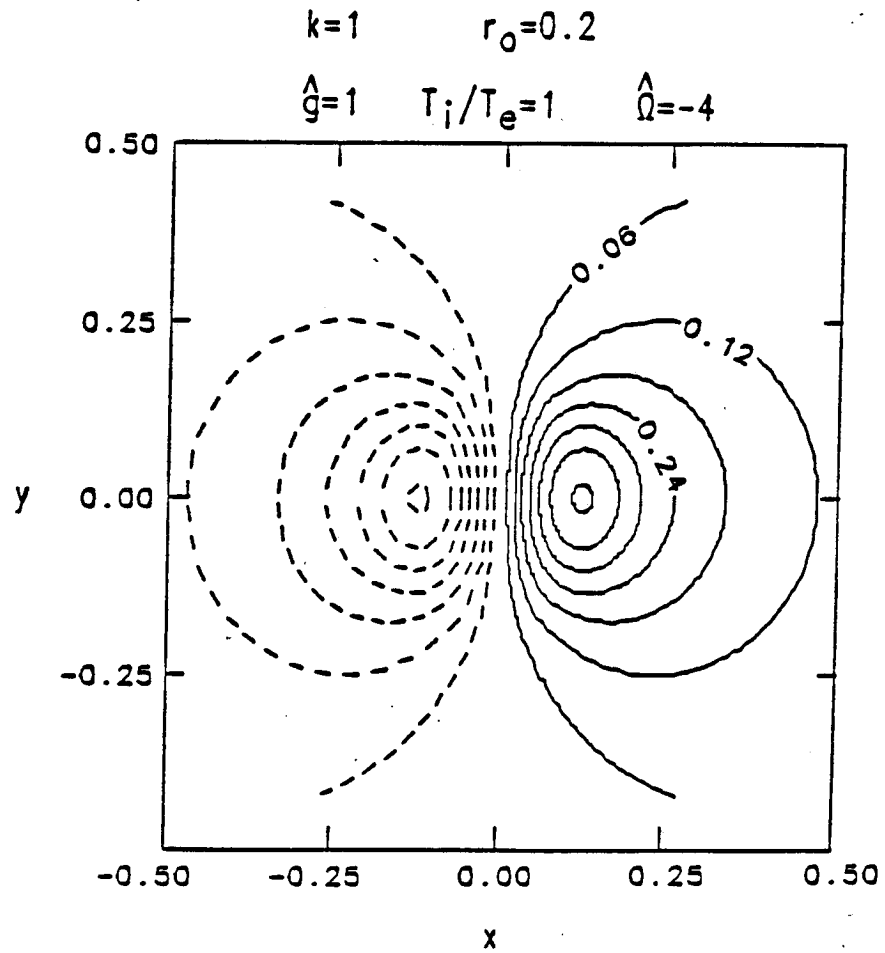


Fig.5.2 The contour of constant  $\phi(r, \theta)$ , notice the dipolar structure.

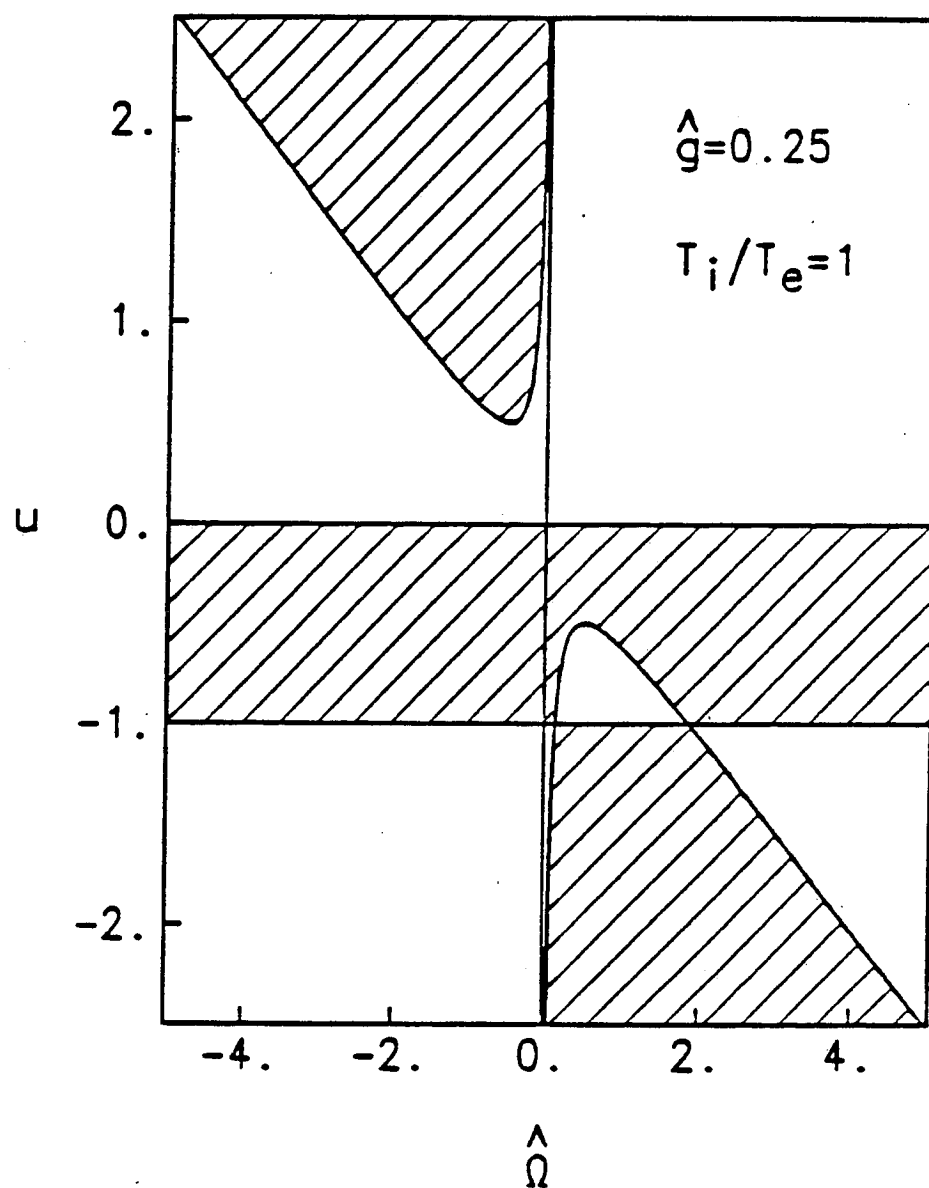


Fig.5.3 Propagation regions of vortices and linear wave modes. Vortices occur in the unhatched regions, and wave modes occur in the hatched regions of the parameter space. The boundary curves are  $u = -v_g/v_c$ ,  $u = -T_i/T_e$ , and  $u = 0$ .

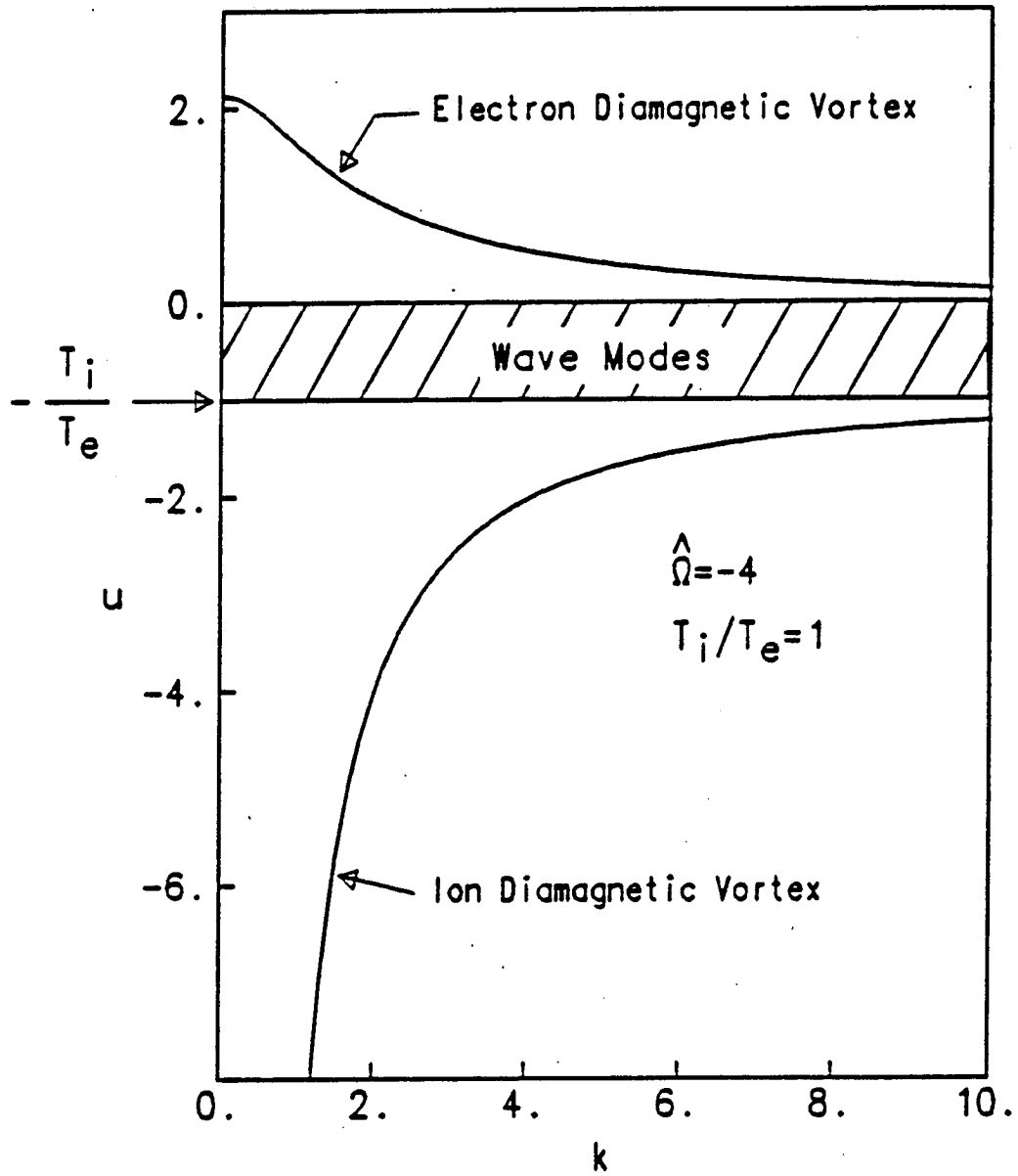


Fig.5.4 The vortex propagation speed versus inverse external scale size for  $\hat{\Omega} < 0$ ,

$$T_i/T_e = 1, \hat{g} = 1, \text{ and } r_o/r_n = 1/5.$$



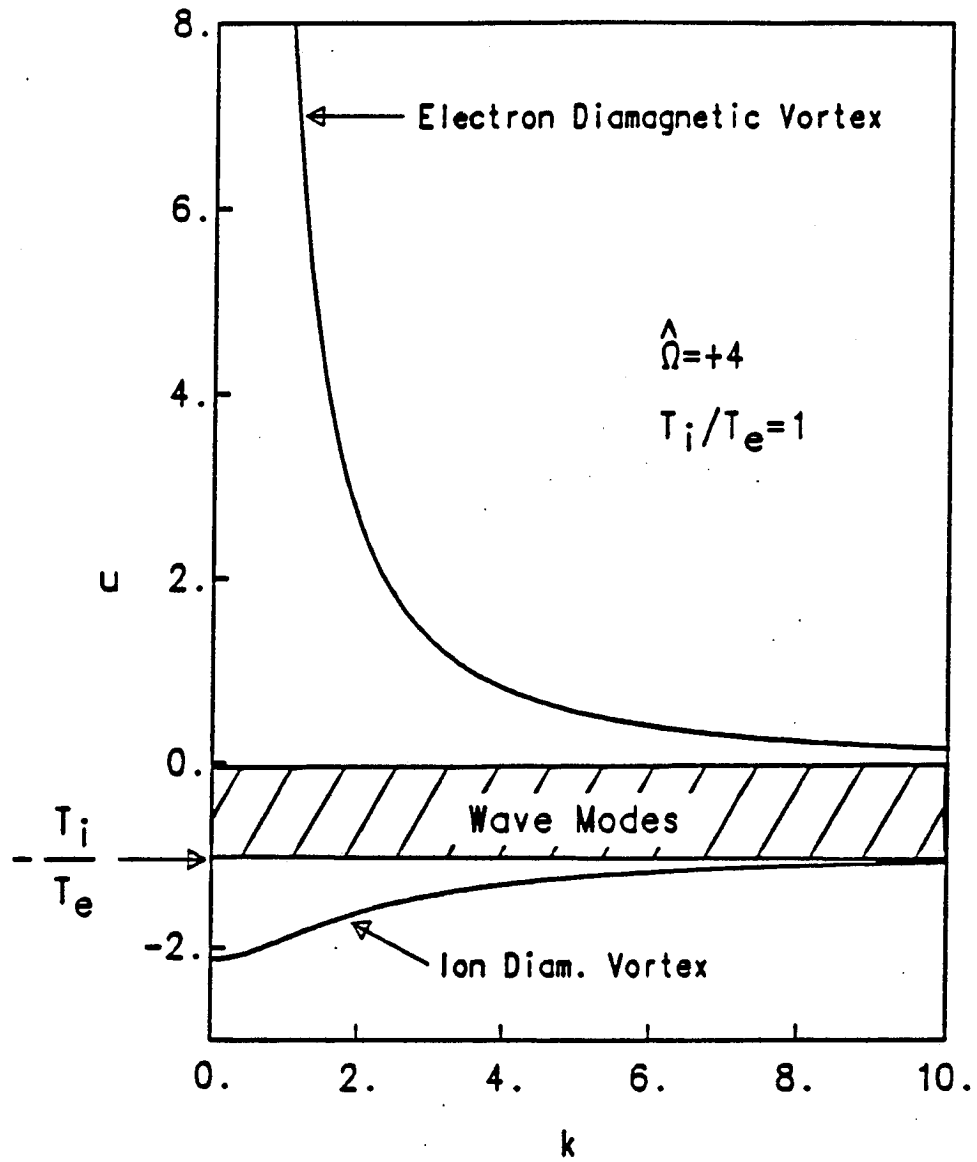


Fig.5.5 The vortex propagation speed versus inverse external scale size for  $\hat{\Omega} > 0$ ; other parameters are the same as Fig.5.4.

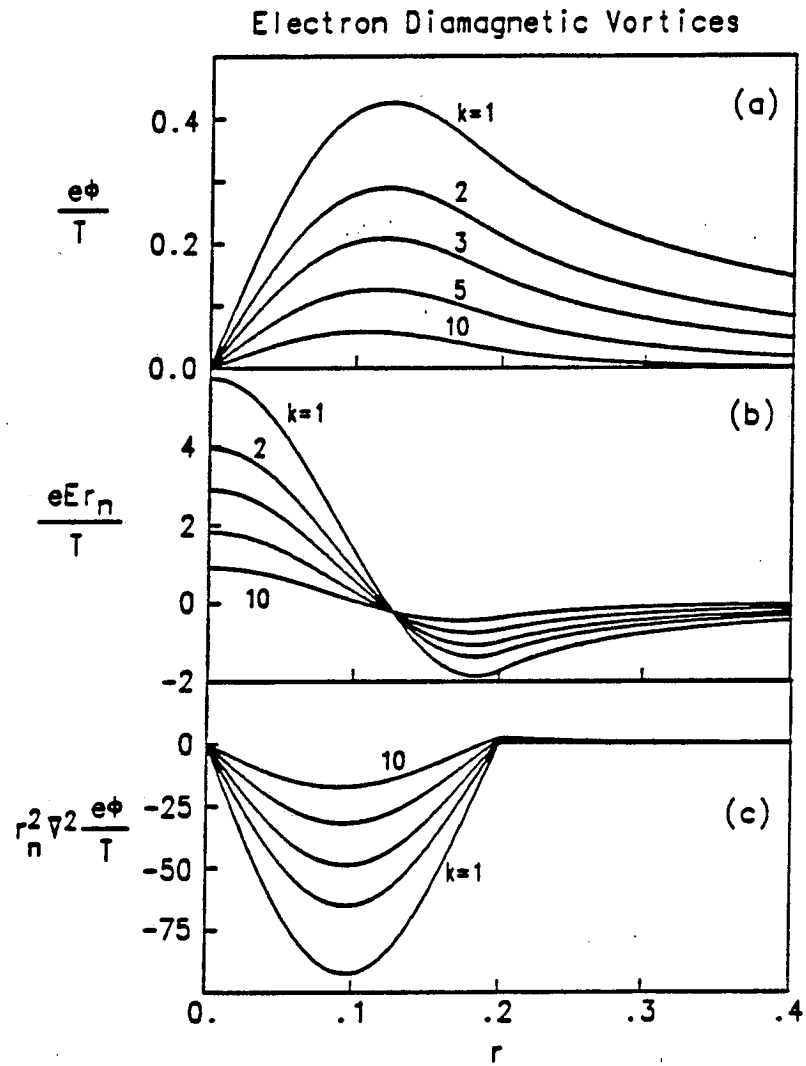


Fig.5.6 The radial structure of electron diamagnetic vortices ( $u > 0$ ): (a) potential, (b) electric field, (c) vorticity. (The parameters are the same as Fig.5.4.)

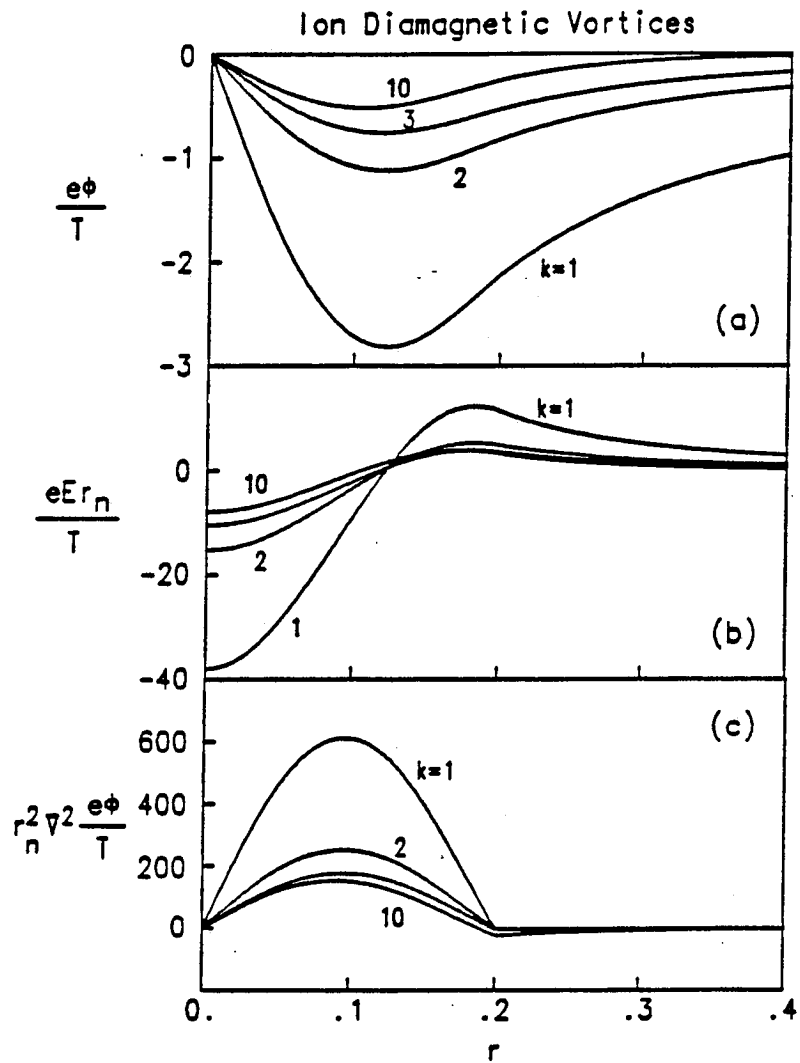


Fig.5.7 The radial structure of ion diamagnetic vortices ( $u < 0$ ): (a) potential, (b) electric field. (c) vorticity. (The parameters are the same as Fig.5.4.)

## V.6 Summary and conclusions

In summary, in this chapter we have reduced the nonlinear equation for the uniformly rotating plasma to a proper form for pursuit of the solitary vortex solution. We obtained two localized solutions of two equations corresponding to solitary dipolar vortices. We discussed the nonlinear dispersion relation, the allowed regions of propagation speeds, the structure of the vortices, and the complementary regions of linear modes.

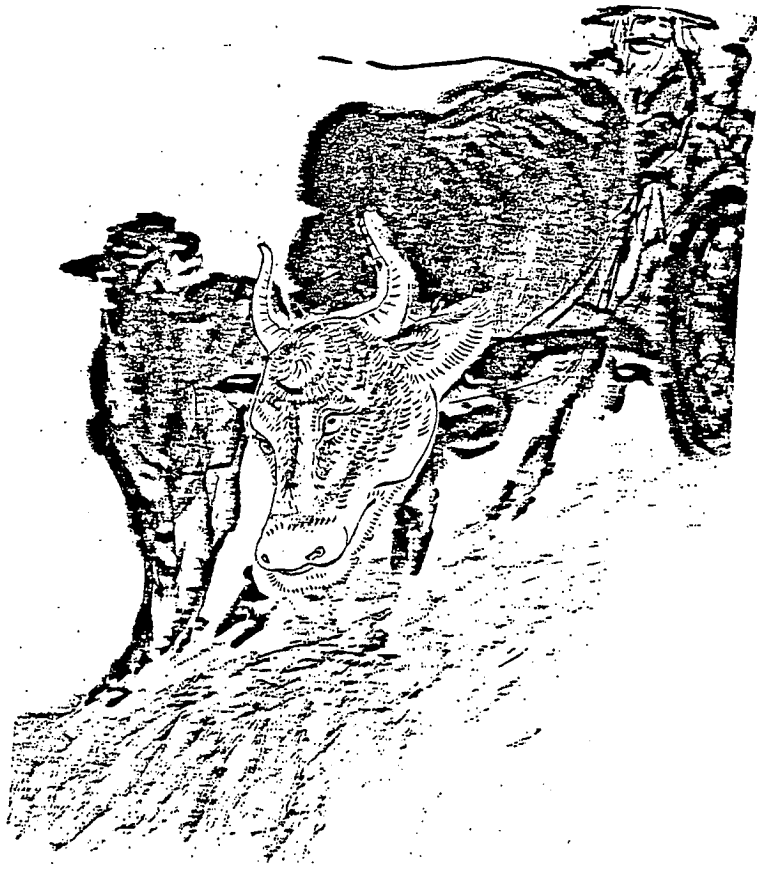
The vortex solutions given here describe the convection of density and vorticity of background plasma on space scales small compared with the radius of the plasma column. The electron motion in these vortex solutions is basically flute-like compared with those given earlier by Meiss and Horton [1983] and Makino et al [1981] which considered adiabatic electrons ( $k_{\parallel}v_e > k_{\perp}u$ ), but in the second solitary vortex solution we considered the effect of small amount of these adiabatic electrons. A principal difference is that for the drift wave vortex the electron diamagnetic drift velocity  $v_{de}$  determines the speed of propagation, whereas for the dipolar vortex it is the Coriolis force  $2m_j\mathbf{V} \times \boldsymbol{\Omega}$  and the finite ion Larmor radius drift velocity that determine the speed of propagation of the vortex. For small ion-to-electron temperature ratios the speed of propagation in the direction of plasma rotation is given approximately by  $u = 2\Omega/k_{\perp}^2 r_n$ .

The dominant direction of flute vortex propagation is in the direction of the plasma rotation although counter streaming solutions also occur.

We show that the scale of the maximum potential  $\phi_m$  in the vortex scales as  $e\phi_m/T \sim 1/(k_{\perp}r_n)$  consistent with the usual estimate for nonlinear  $\mathbf{E} \times \mathbf{B}$  convective motion in an inhomogeneous plasma. We show that vortices propagating in the ion diamagnetic direction have a larger maximum potential (by a factor  $\simeq 5$ ) and a much larger vorticity than those propagating in the electron diamagnetic direction. The difference in the strength of the vorticity arises from the partial cancellation of the convective derivative proportional to  $u + T_i/T_e$  for the ion diamagnetic vortices.

Finally, we remark that although the nature of the vortex-wave interaction dynamics remains to be investigated theoretically, the experimental evidence [Antipov et al 1982, 1983; Antonova et al 1983; Flier et al 1983] as well as the computer simulations in [Makino et al 1981; McWilliams and Zabusky 1982; Zabusky and McWilliam 1982] show the importance of the interactions between these two components of the field. A vortex with its four parameters  $x_o, y_o$ , (initial position of the vortex core) amplitude and speed contain an infinite spectrum of coherent  $\mathbf{k}$  modes. We suggest that a theoretical description based on field containing both vortices and wave modes may be more nearly diagonal than a pure modal description.

*Walking and pulling, where is the destination?*



## Chapter VI

### CONCLUSIONS

In this thesis we have studied the linear stability and the nonlinear motion of magnetically confined rotating plasma.

By using a two fluid model including gyroviscosity, two coupled nonlinear equations which describe the low frequency flute dynamics of a low  $\beta$ , collisionless, isothermal, inhomogeneous plasma column confined in a constant axial magnetic field in the presence of a radial equilibrium electric field are derived. The equations include an effective gravity term to model magnetic field line curvature or RF pondermotive force effect. For a closed system the total mass, entropy, energy, and angular momentum are conserved by the coupled nonlinear equations.

The conclusions drawn from the linear stability analysis carried out in Chapter III and Chapter IV follow.

A new sufficient condition of stability for the rotating system against the flute perturbation is obtained. We find that as long as the equilibrium profiles satisfy the condition

$$|\omega_{*i}/m| = \left| \frac{cT_i}{Be} \frac{1}{r} \frac{d \ln n_o(r)}{dr} \right| \geq \Omega(r) \geq 0,$$

the rotating system is stable. In low  $\beta$  plasma, this new stability condition generalizes the one given by Freidberg and Pearstein [1978] for the constant  $\omega_{*i}$  and  $\Omega$  case. The new condition is valid for both constant and radially dependent

diamagnetic drift frequency and plasma rotation frequency.

An analytic solution of the linear stability equation for a plasma column with Gaussian-density profile, constant rotation frequency, effective gravity linear in the radius, and bounded by a conducting wall at finite distance, is obtained. Analysis of this model reveals several important aspects of the stability of rotating plasma. (1) Due to the combination effect of the Coriolis force and FLR, the stability of the system strongly depends on the rotation direction. For the plasma column with negative radial density gradient, the positive rotation state is more stable than the negative one, provided other relevant parameters are the same. This result suggests that modeling a rotational stability problem as a gravity stability problem by simply taking the centrifugal force as an effective gravity in principle is not correct, and will lead to error. This result also indicates that controlling the direction of the radial electric field inward to the plasma is a possible means to stabilizing the rotational flute instability. (2) The FLR stabilizing effect, unlike the gravity stability problem, FLR contribution is not absolutely stabilizing in rotating problem. Depending on the direction of rotation and the magnitude of  $\omega_{*i}$  and  $\Omega$ , the FLR can stabilize or destabilize the system. (3) The location of the conducting wall effects the (1,0) mode differently from the other modes. While decreasing the wall distance always stabilizes the mode with  $m > 1, n \geq 0$ , beyond a characteristic distance determined by equilibrium parameters



it destabilizes the (1,0) mode. We also found that the well-known result about the marginal instability of the (1,0) mode for this model profile is actually correct in the limiting case of putting the boundary at infinity, as is the conventional belief of (1,0) mode being rigid.

The analysis of sheared rotation stability for three simple equilibrium density and rotation frequency profiles indicates the analogy between the shear rotational stability problem and the parallel shear flow stability problem in a perfect fluid. This resemblance suggest applying the results of the relatively well studied latter problem to understand better the former. one.

The investigation of the flute-like rotational trapped particle modes for a three cell axisymmetric Tandem mirror system provides some useful quantitative and qualitative knowledge about this mode. (1) By modifying the equation we used in section III.3, considering the flute-like mode, we obtain an analytically solvable stability equation for the trapped particle modes in a model Tandem mirror system, and the solution of this equation quantitatively gives the radial structure, oscillation frequency, and growth rate of the modes. These results should be considered as the quantitative counterpart of the qualitative analysis of the rotational trapped particle mode reported recently [Kesner and Lane, 1985]. (2) The analytic dispersion relation obtained in section IV.2 shows the fact that the effect of the passing electrons is always canceling the FLR effect, hence when the

two effects have comparable magnitude this system is more unstable than the one we discussed in section **III.3**. When the passing electron fraction is larger than some critical value, given by Eq. (IV.34), then the FLR effect is negligible and the system can be stabilized. (3) The numerical results presented in section **IV.3** give us much new information about the stability of systems with sheared rotation frequency and sheared diamagnetic frequency profiles. Comparison between the analytic and numerical results seem to suggest that the results for the Gaussian density and uniform rotation model overestimate the instability of the real system. Although some possible explanations of the numerical results were suggested, we feel that to get a better understanding of this new topic more works are needed.

The nonlinear analysis carried out in Chapter **V** gives two exact localized solutions of the nonlinear equations, the solitary flute-vortex in rotating plasma and the similar one modified by including the passing electron population.

These vortices are two-dimensional, localized, and travel in the azimuthal direction with speeds limited by the relevant equilibrium plasma parameters. Most interesting, the allowed region for the travelling speeds of these vortices is complementary to the allowed region of the phase velocity of the corresponding linear modes. All these features of our solitary vortex solution are common to the ones obtained from the nonlinear Rossby wave equation in planetary atmosphere studies and the drift vortex from the nonlinear drift wave equation in magnetized plasma.

For the latter two vortices, there are numerical simulations which indicate their robustness under collisions as well as evidence from laboratory experiments which shows their existence in nature. In addition, further investigations about the spectrum and other properties of the drift vortex also have been carried out [Meiss and Horton, 1982; Meiss, 1984].

The existence of these vortex solutions to the nonlinear equations describing flute dynamics of low  $\beta$  rotating plasma and the complementary relation between the vortices and the phase velocity of the linear modes suggest a possible new picture of the dynamics: the complete description of the fluctuations in low  $\beta$  rotating plasma should include both the coherent vortices component and the conventional modes.

## Appendix A

### Derivation of Equation (III.9)

In this appendix we derive the linear stability equation (III.9) from Eqs. (III.5) and (III.6).

Substituting normal mode of perturbation

$$\delta\phi_m(r, \theta, t) = \delta\phi_m(r)e^{i(m\theta - \omega t)}, \quad \delta n_m(r, \theta, t) = \delta n_m(r)e^{i(m\theta - \omega t)}$$

into Eq. (III.5), we have

$$-i\omega\delta n_m + i\frac{c}{B}\frac{d\phi_o}{dr}\frac{m}{r}\delta n_m - i\frac{c}{B}\frac{m}{r}\frac{dn_o}{dr}\delta\phi_m = 0. \quad (A.1)$$

Remember  $\Omega = \frac{1}{r}\frac{c}{B}\frac{d\phi_o}{dr}$ ,  $\tilde{\omega} = \omega - m\Omega$ , immediatly we have

$$\delta n_m(r) = -\frac{cm}{Br\tilde{\omega}}\delta\phi_m(r). \quad (A.2)$$

Substituting the normal mode  $\delta\phi_m(r, \theta, t), \delta n_m(r, \theta, t)$  into Eq. (III.6) yields

$$\begin{aligned} & \frac{c}{B}\nabla \cdot (n_o\frac{\partial}{\partial t}\nabla\delta\phi_m + \delta n_m\frac{\partial}{\partial t}\nabla\phi_o) + \\ & (\frac{c}{B})^2\nabla \cdot (\delta n_m[\phi_o, \nabla\phi_o] + n_o[\delta\phi_m, \nabla\phi_o] + n_o[\phi_o, \nabla\delta\phi_m]) + \\ & (\frac{c}{B})^2\frac{T_i}{e}\nabla \cdot ([\delta n_m, \nabla\phi_o] + [n_o, \nabla\delta\phi_m]) + [\delta n_m U(r)] \\ & = \frac{c}{B}(\nabla n_o \cdot \frac{\partial}{\partial t}\nabla\delta\phi_m + n_o\frac{\partial}{\partial t}\nabla^2\delta\phi_m) + (\frac{c}{B})^2\nabla n_o \cdot ([\phi_o, \nabla\delta\phi_m]) + \end{aligned}$$

$$\begin{aligned}
& [\delta\phi_m, \nabla\phi_o] + \left(\frac{c}{B}\right)^2 n_o ([\delta\phi_m, \nabla^2\delta\phi_m]) + \\
& \left(\frac{c}{B}\right)^2 \nabla\delta n_m \cdot [\phi_o, \nabla\phi_o] + \left(\frac{c}{B}\right)^2 \frac{T_i}{e} ([\nabla\delta n_m, \nabla\phi_o] + [\delta n_m, \nabla^2\phi_o]) + \\
& [\nabla n_o, \nabla\delta\phi_m] + [n_o, \nabla^2\delta\phi_m] + [\delta n_m, U(r)] = 0 \tag{A.3}
\end{aligned}$$

Notice that

$$\nabla n_o \cdot \frac{\partial}{\partial t} \nabla\delta\phi = -i\omega \frac{dn_o}{dr} \frac{d\delta\phi_m}{dr}, \tag{A.4}$$

$$n_o \frac{\partial}{\partial t} \nabla\delta^2\phi_m = -i\omega n_o \nabla^2\delta\phi_m, \tag{A.5}$$

$$\begin{aligned}
\frac{c}{B} \nabla n_o \cdot [\phi_o, \nabla\delta\phi_m] &= \frac{c}{B} \frac{dn_o}{dr} [\phi_o, \nabla\delta\phi_m]_{\hat{r}} \\
&= i \frac{m}{r} \Omega \frac{dn_o}{dr} \left(-\delta\phi_m + r \frac{d\delta\phi_m}{dr}\right), \tag{A.6}
\end{aligned}$$

$$\begin{aligned}
\frac{c}{B} \nabla n_o \cdot [\delta\phi_m, \nabla\phi_o] &= \frac{c}{B} \frac{dn_o}{dr} [\delta\phi_m, \nabla\phi_o]_{\hat{r}} \\
&= -i \frac{m}{r} \frac{dn_o}{dr} \frac{d}{dr} (r\Omega) \delta\phi_m \tag{A.7}
\end{aligned}$$

$$\frac{c}{B} n_o [\delta\phi_m, \nabla^2\phi_o] = -i \frac{m}{r} n_o \frac{d}{dr} \left\{ \frac{1}{r} \frac{d}{dr} (r^2\Omega) \right\} \delta\phi_m \tag{A.8}$$

$$\frac{c}{B} n_o [\phi_o, \nabla^2\delta\phi_m] = imn_o \Omega \nabla^2\delta\phi_m, \tag{A.9}$$

$$\begin{aligned} \frac{c}{B} [\nabla \delta n_m, \nabla \phi_o] &= - \left[ \frac{d\phi_o}{dr} \hat{r}, \nabla \delta n_m \right] \\ &= -im \frac{d\Omega}{dr} \left( \frac{d\delta n_m}{dr} - \frac{\delta n_m}{r} \right), \end{aligned} \quad (\text{A.10})$$

$$\frac{c}{B} [\delta n_m, \nabla^2 \phi_o] = -i \frac{m}{r} \frac{d}{dr} \left( \frac{1}{r} \frac{d}{dr} (r^2 \Omega) \right) \delta n_m, \quad (\text{A.11})$$

$$\begin{aligned} [\nabla n_o, \nabla \delta \phi_m] &= \left[ \frac{dn_o}{dr} \hat{r}, \nabla \delta \phi_m \right] \\ &= i \frac{m}{r} \left( \frac{d^2 n_o}{dr^2} - \frac{1}{r} \frac{dn_o}{dr} \right) \left( \frac{d\delta \phi_m}{dr} - \frac{\delta \phi_m}{r} \right), \end{aligned} \quad (\text{A.12})$$

$$[n_o, \nabla^2 \delta \phi_m] = i \frac{m}{r} \frac{dn_o}{dr} \nabla^2 \delta \phi_m, \quad (\text{A.13})$$

$$\left( \frac{c}{B} \right)^2 \nabla \delta n_m \cdot [\phi_o, \nabla \phi_o] = im \Omega^2 \delta n_m, \quad (\text{A.14})$$

$$[\delta n_m, U(r)] = -i \frac{m}{r} \frac{dU}{dr} \delta n_m = i \frac{m}{r} g(r) \delta n_m. \quad (\text{A.15})$$

Substituting (A.4)-(A.15) into (A.3) yields

$$\begin{aligned} &(\tilde{\omega} - \omega_{*i}) n_o \nabla^2 \delta \phi_m + \tilde{\omega} \frac{dn_o}{dr} \frac{d\delta \phi_m}{dr} + \\ &\left\{ \left( \frac{2m\Omega}{r} + m \frac{d\Omega}{dr} \right) \frac{dn_o}{dr} + n_o \frac{m}{r} \frac{d}{dr} \left[ \frac{1}{r} \frac{d}{dr} (r^2 \Omega) \right] \right\} \delta \phi_m - \\ &\frac{cT_i}{Be} m \left( \frac{d^2 n_o}{dr^2} - \frac{1}{r} \frac{dn_o}{dr} \right) \frac{d}{dr} \left( \frac{\delta \phi_m}{r} \right) + \frac{T_i}{e} \frac{m}{r} \frac{d}{dr} \left[ \frac{1}{r} \frac{d}{dr} (r^2 \Omega) \right] \delta n_m - \end{aligned}$$

$$\frac{B}{c} \frac{m}{r} (r\Omega^2 + g) \delta n_m + \frac{T_i}{e} m \frac{d\Omega}{dr} r \frac{d}{dr} \left( \frac{\delta n_m}{r} \right) = 0. \quad (\text{A.16})$$

Notice that

$$\begin{aligned} \nabla \cdot [(\tilde{\omega} - \omega_{*i}) n_o \nabla \delta \phi_m] &= (\tilde{\omega} - \omega_{*i}) n_o \nabla^2 \delta \phi_m + \tilde{\omega} \frac{dn_o}{dr} \frac{d\delta \phi_m}{dr} - \\ &- m \frac{d\Omega}{dr} n_o \frac{d\delta \phi_m}{dr} - \frac{d}{dr} (n_o \omega_{*i}) \frac{d\delta \phi_m}{dr}, \end{aligned} \quad (\text{A.17})$$

and

$$\frac{cT_i}{Be} m \left( \frac{d^2 n_o}{dr^2} - \frac{1}{r} \frac{dn_o}{dr} \right) \frac{d}{dr} \frac{\delta \phi_m}{r} = - \frac{d}{dr} (n_o \omega_{*i}) \frac{d\delta \phi_m}{dr} + \frac{1}{r} \frac{d}{dr} (n_o \omega_{*i}) \delta \phi_m. \quad (\text{A.18})$$

Substituting (A.2) into the terms with  $\delta n_m$  in (A.16), eliminating  $\delta n_m$ , and notice that

$$\frac{T_i}{e} m \frac{d\Omega}{dr} r \frac{d}{dr} \left( \frac{\delta n_m}{r} \right) = \frac{cT_i}{Be} \frac{1}{\tilde{\omega}} \frac{m^2}{r^2} \frac{dn_o}{dr} \frac{d\Omega}{dr} \delta \phi_m - m \frac{d\Omega}{dr} \frac{d}{dr} \left( \frac{\omega_{*i}}{\tilde{\omega}} n_o \delta \phi_m \right), \quad (\text{A.19})$$

$$- \frac{B}{c} \frac{m}{r} (r\Omega^2 + g) \delta n_m = \frac{1}{\tilde{\omega}} m^2 (\Omega^2 + g/r) \frac{1}{r} \frac{dn_o}{dr} \delta \phi_m, \quad (\text{A.20})$$

$$\frac{T_i}{e} \frac{m}{r} \frac{d}{dr} \left[ \frac{1}{r} \frac{d}{dr} (r^2 \Omega) \right] \delta n_m = - \frac{m}{r} \frac{\omega_{*i}}{\tilde{\omega}} n_o \frac{d}{dr} \left[ \frac{1}{r} \frac{d}{dr} (r^2 \Omega) \right] \delta \phi_m. \quad (\text{A.21})$$

Substituting (A.17)-(A.21) into (A.16), arranging each term properly, we obtain

$$\begin{aligned}
& \nabla_{\perp} \cdot [n_o(\tilde{\omega} - \omega_{*i})\nabla_{\perp}\delta\phi_m] + m\frac{d\Omega}{dr}\frac{d}{dr}[n_o(1 - \frac{\omega_{*i}}{\tilde{\omega}})\delta\phi_m] \\
& + \{[2m\Omega + \frac{m^2(\Omega^2 + g/r)}{\tilde{\omega}} - \frac{m^2cT_i}{\tilde{\omega}Be}\frac{d^2(r\Omega)}{dr^2}]\}\frac{1}{r}\frac{dn_o}{dr} \\
& \frac{m}{r}n_o\frac{d}{dr}(\frac{1}{r}\frac{d}{dr}(r^2\Omega)) + \frac{1}{r}\frac{d}{dr}(n_o\omega_{*i})\}\delta\phi_m = 0. \tag{III.9}
\end{aligned}$$

Notice That

$$\frac{d^2}{dr^2}(r\Omega) = \frac{d}{dr}(r^2\frac{d\Omega}{dr}).$$



## Appendix B

### Derivation of Equation (III.10)

In this appendix we give the derivation of equation (III.10).

Rewrite the linearized equation (A.16) as

$$\begin{aligned}
 & (\tilde{\omega} - \omega_{*i})n_o \nabla_{\perp}^2 \delta\phi_m + \tilde{\omega} \frac{dn_o}{dr} \frac{d\delta\phi_m}{dr} \\
 & + \frac{m}{r} \frac{dn_o}{dr} \left(2\Omega + r \frac{d\Omega}{dr}\right) \delta\phi_m + \frac{m}{r} n_o \frac{d}{dr} \left[ \frac{1}{r} \frac{d}{dr} (r^2 \Omega) \right] \delta\phi_m \\
 & - m \frac{cT_i}{Be} r \frac{d}{dr} \left( \frac{1}{r} \frac{dn_o}{dr} \right) \frac{d}{dr} \left( \frac{\delta\phi_m}{r} \right) - \frac{B}{c} m \left( \Omega^2 + \frac{g}{r} \right) \delta n_m \\
 & + \frac{T_i}{e} \frac{m}{r} \frac{d}{dr} \left[ \frac{1}{r} \frac{d}{dr} (r^2 \Omega) \right] \delta n_m + \frac{T_i}{e} m r \frac{d\Omega}{dr} \frac{d}{dr} \left( \frac{\delta n_m}{r} \right) = 0. \tag{B.1}
 \end{aligned}$$

Introduce radial Lagrangian displacement  $\xi_m(r, \theta, t)$  corresponding to the normal mode  $\delta\phi_m(r, \theta, t)$ ,  $\delta n_m(r, \theta, t)$  such that

$$\frac{d\xi_m}{dt} = v_r(r, \theta, t) = -i \frac{c}{B} \frac{m}{r} \delta\phi_m. \tag{B.2}$$

Solving equation (B.2) we have

$$\xi_m(r, \theta, t) = \frac{c}{B} \frac{m}{r\tilde{\omega}} \delta\phi_m(r) e^{i(m\theta - \omega t)}. \tag{B.3}$$

Substituting (B.3) into (A.2) gives

$$\delta n_m = -\frac{dn_o}{dr} \delta\phi_m. \tag{B.4}$$

Now we intend to express equation (B.1) in terms of  $\xi_m$ . Substituting the relation

$$\delta\phi_m = \frac{B}{cm} r\tilde{\omega}\xi_m$$

into each term of equation (B.1), we obtain

$$\begin{aligned} n_o\tilde{\omega}\nabla_{\perp}^2\delta\phi_m &= \frac{B}{cm} \left\{ \frac{n_o}{r^2} \left[ (r\tilde{\omega}^2 + 3r^2\tilde{\omega}\frac{d\tilde{\omega}}{dr} + r^2\frac{d^2\tilde{\omega}}{dr^2})\xi_m + 3r\tilde{\omega}^2\frac{d\xi_m}{dr} \right. \right. \\ &\quad \left. \left. + 2r^3\frac{d\tilde{\omega}}{dr}\frac{d\xi_m}{dr} + r^3\tilde{\omega}\frac{d^2\xi_m}{dr^2} \right] - \frac{m^2}{r}n_o\tilde{\omega}^2\xi_m \right\} \\ &= \frac{B}{cm} \left\{ \frac{n_o}{r^2} \left[ \frac{d}{dr}(\tilde{\omega}^2 r^3 n_o \frac{d\xi_m}{dr}) + 3r^2\tilde{\omega}\frac{d\tilde{\omega}}{dr}\xi_m + r^3\tilde{\omega}\frac{d^2\tilde{\omega}}{dr^2}\xi_m \right] \right. \\ &\quad \left. + \frac{1-m^2}{r}n_o\tilde{\omega}^2\xi_m - \tilde{\omega}^2 r \frac{dn_o}{dr} \frac{d\xi_m}{dr} \right\}, \end{aligned} \quad (B.5)$$

$$\tilde{\omega}\frac{dn_o}{dr}\frac{d\delta\phi_m}{dr} = \frac{B}{cm} \left[ r\tilde{\omega}^2\frac{dn_o}{dr}\frac{d\xi_m}{dr} + (\tilde{\omega}^2 + r\tilde{\omega}\frac{d\tilde{\omega}}{dr})\frac{dn_o}{dr}\xi_m \right], \quad (B.6)$$

$$\frac{m}{r}\frac{dn_o}{dr}(2\Omega + r\frac{d\Omega}{dr})\delta\phi_m = \frac{B}{cm}\frac{1}{r^2}\frac{dn_o}{dr}(2mr^2\Omega\tilde{\omega} - r^3\tilde{\omega}\frac{d\tilde{\omega}}{dr})\xi_m. \quad (B.7)$$

in derivation of (B.7) the relation

$$\frac{d\tilde{\omega}}{dr} = -m\frac{d\Omega}{dr}, \quad (B.8)$$

is used.

$$\frac{m}{r} n_o \frac{d}{dr} \left[ \frac{1}{r} \frac{d}{dr} (r^2 \Omega) \right] \delta \phi_m = - \frac{B}{cm} \frac{n_o}{r^2} \left( 3r^2 \tilde{\omega} \frac{d\tilde{\omega}}{dr} + r^3 \tilde{\omega} \frac{d^2 \tilde{\omega}}{dr^2} \right) \xi_m, \quad (B.9)$$

Summing up the results obtained, after many cancelations

$$\begin{aligned} (B.5) + (B.6) + (B.7) + (B.8) + (B.9) &= \left( \frac{B}{cm} \right) \frac{1}{r^2} \left\{ \frac{d}{dr} (\tilde{\omega}^2 r^3 n_o \frac{d\xi_m}{dr}) \right. \\ &\quad \left. + [(1 - m^2) r n_o \tilde{\omega}^2 \xi_m + \frac{dn_o}{dr} r^2 (\omega^2 - m^2 \Omega^2)] \xi_m \right\}, \end{aligned} \quad (B.10)$$

$$- \frac{B}{c} m (\Omega^2 + g/r) \delta n_m = \frac{B}{cm} [m^2 r^2 (\Omega^2 + g/r)] \frac{1}{r^2} \frac{dn_o}{dr} \xi_m \quad (B.11)$$

$$\begin{aligned} &-m \frac{cT_i}{Be} \left( \frac{d^2 n_o}{dr^2} - \frac{1}{r} \frac{dn_o}{dr} \right) \frac{d}{dr} \left( \frac{\delta \phi_m}{r} \right) \\ &= -mr \frac{cT_i}{Be} \frac{d}{dr} \left( \frac{1}{r} \frac{dn_o}{dr} \right) \frac{d}{dr} \left( \frac{\delta \phi_m}{r} \right) \\ &= - \frac{B}{cm} r \frac{d(n_o \omega_{*i})}{dr} \frac{d}{dr} (\tilde{\omega} \xi_m) \\ &= - \frac{B}{cm} \left\{ r n_o \tilde{\omega} \frac{d\omega_{*i}}{dr} \frac{d\xi_m}{dr} + r n_o \frac{d\omega_{*i}}{dr} \frac{d\tilde{\omega}}{dr} \xi_m \right. \\ &\quad \left. + r \omega_{*i} \frac{dn_o}{dr} \left( \frac{d\tilde{\omega}}{dr} \xi_m + \tilde{\omega} \frac{d\xi_m}{dr} \right) \right\} \end{aligned} \quad (B.12)$$

$$\begin{aligned} &\frac{T_i}{e} \frac{m}{r} \left\{ \frac{d}{dr} \left[ \frac{1}{r} \frac{d}{dr} (r^2 \Omega) \right] \right\} \delta n_m \\ &= - \frac{T_i}{e} \frac{m}{r} \frac{dn_o}{dr} \left\{ \frac{d}{dr} \left[ \frac{1}{r} \frac{d}{dr} (r^2 \Omega) \right] \right\} \xi_m \end{aligned}$$

$$\begin{aligned}
&= -\frac{B}{c} n_o \omega_{*i} \left( 3 \frac{d\Omega}{dr} + r \frac{d^2\Omega}{dr^2} \right) \xi_m \\
&= \frac{B}{cm} n_o \omega_{*i} \left( 3 \frac{d\tilde{\omega}}{dr} + r \frac{d^2\tilde{\omega}}{dr^2} \right) \xi_m
\end{aligned} \tag{B.13}$$

$$\begin{aligned}
&\frac{T_i}{e} m r \frac{d\Omega}{dr} \frac{d}{dr} \left( \frac{\delta n_m}{r} \right) = \frac{B}{cm} r \frac{d\tilde{\omega}}{dr} \frac{d}{dr} \left( n_o \omega_{*i} \xi_m \right) \\
&= \frac{B}{cm} \left\{ r n_o \frac{d\tilde{\omega}}{dr} \frac{d\omega_{*i}}{dr} \xi_m + r n_o \frac{d\tilde{\omega}}{dr} \omega_{*i} \frac{d\xi_m}{dr} + r \frac{dn_o}{dr} \frac{d\tilde{\omega}}{dr} \omega_{*i} \xi_m \right\}
\end{aligned} \tag{B.14}$$

$$\begin{aligned}
-n_o \omega_{*i} \nabla^2 \delta \phi_m &= -\frac{B}{cm} \left\{ \frac{n_o \omega_{*i}}{r} \left[ \tilde{\omega} \xi_m + 3r \frac{d\tilde{\omega}}{dr} \xi_m + r^2 \frac{d^2\tilde{\omega}}{dr^2} \xi_m + \right. \right. \\
&\quad \left. \left. 3r\tilde{\omega} \frac{d\xi_m}{dr} + 2r^2 \frac{d\tilde{\omega}}{dr} \frac{d\xi_m}{dr} + r^2 \tilde{\omega} \frac{d^2\xi_m}{dr^2} \right] - \frac{m^2 n_o}{r} \tilde{\omega} \omega_{*i} \xi_m \right\} \\
&= -\frac{B}{cm} \left\{ \frac{1}{r^2} \frac{d}{dr} \left( n_o \tilde{\omega} \omega_{*i} r^3 \frac{d\xi_m}{dr} \right) + \frac{n_o}{r^2} \left[ r(1-m^2) \tilde{\omega} \omega_{*i} \xi_m + \right. \right. \\
&\quad \left. \left. 3r^2 \frac{d\tilde{\omega}}{dr} \omega_{*i} \xi_m + r^3 \frac{d^2\tilde{\omega}}{dr^2} \omega_{*i} \xi_m + r^3 \frac{d\tilde{\omega}}{dr} \omega_{*i} \frac{d\xi_m}{dr} \right] - \right. \\
&\quad \left. - \frac{1}{r^2} \tilde{\omega} \left[ \frac{dn_o}{dr} \omega_{*i} r^3 \frac{d\xi_m}{dr} + r^3 n_o \frac{d\omega_{*i}}{dr} \frac{d\xi_m}{dr} \right] \right\}
\end{aligned} \tag{B.15}$$

Summig up Eqs (B.12)-(B.15) gives

$$\begin{aligned}
&(B.12) + (B.13) + (B.14) + (B.15) = \\
&= -\frac{B}{cm} \frac{1}{r^2} \left\{ \frac{d}{dr} \left( \tilde{\omega} \omega_{*i} n_o r^3 \frac{d\xi_m}{dr} \right) + n_o (1-m^2) r \tilde{\omega} \omega_{*i} \xi_m \right\}
\end{aligned} \tag{B.16}$$

Finally, adding Eqs. (B.10), (B.11), and (B.16) yields

$$\frac{d}{dr} \left[ \tilde{\omega}^2 \left( 1 - \frac{\omega_{*i}}{\tilde{\omega}} \right) r^3 n_o \frac{d\xi_m}{dr} \right] + \left[ (1-m^2) \tilde{\omega}^2 \left( 1 - \frac{\omega_{*i}}{\tilde{\omega}} \right) n_o r + r^2 (\omega^2 + g/r) \frac{dn_o}{dr} \right] \xi_m = 0. \tag{III.10}$$

## Appendix C

### Derivation of Equation (III.11)

In this Appendix we give the derivation of Eq.(III.11).

From (A.1), we have

$$m \frac{cT_e}{Be} \frac{1}{r} \frac{d\tilde{\phi}_o}{dr} \delta n_m - m \frac{cT_e}{Be} \frac{1}{r} \frac{dn_o}{dr} \delta \tilde{\phi}_m = \omega \delta n_m, \quad (C.1)$$

where we denote  $\tilde{\phi} = \frac{e\phi}{T_e}$ .

Notice that

$$\frac{cT_e}{Be} \frac{1}{r} \frac{d\tilde{\phi}_o}{dr} = \Omega(r),$$

and

$$-\frac{cT_e}{Be} \frac{1}{r} \frac{1}{n_o} \frac{dn_o}{dr} = \omega_{*e},$$

Eq.(C.1) can be written as

$$m\Omega \delta \tilde{n}_m + m\omega_{*e} \delta \tilde{\phi}_m = \omega \delta \tilde{n}_m. \quad (C.2)$$

Linearizing Eq.(II.38) yields

$$\hat{L}_1 \delta n_m + \hat{L}_2 \delta \tilde{\phi}_m = \omega (\hat{L}_3 \delta n_m + \hat{L}_4 \delta \tilde{\phi}_m) \quad (C.3)$$

where

$$\hat{L}_1 = (im) \left\{ \frac{T_i}{T_e} \left[ \frac{1}{r^2} \frac{d\tilde{\phi}_o}{dr} - \frac{1}{r} \frac{d^2 \tilde{\phi}_o}{dr^2} \right] \frac{d}{dr} + \left[ \frac{1}{r^2} \left( \frac{d\tilde{\phi}_o}{dr} \right)^2 + g/r - \frac{T_i}{T_e} \frac{1}{r} \frac{d^3 \tilde{\phi}_o}{dr^3} \right] \right\} \quad (C.4)$$

$$\hat{L}_2 = imn_o \left( \hat{O}_1 \frac{d^2}{dr^2} + \hat{O}_2 \frac{d}{dr} + \hat{O}_3 \right) \quad (C.5)$$

$$\hat{O}_1 = \frac{1}{r} \frac{d\tilde{\phi}_o}{dr} + \frac{T_i}{T_e} \frac{1}{r} \frac{d \ln n_o}{dr} \quad (C.6)$$

$$\hat{O}_2 = \frac{1}{r} \frac{d\tilde{\phi}_o}{dr} \left( \frac{1}{r} + \frac{d \ln n_o}{dr} \right) + \frac{T_i}{T_e} \frac{1}{rn_o} \frac{d^2 n_o}{dr^2} \quad (C.7)$$

$$\begin{aligned} \hat{O}_3 = & -\frac{1}{r} \frac{d^2 \tilde{\phi}_o}{dr^2} \left( \frac{1}{r} + \frac{d \ln n_o}{dr} \right) + \frac{1}{r^2} \frac{d\tilde{\phi}_o}{dr} \left( \frac{1}{r} - \frac{d \ln n_o}{dr} \right) - \\ & - \frac{m^2}{r^3} \frac{d\tilde{\phi}_o}{dr} - \frac{1}{r} \frac{d^3 \tilde{\phi}_o}{dr^3} + \frac{T_i}{T_e} \left( -\frac{1}{r^2} \frac{1}{n_o} \frac{d^2 n_o}{dr^2} + \frac{1-m^2}{r^3} \frac{d \ln n_o}{dr} \right) \end{aligned} \quad (C.8)$$

$$\hat{L}_3 = 0 \quad (C.9)$$

$$\hat{L}_4 = in_o \left\{ \frac{d^2}{dr^2} + \left( \frac{1}{r} + \frac{d \ln n_o}{dr} \right) \frac{d}{dr} - \frac{m^2}{r^2} \right\} \quad (C.10)$$

Taking dimensionless quantities

$$\delta \tilde{n}_m = \frac{\delta n_m}{n_o(r)}$$

$$x = \frac{r^2}{a^2}$$

$$\hat{\Omega} = \Omega / \left( \frac{\rho_s v_s}{a^2} \right)$$

where  $a^2$  is radial scale length of plasma, and

$$v_s = \left(\frac{T_e}{m_i}\right)^{\frac{1}{2}}, \quad \rho_s = v_s/\omega_{ci}.$$

Eqs. (C.2) and (C.3) have the forms of

$$A_{11}(x)\delta\tilde{n}_m(x) + A_{12}(x)\delta\tilde{\phi}_m(x) = \omega(B_{11}(x)\delta\tilde{n}(x) + B_{12}x\delta\tilde{\phi}_m(x)) \quad (C.11)$$

$$A_{21}(x)\delta\tilde{n}_m(x) + A_{22}(x)\delta\tilde{\phi}_m(x) = \omega(B_{21}(x)\delta\tilde{n}_m(x) + B_{22}(x)\delta\tilde{\phi}_m(x)) \quad (C.12)$$

where

$$A_{11} = m\hat{\Omega}(x), \quad (C.13)$$

$$A_{12} = m\omega_{*e}(x), \quad (C.14)$$

$$B_{11} = 1, \quad (C.15)$$

$$B_{12} = 0. \quad (C.16)$$

$$A_{21} = m \left\{ -\frac{T_i}{T_e} x \frac{d\hat{\Omega}}{dx} \frac{d}{dx} + \frac{1}{4} \left( \hat{\Omega}^2 + \frac{g}{\sqrt{x}} \right) - \right.$$

$$-\frac{T_i}{T_e} \left[ \frac{1}{\sqrt{x}} \frac{d}{dx} \left( \sqrt{x^3} \frac{d\hat{\Omega}}{dx} \right) + x \frac{d\hat{\Omega}}{dx} \frac{d \ln n_o}{dx} \right] \quad (C.17)$$

$$A_{22} = m \left\{ x(\hat{\Omega} + 2 \frac{T_i}{T_e} \frac{dn_o}{dx}) \frac{d^2}{dx^2} + [\hat{\Omega} \frac{1}{n_o} \frac{d}{dx} (xn_o) + 2 \frac{T_i}{T_e} \frac{1}{n_o} \frac{d}{dx} (x \frac{dn_o}{dx})] \frac{d}{dx} - [\frac{1}{x} \frac{d}{dx} (x^2 \frac{d\hat{\Omega}}{dx}) + \frac{d \ln n_o}{dx} \frac{d}{dx} (x\hat{\Omega}) + \frac{m^2}{4x} \hat{\Omega} + \frac{T_i}{T_e} \frac{1}{n_o} (\frac{d^2 n_o}{dx^2} + \frac{1}{2} \frac{m^2}{x} \frac{dn_o}{dx})] \right\}, \quad (C.18)$$

$$B_{21} = 0, \quad (C.19)$$

$$B_{22} = x \frac{d^2}{dx^2} + \frac{1}{n_o} \frac{d}{dx} (xn_o) \frac{d}{dx} - \frac{1}{4} \frac{m^2}{x}. \quad (C.20)$$

Writing Eqs.(C.11) and (C.12) together gives a matrix form of equation

$$\mathbf{A} \begin{pmatrix} \delta \tilde{n}_m \\ \delta \tilde{\phi}_m \end{pmatrix} = \omega \mathbf{B} \begin{pmatrix} \delta \tilde{n}_m \\ \delta \tilde{\phi}_m \end{pmatrix} \quad (III.11)$$

where

$$\mathbf{A} = \begin{pmatrix} A_{11}, & A_{12} \\ A_{21}, & A_{22} \end{pmatrix}$$

$$\mathbf{B} = \begin{pmatrix} B_{11}, & B_{12} \\ B_{21}, & B_{22} \end{pmatrix}.$$



## Appendix D

### The Nonlinear Dispersion Relations of Solitary Vortices in Magnetized Plasma

For recent few years, various solitary vortex solutions have been obtained in magnetized plasma and the number of publications on this topic is growing. In this Appendix we intend to list these solutions for reference. Since all these solutions have the same localized dipolar structure as the one obtained in nonlinear Rossby wave equation, here we classify these solutions according to their nonlinear dispersion relations.

#### 1. Solitary Drift Vortex

Single field,  $\phi(x, y, t) \equiv \phi(x, y - ut)$ .

Nonlinear Dispersion Relation:

$$k^2 = \frac{u - v_{de}}{u}$$

(T. Taniuti and A. Hasegawa, 1982)

#### 2. Solitary Electron-Drift and Ion-Acoustic Vortex

Single field,  $\phi(x, y, z, t) \equiv \phi(x, y + \alpha z - ut)$

Nonlinear Dispersion Relation:

$$k^2 = \frac{u(u - v_d) - \alpha^2}{u^2}$$

(J.Meiss and W.Horton, 1983)

**3. Solitary Flute Vortex**Two fields,  $n(x, y - ut)$ ,  $\phi(x, y - ut)$ 

Nonlinear Dispersion relation:

$$k^2 = \frac{v}{u(u+1)}, \quad (v = gr_n/v_{di}^2)$$

(V.Pavlenko and V.Petviashvili, 1983)

**4. Ballooning Vortex**Single field,  $\phi(x, y + \alpha z - ut)$ 

Nonlinear Dispersion Relation:

$$k^2 = \frac{-g/r_n}{u^2 - \alpha^2 C_A^2}, \quad (C_A^2 = B_o^2/4\pi\rho_o)$$

(A.Mikhailovskii et al., 1984)

**5. Alfvén Vortex**Two fields,  $\phi(x, y + \alpha z - ut)$ ,  $\psi(x, y + \alpha z - ut)$ 

Nonlinear Dispersion Relation:

$$k^2 = \frac{\alpha^2 c_A^2 - u^2}{\alpha^2 c_A^2 \rho_s^2}$$

(A.Mikhailovskii et al., 1984)

**6. Short-Wavelength Drift Vortex**Single field,  $\phi(x, y + \alpha z - ut)$

Nonlinear Dispersion Relation:

$$k^2 = \frac{1 - v_{di}/u - \alpha^2 v_{es}^2/u^2}{\rho_{es}^2}, \quad (v_{es} \equiv \sqrt{\frac{T_i}{m_e}}, \rho_{es}^2 \equiv \frac{T_i}{m_e \omega_{ce}^2})$$

(A.Mikhailovskii et al., 1984)

### 7. Electron Gradient Vortex

Single field,  $\phi(x, y + \alpha z - ut)$

Nonlinear Dispersion Relation:

$$k^2 = \frac{\alpha^2 \omega_{pe}^2 \delta}{u^2 (1 + \omega_{pe}^2/\omega_{ce}^2)}, \quad (\delta \equiv \frac{u}{r_n \omega_{ce} \alpha^2} - 1)$$

(G.Aburdzhaniya et al., 1984)

### 8. Convective Cell Vortex

Three fields,  $n, \phi$ , and  $v_{\parallel} \equiv f(x, y + \alpha z - ut)$

Nonlinear Dispersion Relations:

$$k^2 = \frac{\alpha}{\alpha^2 - u^2}$$

(P.Shukla et al., 1985)

### 9. Shear Alfvén Vortex in Very Low $\beta$ Plasma

Two fields,  $\phi(x, y + \alpha z - ut), A_{\parallel}(x, y + \alpha z - ut)$

Nonlinear Dispersion Relation:

$$k^2 = \frac{1 - \alpha^2/u^2}{2m_e/m_i \beta}, \quad (\beta = \frac{8\pi n_o T_e}{B_o^2})$$

(P.Shukla et al., 1985)

**10. Drift-Alfvén Vortex**Three Fields,  $\phi, A_{\parallel},$  and  $n \equiv f(x, y + \alpha z - ut)$ 

Nonlinear Dispersion Relation:

$$k^2 = -\frac{(u - v_{de})(u^2 - uv_{di} - \alpha^2)}{(u - v_{di})\alpha^2}$$

(P.Shukla, M.Yu, and R.Varma, 1985)

**11. Kinetic Alfvén Vortex**

Three fields, as in 10.

Nonlinear Dispersion Relation:

$$k^2 = 1 - u^2/\alpha^2$$

(P.Shukla, Y.Yu, and R.Varma, 1985)

**12. Flute Vortex in Rotating Plasma**Two fields,  $n(x, y - ut), \phi(x, y - ut)$ 

Nonlinear Dispersion Relation:

$$k^2 = \frac{uv_c + v_g}{u(u + T_i/T_e)}$$

(W.Horton, J.Liu, J.Meiss, and J.Sedlak, 1985)

**13. Modified Flute Vortex in Rotating Plasma**

Two fields, same as in 12.

Nonlinear Dispersion Relation:

$$k^2 = \frac{u[v_c + A_p(u - v_{de})] + v_g}{u(u + T_i/T_e)}$$

(J.Liu, 1985)

## REFERENCES

- G.D.Aburdzheniya, A.B.Michailovskii, and Shapov, *Phys.Lett.* **100A** (1984) 134.
- G.D.Aburdzheniya, F.F.Kamenets, V.P.Lakhin, A.B.Mikhailovskii, and O.G. Onishchenko, *Phys.Lett.* **105A** (1984) 48.
- S.V.Antipov, M.V.Nezlin, E.N.Snezhkin, and A.S.Trubnikov, *JETP* **55** (1982) 85.
- S.V.Antipov, M.V.Nezlin, V.K.Rogianov, E.N.Snezhkin, and A.S.Trubnikov *JETP* **57** (1983) 786.
- R.A.Antonova, V.P.Zhvaniya, D.G.Lominadze, D.I.Nanobashivili, and V.I.Petviashvili, *JETP lett.* **37** (1983) 786
- L.A. Artsimovich, *Controlled Thermonuclear Reaction* (Gordon and Breach, New York) 1964.
- G.K.Batchelor, *An Introduction to Fluids Dynamics* (Combridge University press, Cambridge) 1967, Chapter 7.
- H.Berk and B.Lane, *IFS Rept.* **178** 1985
- H.Berk, M.N.Rosenbluth, V.Wong, T.M.Antonsen, and D.Boldwin *Sov.J.Plasma Phys.* **9** (1983) 176.
- G.Berge, in *Plasma Physics and Controlled Nuclear Fusion*, (IAEA, Vienna) 1966, vol.1, p.767.
- A.S.Bishop, Project Sherwood, The U.S Program in Controlled Fusion (Addison-Wesley, Reading, Mass.) 1958, p.127
- E.C.Bowers and M.G.Haines, *Phys. Fluids* **14** (1971) 165.

- S.I.Braginskii, in *Review of Plasma Physics* ed. by M.A.Leontovich (Consultants Bureau, New York) 1965, vol.1, p.205
- B.N.Breizman and F.A.Tsel'nik, *Sov.J.Plasma Phys.* **9** (1983) 666.
- H.Buchholz, *The Confluent Hypergeometric Function* (Spring-Verlag, New York) 1969.
- J.A.Byers and R.H.Cohen, *Phys. Fluids* **28** (1985) 1589
- S.Chandrasekhar, *Hydrodynamic and Hydromagnetic Stability* (Clarendon, Oxford) 1961, Chapter 11.
- J.G.Charney, *Geophys.Public.Kosjones Nors.Videnshap.-Akad. Osdlo* **17** (1948) 3.
- F.F.Chen, *Phys.Fluids* **9** (1966) 965.
- F.F.Chen, *Phys. Fluids* **10** (1967) 1647
- R.C.Davidson, *Phys. Fluids* **19** (1976) 1189.
- R.C.Davidson, *Theory of Nonneutral plasma* (Benjamin, Reading, Mass.) 1974, Chapter 3.
- P.G.Drazin and W.H.Reid, *Hydrodynamic instability* (Combridge University Press, Cambridge) 1981.
- G.R.Flierl *WHOI-80-53* 1980, p.13
- G.R.Flierl, V.D.Larichev, J.C. McWilliams, and G.M. Reznik *Dyn. Atmo. and Oceans* **5** (1980) 1.
- G.A.Flierl, M.E.Stern, and J.A.Whitehead, *Dyn.Atmos.and Oceans* **7** (1983) 233.
- S.Flügge, *Practical Quantum Mechanics* (Spring-Verlag, New York) 1974 p.166.

- J.P.Freidberg, *Phys. Fluids* **15** (1972) 1102.
- J.P.Freidberg and D.A.D'Ippolito, *Phys. Fluids* **26** (1983) 2657.
- J.P.Freidberg and L.D.Pearlstein, *Phys. Fluids* **21** (1978) 1207.
- J.P.Freidberg and J.A.Wesson, *Phys. Fluids* **13** (1970) 1117.
- A.M.Fridman and V.L.Polyachenko *Physics of Gravitating systems* (Spring-Verlag, New York) 1984. Vol.2, Chapter XI.6.
- R.D.Hazeltine, D.D.Holm, and P.J.Morrison, *IFS Rept.* **173** 1985.
- A.Hasegawa and K.Mima, *Phys. Rev.Lett.* **39** (1977) 205
- A.Hasegawa, C.G.Maclennan, and Y.Kodama, *Phys. Fluids* **22** (1979) 2122
- E.B.Hooper, Jr., G.A.Hallock, and H.H.Foote, *Phys. Fluids* **26** (1983) 314
- W.Horton, *Phys. Fluids* **24** (1981) 1270
- W.Horton and J.Liu, *Physic. Fluids* **27** (1984) 2067.
- W.Horton, J.Liu, J.Meiss, and J.Sedlak, *IFS Rept.* **193** 1985.
- W.Horton, J.Liu, J.D.Meiss, J.E.Sedlak and N.J.Zabusky, *Proceeding of 1985 Sherwood theory confrence 1S-26* Madison, Wis.
- D.B.Ilić, T.D. Rognlien, S.A.Self and F.W. Crafwford, *Phys. Fluids* **16** (1973) 1042.
- P.Janssen, *Physica* **94c** (1978) 251.
- P.Janssen, *Phys. Fluids* **25** (1982) 316
- D.L. Jassby, *Phys. Fluids* **15** (1972) 1590.
- D.L.Jassby and F.W.Perkins, *Phys. Rev.Lett.* **24** (1970) 256.
- G.I.Kent, N.C.Jen, and F.F. Chen, *Phys. Fluids* **12** (1969) 2140.



- J.Kesner and B.Lane, *Phys. Fluids* **28** (1985) 634.
- E.M.Laedke and K.H.Spatschek, *Phys. Fluids* **28** (1985) 1008.
- H. Lamb, *Hydrodynamics* 4th ed. (Combridge University Press, Cambridge) 1916, section. 165.
- V.D.Larichev and G.M.Reznik, *Dokl. Akad.Nauk.USSR* **231** (1976) 1077.
- B.Lehnert, *Nuclear Fusion* **11** ( 1971) 485.
- X.S.Lee, P.J.Catto, and R.E. Aamodt, *Phys. Fluids* **25** (1982) 1491
- C.C.Lin, *The theory of Hydrodynamic instability* (Cambridge University press, Cambridge) 1966, pp. 56-58.
- J.Liu, W.Horton, and J.Sedlak, *IFS Rept.***195**. 1985.
- M.Makino, T.Kamimura, and T.Tanuiti, *J.Phys.Soc.Jap.* **50** (1981) 980.
- J.C.McWilliams and N.J.Zabusky, *Geophys.Astrophs.Fluid Dyn.* **19** (1982) 207.
- J.J.McLure and N.Nathrath, *Proceeding XIIIth ICPIG*, Berlin, p.693.
- J.D. Meiss, in *Radiation in Plasma* ed. by B.McNamara, (World Scientific, Singapole) 1984, Vol.1, p.321.
- J.D.Meiss and W.Horton *Phys. Fluids* **25** (1983) 990.
- A. B. Michailovskii, *Theory of Plasma Inatability* 2nd ed. (Atomizdat. Moscow) 1977, Vol.2, Chapt.7,9. (in Russian)
- A.B. Michailovskii, G.D.Aburdzheniya, O.G.Onishchenko, and S.E.Sharpov, *Phys. Lett.* **100A** (1984) 503; **104A** (1984) 94.
- A.B.Mikhailovskii, G.D.Aburzheniya, O.G.Onishchenko, and A.P.Churikov, *Phys. Lett.* **101A** (1984) 263.

- A.B.Mikhailovskii, V.P.Lakhin, L.A.Mikhailovskaya, and O.G.Onishchenko, *JETP* **86** 2061. (in Russian)
- M.V.Nezlin, *Sov. Astron. Lett.* **10** (1984) 221.
- V.P.Pavlenko and V.I.Petviashvili, *Sov.J.Plasma Phys.* **9** (1983) 603.
- F.W.Perkins and D.L.Jassby, *Phys.Fluids* **14** (1971) 102.
- K.V.Robert and J.B.Taylor *Phys.Rev.Lett.* **8** (1962) 197.
- V.I.Petviashvili, *Sov.J. Plasma Phys.* **3** (1977) 150.
- V.I.Petviashvili, *JETP Lett.* **32** (1980) 619
- V.I.Petviashvili, *Sov.Astron.Lett.* **9** (1983) 137
- V.I.Petviashvili and V.Pogutse, *JETP Lett.* **39** (1984) 436.
- H.U.Rahman and J.Weiland, *Phys.Rev.A* **28** (1982) 1678
- T.D.Rognlien, *J. of Appl. Phys.* **44** (1973) 3515.
- M.N.Rosenbluth, *Physica Scripta* **T2/2** (1982) 104
- M.N.Rosenbluth, N.A.Krall, and N.Rostoker, *Nuclear Fusion Suppl. Pt.1.* (1962) 143.
- M.N.Rosenbluth and A.Simon, *Phys. Fluids* **8** (1965) 1300.
- M.N.Rosenbluth and A.Simon *Phys. Fluids* **9** (1966) 726.
- C.E.Seyler, *Phys. Fluids* **22** (1979) 2324.
- P.K.Shukla,D.Anderson, M.Lidak, and H.Wilhelmsson, *Phys.Rev.A* **31** (1985) 1946.
- P.K.Shukla, K.H.Spatschek, and R. Balescu, *Phys.Lett.* **107A** (1985) 461
- P.K.Shukla, M.Y.Yu, and R.A.Varma, *Phys. Fluids* **28** (1985) 1719.

- P.K.Shukla, M.Y.Yu, and R.A.Varma, *Phys.Lett.* **109A** (1985) 322.
- G.O.Spies *Physic. Fluids* **21** (1978) 580
- M.E.Stern, *J.Mar.Res.* **33** (1975) 1.
- T.Taniuti and A.Hasegawa, *Physica Scripta* **T2/2** (1982) 529.
- J.B.Taylor *J. Nuclear Energy, Pt.3* **4** (1962) 406.
- J.Wright,D.F.R.Pott,and M.G.Haines, *Plasma Phys.***18** (1976) 1.
- N.J.Zabusky and J.C.McWilliams, *Phys. Fluids* **25** (1982) 2175.
- V.V. Zheleznyakov, *Electromagnetic Waves in The Cosmic Plasma* (Nauka, Moscow) 1977, p.24. (in Russian).

## VITA

Jixing Liu was born in Lingshi County, Shanxi Province, China on November 8, 1938, the son of Jian Lian and Kang Liu. While his parents were fighting the Japanese invaders, he was brought up by Mr. and Mrs. Pang, a farmer family in Lingshi County, Shanxi Province, China and he stayed with them until the spring of 1947. After completing his work at the 41st High School, Chungqin City, Sichuang Province China in 1957, he entered the Physics Department of The Peking University, Beijing, China. He received his Bachelor of Science degree in physics from The Peking University in July, 1964. During the following years he worked as a research assistant in the theoretical division of The Institute of Atomic Energy, Academia Sinica, Beijing, China from October 1964 to August 1968; as a farmer in Lishui County, Jianshu Province, China from October 1968 to October 1970; and first as a technician and later an engineer in The Institute of Electromagnetic Wave Propagation, Beijing, China from May 1971 to August 1978. In September 1978 he entered The Institute of Theoretical Physics, Academia Sinica, Beijing, China, as a graduate student.

In August 1980, he entered the graduate school of The University of Texas at Austin. Since that time he has been employed as a Teaching Assistant I & II in the Department of Physics and as a Research Assistant I, II, & III in the Institute for Fusion Studies. He married Shu-kun Wang from Heicheng County, Liaoning Province, China in 1966 and they have two sons, Yi Liu, born in 1969, and Zhi Liu, born in 1971.

Permanent Address:     The Institute of Theoretical  
                                  Physics, Academia Sinica.  
                                  P.O. Box 2735  
                                  Beijing, China.